DOI:10.14753/SE.2017.2251

SIGMA-1 RECEPTOR AGONISM: THE NOVEL TREATMENT OPTION IN RENAL DISEASE

Ph.D. Thesis

Ádám Hosszú

Doctoral School of Clinical Medicine

Semmelweis University

Supervisor: Andrea Fekete, M.D., Ph.D.

Official reviewers:
Attila Szijártó, M.D., D.Sc.
Szilveszter Dolgos, M.D., Ph.D.

Head of the Final Examination Commitee:
Prof. Zoltán Benyó, M.D., Ph.D.

Members of the Final Examination Commitee:
Gábor Kökény, M.D., Ph.D.
Kristóf Dede, M.D., Ph.D.

Budapest, 2016

DOI:10.14753/SE.2017.2251

Table of Contents

DOI:10.14753/SE.2017.2251

DOI:10.14753/SE.2017.2251

1. List of Abbreviations

ADP - adenosine diphosphate
AKI - acute kidney injury
Akt - protein kinase B
AMP - adenosine monophosphate
AST- aspartate transaminase
ATF6 - activating transcription factor 6
ATP - adenosine triphosphate
BDNF - brain-derived neurotrophic factor
BUN - blood urea nitrogen
CKD - chronic kidney disease
CNS - central nervous system
DAB - 3,3’ diaminobenzidine
DHEA - dehydroepiandrosterone
DM - diabetes mellitus
DM1 – type 1 diabetes mellitus
DM2 - type 2 diabetes mellitus
DNA – deoxyribonucleid acid
DNP - diabetic nephropathy
eNOS - endothelial nitric oxide synthase
ER - endoplasmic reticulum
ESRD - end stage renal disease
FLU - fluvoxamine
GFR - glomerular filtration rate
HIF-1α - hypoxia inducible factor 1 alpha
HK2 - human kidney-2 cell line
HLA - human leukocyte antigene
H_2O_2 - hydrogen peroxide
HSP - heat shock protein
IL-1 - interleukin 1
IL-4 - interleukin 4

IL-6 - interleukin 6

IL-10 - interleukin 10

IOD – integrated optical density

IRE1 - inositol requiring enzyme 1

IRI - ischemia/reperfusion injury

KDIGO - Kidney Disease Improving Global Outcomes

KIM-1 - kidney injury molecule 1

KTx - kidney transplantation

MCP-1 - monocyte chemoattractant protein 1

mRNA - messenger ribonucleic acid

miR21- micro ribonucleic acid 21

miR17-5p - micro ribonucleic acid 17-5p

mTOR - mammalian target of rapamycin

MTT - methyl-thiazoletetrazolium assay

NE100 - N,N-dipropyl-2-[4-methoxy-3-(2-phenylethoxy)-phenyl]-thylaminemonohydrochloride

NGAL - neutrophil gelatinase-associated lipocalin

NO - nitric oxide

nNOS - neuronal nitric oxide synthase

pAkt - phosphorylated protein kinase B

PAS - periodic acid-Schiff

peNOS - phsophorylated endothelial nitric oxide synthase

PERK - protein kinase RNA-like endoplasmic reticulum kinase

PI3K - phosphoinositide 3-kinase

RAAS - renin angiotensin aldosterone system

RIFLE - Risk, Injury, Failure, Loss, End stage renal disease

ROS - reactive oxygen species

RT – room temperature

RT-PCR - reverse transcriptase polymerase chain reaction

RRT - renal replacement therapy

S1R - Sigma-1 receptor

SCr - serum creatinine

siRNA - short interfering ribonucleic acid

SSRI – selective serotonin reuptake inhibitors

Tx - transplantation

TNF- α - tumor necrosis factor alpha

US – United States

XBP1 - X-box binding protein 1

WHO - World Health Organization

DOI:10.14753/SE.2017.2251

1.2 List of Figures and Tables

DOI:10.14753/SE.2017.2251

2. Introduction

2.1 End-stage renal disease

Prevalence: End-stage renal disease (ESRD) is the final stage of chronic kidney disease (CKD) characterized by complete loss of kidney function. It is a leading cause of morbidity and mortality worldwide, its global prevalence is estimated to be 8-16% (*Figure 1*) and the overall years of life lost due to premature death is third behind AIDS and diabetes mellitus (DM).[1] Similarly to global trends the prevalence of CKD has been increasing rapidly in the past decades in Hungary (ca. 8%) as well.

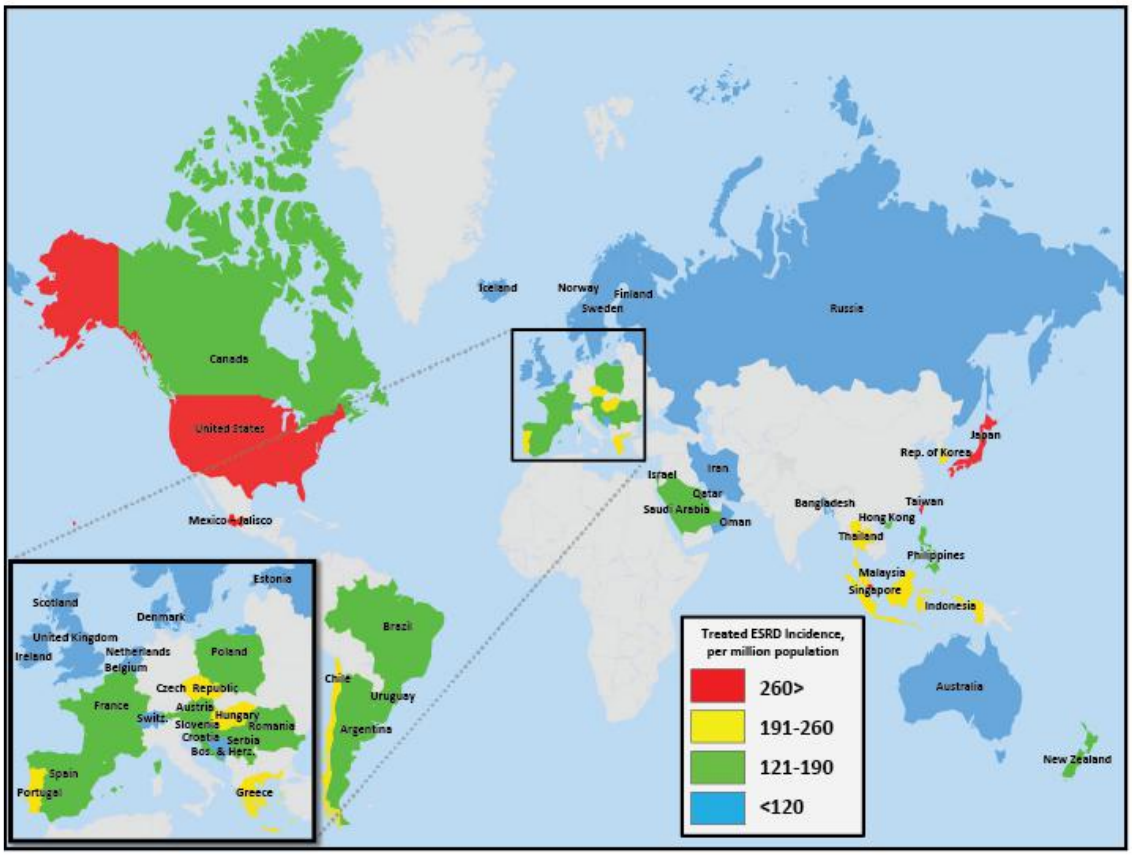

Figure 1. Incidence of treated end-stage renal disease (ESRD) per million population (*US Renal Data System ESRD Database 2015*).

Etiology: The leading causes of CKD are mostly lifestyle-related and show geographic differences. In the Euro-Atlantic population DM and hypertension are responsible for the majority of adult cases (45% and 28%, respectively). More than 400

million people suffer from DM worldwide and by 2040 this number will exceed 640 million (*International Diabetes Federation Diabetes Atlas, 7th Edition*). Diabetic nephropathy (DNP) develops in around one-third of the cases (30-40% of Type 1 DM (DM1) and 10-20% of Type 2 DM (DM2))[2] and significantly amplifies the risk of cardiovascular disease and death.[3] Increasing global trends suggest that DNP will continue to drive the prevalence of CKD and ESRD in the foreseeable future.

In low-income countries different types of glomerulonephritis, polycystic kidney disease and infectious diseases are mainly responsible for CKD, while in children anatomical abnormalities, hereditary disorders, glomerular diseases and secondary causes of glomerulonephritides are the leading causes (*US Renal Data System Annual Report 2015*).

Acute kidney injury (AKI) is also a relevant risk factor for the development of CKD that accounts for 2 to 3% of ESRD cases annually. However AKI represents a much larger portion of renal disease burden on the long run, due to the significantly increased long-term risk of CKD and ESRD following AKI, even if renal function recovers initially.[4] This relation seems to be bi-directional as CKD patients are more vulnerable to AKI as well.[5] AKI will be discussed in detail in the following part of the dissertation.

Diagnosis: The severity of CKD can be defined based on the level of kidney function (*Table 1*). CKD exists if glomerular filtration rate (GFR) is below 60 mL/min/1.73m^2 for at least 3 months, irrespective of the cause. In many diseases kidney damage can also be confirmed by the presence of albuminuria, defined as albumin-to-creatinine ratio >30 mg/g in at least two urine spot samples.[6]

Table 1. Stages of chronic kidney disease (CKD). GFR: glomerular filtration rate (*Kidney Disease Outcomes Quality Initiative Guidelines*).

Stage 1	Kidney damage with normal or ↑ GFR	GFR ≥90 mL/min/1.73m^2
Stage 2	Kidney damage with mild ↓ GFR	GFR 60-89 mL/min/1.73m^2
Stage 3	Moderate ↓ GFR	GFR 30-59 mL/min/1.73m^2
Stage 4	Severe ↓ GFR	GFR 15-29 mL/min/1.73m^2
Stage 5	Kidney failure	GFR <15 mL/min/1.73m^2

Treatment: If a patient's GFR falls below 20 mL/min/1.73m^2 renal replacement therapy (RRT) (dialysis or kidney transplantation (KTx)) should be considered. Today more than 2.6 million people receive RRT worldwide, but even according to a conservative estimation only less than half of the patients in need get treatment.[7] Parallel to international trends in Hungary the number of patients on RRT has also doubled in the last 15 years and now is over 10,000 (*Figure 2*).[8]

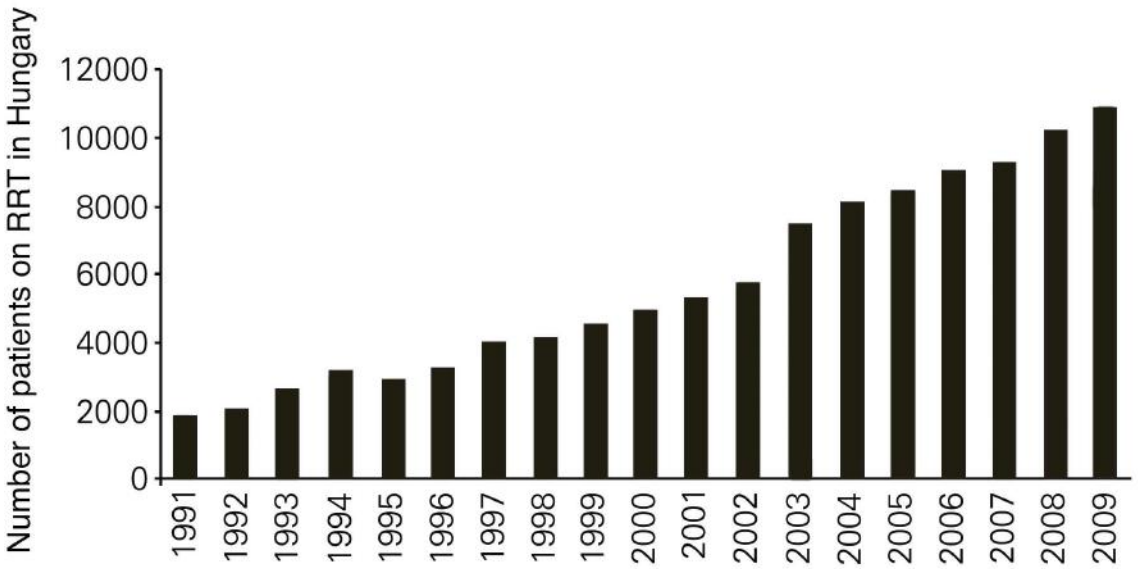

Figure 2. The number of patients on renal replacement therapy (RRT) in Hungary by year (modified image of *Kulcsar et al. 2010*).[8]

Dialysis (peritoneal or hemodialysis) can be a good option in patients not suitable for KTx or awaiting a kidney transplant. However it has several disadvantages; dialysis opportunities are not available in a lot of areas, transportation of patients is difficult, several side effects can occur and a stable access to the bloodstream is required. Dialysis is not only a health problem, but also imposes a massive economic burden both on affected individuals and health care systems. In the US expenditures are over $40 billion, while in the European Union dialysis alone costs more than €15 billion each year (*US Renal Data System Annual Report 2015*; http://www.niddk.nih.gov/health-information/health-statistics). KTx is considerably less expensive. The yearly cost for transplant patients in the US is about $29,000, while the cost for dialysis is over $80,000 per patient (*US Renal Data System Annual Report 2015*).

DOI:10.14753/SE.2017.2251

2.2 Kidney transplantation

The primary RRT treatment option for ESRD is KTx; which is associated with improved survival and quality of life. In a recent review of 110 studies including almost 2 million participants with kidney failure, KTx was associated with reduced risk of mortality and cardiovascular events as well as better quality of life than treatment with chronic dialysis.[9]

While the number of kidney transplants has not changed in the past decade, the total number of patients living with a functioning kidney transplant continues to grow (*US Renal Data System Annual Report 2015*). One-year graft survival is 97% for living donor and 92% for deceased donor transplant recipients.

Living donor transplants have superior outcomes as these donors are usually younger and healthier. Cold ischemia time can be markedly reduced also as these Txs can be planned in advance. Graft survival can be further improved by performing preemptive Tx, transplanting when the recipient is in the best medical and social condition. Beside the obvious advantages of living donor Tx, the possible harm of a healthy person should always be considered as well.[10]

Roughly one third of kidney transplants are from living donors in the US, while this number is around only 12% in Hungary (*National Organ Donation Registry/Nemzeti Szervdonációs Regiszter*) (*Figure 3*). Hungary joined the Eurotransplant Foundation in 2012. This is a network of 8 countries with an aim to mediate and improve the allocation and distribution of donor organs for Tx.

DOI:10.14753/SE.2017.2251

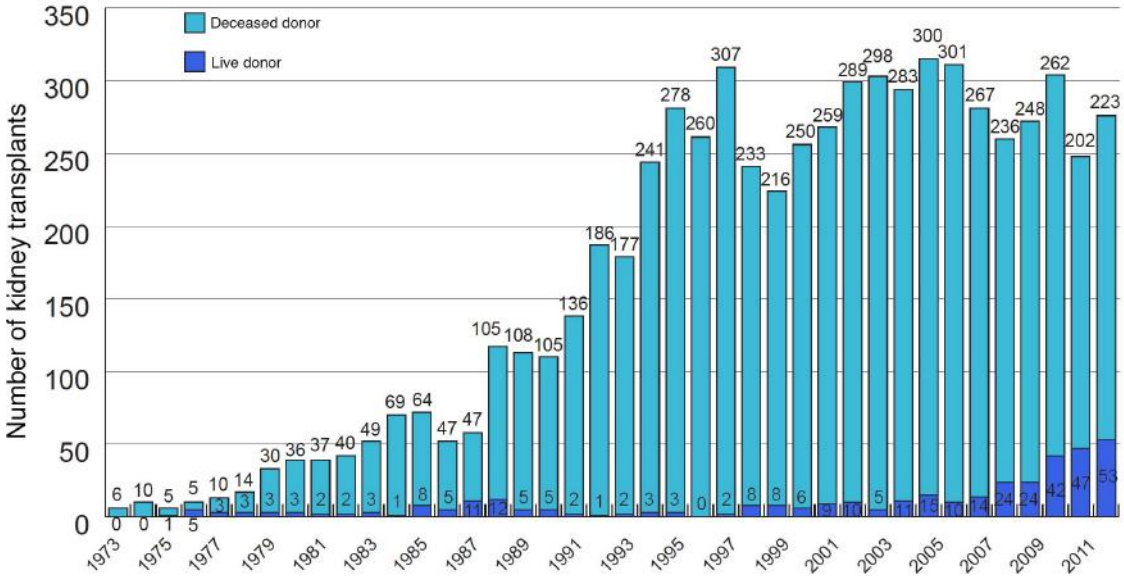

Figure 3. Number of kidney transplants in Hungary (modified image of *Szederkenyi E et al. 2013*).[11]

Although short-term outcomes of KTx have improved substantially due to advances in surgical technique and immunosuppression, long-term outcomes have remained largely unchanged over the past decades.[12] The factors affecting long-term outcome may be either alloantigen-dependent (e.g. HLA matching, HLA immunization etc.) or alloantigen-independent (e.g. donor type and age of both the donor and recipient), disease recurrence, comorbidities or time on dialysis).[13] Among alloantigen-independent factors ischemia/reperfusion injury (IRI) is a major complication that has special influence on long-term survival after KTx. IRI is unavoidable and the duration of storage and cold ischemia time correlate with delayed graft function.

Treatment: Although effective immunosuppressive regimen is the key to successful Tx, immunosuppressants also have several undesirable effects on the kidney. They may provoke or reactivate infections (e.g. severe polyoma BK virus, cytomegalovirus and herpes viruses resulting in interstitial nephritis, or urinary tract infections, etc.). Calcineurin-inhibitors (tacrolimus and cyclosporin A) are nephrotoxic by causing persistent vasoconstriction, interstitial fibrosis and tubular atrophy that can eventually lead to chronic graft dysfunction.[10] Mainly due to steroids tacrolimus, and mTOR inhibitors about a quarter of KTx patients develop '*de novo*' post-transplant DM, which can lead to DNP and graft dysfunction.[14] For all these reasons continuous

and tight control of the immunsuppressive protocol is of special interest during post-transplant nephrological care.

2.3 Acute kidney injury

Etiology: AKI is the abrupt loss of kidney function, resulting in a failure to maintain fluid, acid-base and electrolyte homeostasis. It is a wide-ranging clinical syndrome embodying distinct etiologies, including kidney diseases such as acute glomerular, interstitial or vascular problems. Non - kidney-specific, systemic conditions including global ischemia, hypovolemia or toxic injury along with extrarenal pathology also result in AKI.[15]

Diagnosis: Traditionally AKI was characterized by severe reduction in kidney function, with severe azotemia and often oliguria or even anuria. According to the most recent Kidney Disease Improving Global Outcomes (KDIGO) guidelines AKI is actually defined as any of the following (*KDIGO AKI Guideline 2013*):

- Increase in serum creatinine (SCr) by ≥0.3 mg/dL (≥26.5 μmol/L) within 48 hours
- Increase in SCr to ≥1.5 times baseline, which is known or presumed to have occurred within the prior 7 days
- Urine volume <0.5 ml/kg/h for 6 hours

In the past decades to further classify acute impairment of kidney function the RIFLE criteria was developed through a broad consensus of experts. RIFLE stands for the increasing severity classes: Risk, Injury, Failure; and two outcome classes: Loss and End-stage Renal Disease. Risk, Injury and Failure are defined by the changes SCr or urine output (*Figure 4*). In the past few years however, even moderate decreases of kidney function have been shown to be important. Therefore the Acute Kidney Injury Network added a minor modification to the RIFLE criteria with the inclusion of small changes in SCr (≥26.5 μmol/L) when they occur within 48 hours.[16]

DOI:10.14753/SE.2017.2251

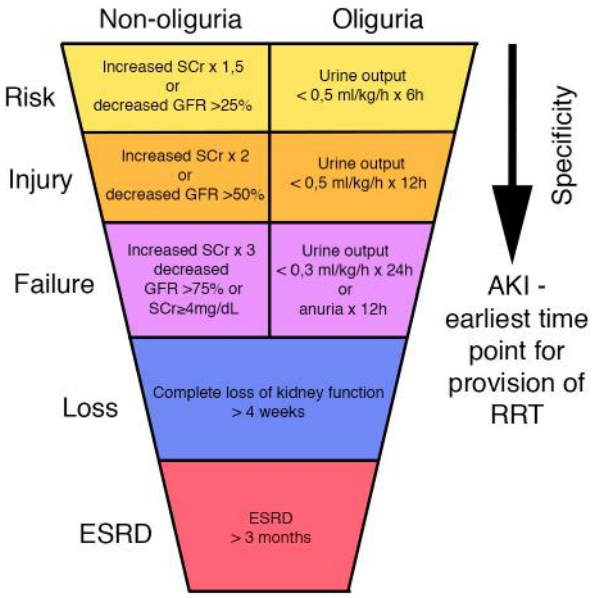

Figure 4. RIFLE criteria of acute kidney injury (AKI); ESRD: end stage renal disease; GFR: glomerular filtration rate; RRT: renal replacement therapy; SCr: serum creatinine (modified image of *Bellomo et al. 2004*).[17]

The most frequently used indicators of renal disease are SCr, blood urea nitrogen (BUN) and creatinine clearance, however these are insensitive, non-specific and do not allow early detection. Therefore ongoing efforts are made to identify new, accurate, real-time indicators of AKI. Kidney Injury Molecule 1 (KIM-1) is upregulated mainly in proximal tubules as soon as a few hours after the ischemic insult, where it may play a role in regeneration as well.[18] Neutrophil gelatinase-associated lipocalin (NGAL) is one of the most highly induced genes after ischemia. NGAL protein is upregulated very early in the postischemic kidney and is a marker of distal tubular injury. It is quickly excreted to the urine making it a sensitive and early biomarker. Several experimental studies have shown that NGAL is remarkably protective by inducing proliferation and inhibiting apoptosis in tubular epithelial cells.[19] However these markers are not introduced to the routine clinical use yet, in everyday diagnosis SCr with GFR and BUN still serve as the basic values.

Renal histological changes are also specific and informative for AKI. Notable morphologic features of ischemic AKI include the loss of proximal tubule brush border, depolarization and patchy loss of tubular cells and tubular cast formation[20] as well as peritubular capillary congestion, endothelial damage and leukocyte accumulation

(*Figure 5*). Since the main focus of this dissertation is ischemic AKI, this pathophysiology will be discussed in detail.

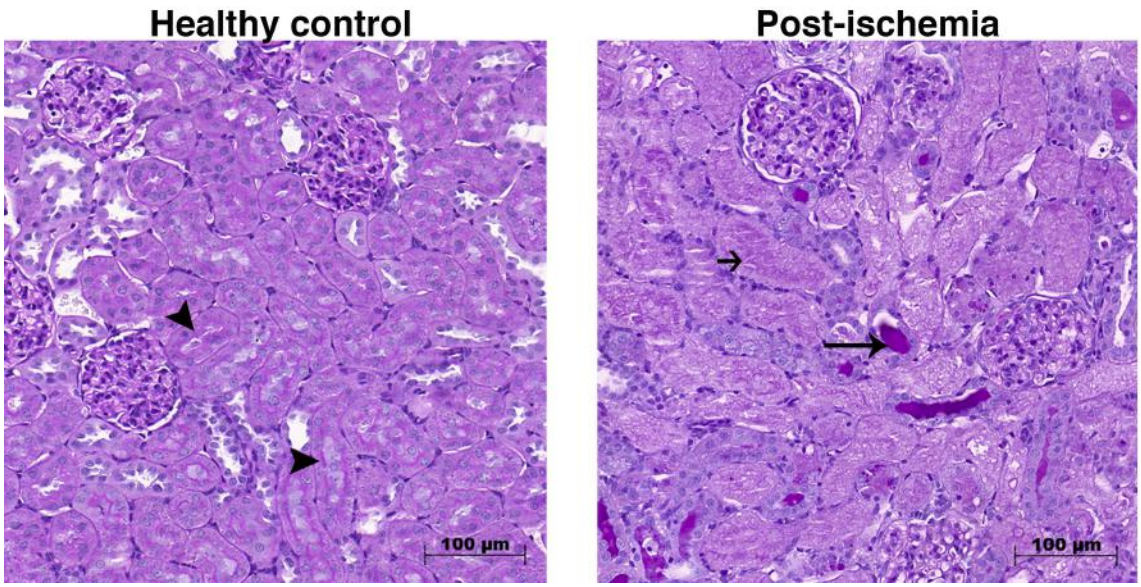

Figure 5. Representative periodic acid-Schiff stained sections of control and post-ischemic rat kidneys. Black quadrilateral arrow points to intact brush border; long, thin arrow shows hyalin accumulation; short black arrow shows necrotic tubule. 200x magnification, scale bar =100 µm.

Pathophysiology of IRI-induced kidney injury: The endothelium of microcirculation plays a pivotal role in the pathophysiology of IRI. Even under normal conditions the kidney regions housing nephron segments with very high energy requirements such as the S3 segment of the proximal tubule or the medullary thick ascending limb, sustain relative hypoxia due to lower blood flow and exchange of oxygen.[21] Relative hypoxia worsens after ischemia, which leads to prolonged cellular injury and cell death. Renal blood flow is reduced by up to 50%, which persists in the outer medulla even during reperfusion. Release of vasoconstrictors such as endothelin is enhanced[22] and abundance of vasodilators such as endothelium-derived NO is decreased[23] causing vasoconstriction in small arterioles and peritubular capillaries.

In parallel, as we previously also showed Na^+K^+-ATP-ase is relocated from the basolateral membrane to the cytoplasm making it dysfunctional.[24] Due to inadequate sodium reabsorption in injured proximal tubules, the tubuloglomerular feedback mechanism contributes to pre-glomerular arterial vasoconstriction. Additionally endothelial damage causes the disruption of cytoskeleton, loss of glycocalyx and

breakdown of the perivascular matrix, which result in increased microvascular permeability and fluid loss to the interstitium.[25] Our group previously described an important role of heat shock proteins (HSPs), especially HSP72, in recovering cellular polarity and structure. HSP72 belongs to the chaperone family and acts by refolding denatured proteins, restoring their function and limiting detrimental peptide interactions.[26]

Oxygen deprivation leads to the degradation of ATP to ADP and AMP, which are further metabolized to adenine nucleotides and hypoxanthine. Hypoxanthine accumulation contributes to the generation of reactive oxygen species (ROS), which in turn cause tubular injury by oxidation of proteins, peroxidation of lipids, DNA damage and apoptosis. ATP depletion also leads to a rise in intracellular free calcium, which activates proteases, phospholipases and leads to cytoskeletal degradation.[27]

In DNP hyperglycemia activates the renin-angiontensin-aldosterone system (RAAS)[28] that leads to ischemia via chronic vasoconstriction as well. Renal blood flow is decreased due to vasoconstriction, which further activates RAAS and increases the production of ROS. Moreover activated RAAS and atherosclerosis increase systemic blood pressure, which in turn not only damages renal perfusion and blood vessels but escalates RAAS activation and atherosclerosis.[29] These processes lead to functional and structural damage of the kidneys.

Inflammation is also an important contributor both of acute and chronic ischemic injury. Innate immunity is responsible for early response and comprises neutrophil granulocytes, macrophages, dendritic cells and natural killer cells. Neutrophils accumulate and attach to the endothelium where they release ROS, proteases and inflammatory cytokines such as IL-1, IL-6, TNF-α, MCP-1, all of which aggravate kidney injury in acute renal injury models[30] and DNP.[31]

Very recently a new molecule, the Sigma-1 receptor (S1R) has become the center of attention in brain ischemia and stroke as a possible mediator of key protective mechanisms, however there is no information about its role in the kidney.

DOI:10.14753/SE.2017.2251

2.4 Sigma-1 receptor

S1R is a unique transmembrane chaperone protein, which consists of 223 amino acids and shows no homology with any other mammalian protein. The receptor consists of two subtypes: the S1R and the S2R, which can be distinguished by molecular weight, tissue distribution and ligand binding profile.[32] The topic of this thesis is S1R, therefore only this isoform will be discussed further on.

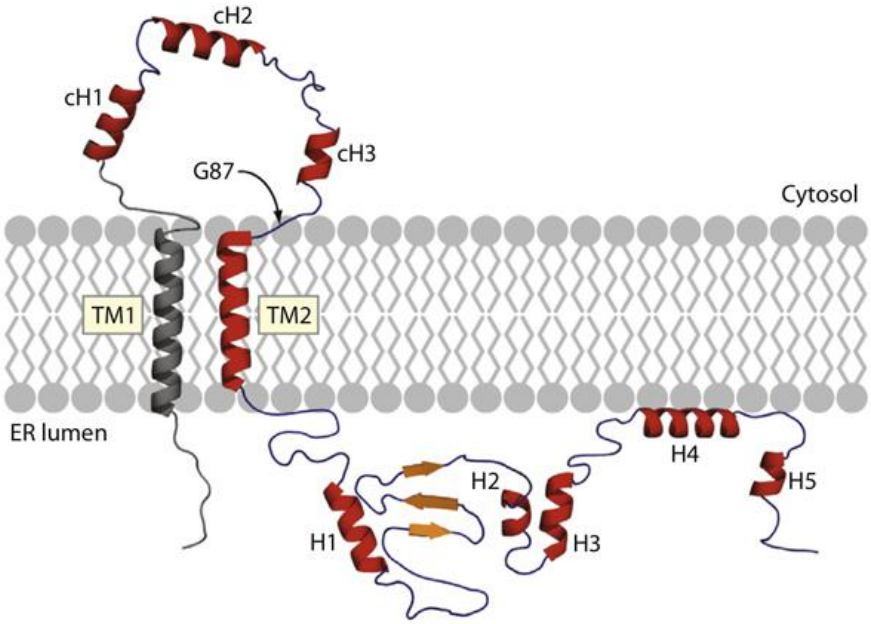

Figure 6. Secondary structure of the Sigma-1 receptor. cH: cytosolic helic; ER: endoplasmic reticulum; TM1: transmembrane helix 1; TM2: transmembrane helix 2, H: helix; G87: the first residue in the GGWMG sequence. (*Ortega-Roldan JL et al. 2015*).[33]

S1R is vastly expressed in the central nervous system (CNS)[34], but has also been detected in various peripheral tissues including the heart, liver and kidney.[35, 36] In the brain S1R is localized in the endoplasmatic reticulum (ER) (*Figure 6*), but upon ligand stimulation it translocates to the cytosol or the cell periphery using the ER-associated reticular network.[37]

S1R has many different ligands and thus has been implicated in a large number of CNS diseases and conditions. The involvement of the receptor in drug and alcohol addiction has been extensively studied, especially in the context of drug self-administration.[38, 39] The effect of S1R agonists on learning and memory has been

studied as well. These compounds seem to improve learning in animal models of amnesia. [40]

Several lines of evidence suggest that S1R agonists also have effective antidepressant properties. Several selective serotonin reuptake inhibitors (SSRI) such as fluvoxamine (FLU) or sertraline bind to S1Rs with very high affinity[41], suggesting a role of S1R in the pharmacological action of these drugs. Other S1R agonists also had effective antidepressant actions in forced swimming, tail suspension or conditioned fear stress tests and these effects were blocked by S1R.[42, 43]

The role of S1R agonists has been demonstrated in models of brain ischemia as well. Most of these studies used the middle cerebral artery occlusion ischemic stroke model to examine the neuroprotective characteristics of S1R agonists. S1R agonist treatment reduced infarct areas, presumably by promoting cell survival and reducing the inflammatory response.[44] However not very much is known about the regulation and function of S1R outside the CNS.

In a recent study S1R stimulation was proven to be effective in minimizing infarct size in a pressure overload induced cardiac hypertrophy model. This protection seemed to be mediated by the upregulation of protein kinase B (Akt)-endothelial nitric oxide synthase (eNOS) signaling.[45] Similarly S1R agonist fluvoxamine attenuated cardiac hypertrophy in another ischemic heart model of transverse aortic constriction.[46]

On the molecular level S1Rs take part in many different processes. The modulation of voltage-dependent ion channels, especially Ca^{2+} channels has been the main area of S1R research. Recent studies demonstrated that S1Rs regulate Ca^{2+} signaling between the ER and mitochondria by modulating inositol triphosphate (IP3) receptors in the ER membrane.[47] A possible protective mechanism of S1R agonists under pathological conditions is rescuing ATP production by restoring mitochondrial Ca^{2+} transport.[48] S1Rs have been shown to modulate potassium, sodium and chloride channels as well.[49, 50]

S1Rs promote cell survival possibly by stabilizing anti-apoptotic protein Bcl-2[51] and suppressing pro-apoptotic proteins Bax and caspase-3[52], however the exact mechanism by which S1Rs are related to caspases and hypoxia-inducible factor alpha (HIF-1α) is yet unknown.

DOI:10.14753/SE.2017.2251

Summarizing the literary data one can conclude that renal IRI plays a central role in the patomechanism of acute kidney injury and KTx, as well as in the development of CKD such as DNP. Via decreased NOS activity and NO production renal vasoconstriction and hypoperfusion occurs leading to the progression of kidney injury both acutely and on the long run. Since renal IRI has high morbidity and mortality and treatment options are still very limited better understanding of the underlying molecular mechanisms are essential for developing novel renoprotective therapies.

Preliminary results in the brain and heart suggest that S1R activates vasodilatative and protective pathways in brain and cardiac ischemia. Therefore it is rather presumable that S1R agonists could trigger similar mechanisms in renal IRI. In our preclinical experiments - during my PhD work - we aimed to investigate this promising option.

DOI:10.14753/SE.2017.2251

3. Objectives

The purpose of our experiments was to investigate the pathomechanisms of IRI-induced AKI in order to identify new therapeutic targets that can be used in KTx as well as in DNP. Based on the current literature demonstrating that S1R is protective in brain and heart ischemia the main aim was to investigate the effect of S1R and its modulation in renal diseases.

Objectives:

The following objectives have been set to fulfill the aims:

1. To investigate the intrarenal and subcellular localization of S1R in the normal and ischemic kidney

2. To analyze the molecular mechanism of S1R - mediated effects

3. To determine the possible renoprotective effect of S1R agonism in acute (renal IRI) and chronic (DNP) models of kidney disease

4. To evaluate the protective effect of S1R agonist pretreatment in KTx

DOI:10.14753/SE.2017.2251

4. Methods

Animals

Adult, male Wistar rats weighing 200±15g (Toxi-Coop Toxicological Research Center, Dunakeszi, Hungary) were used in all experiments (n=8-10/each group). Rats were housed in standard laboratory cages and were allowed free access to food and water. Animal procedures were approved by the Committee on the Care of Laboratory Animals at Semmelweis University, Budapest, Hungary (PEI/001/1731-9/2015).

Renal ischemia/reperfusion injury model and treatment groups

General anesthesia was performed by inhalation of isoflurane (3% vol/vol) mixed with synthetic air (1 L/min) in an isoflurane vaporizer (Eickemeyer Veterinary Equipment Ltd., Twickenham, UK). Renal ischemia was accomplished by cross-clamping the left renal pedicles for 50 min with an atraumatic vascular clamp, ischemia was visually confirmed. Before the end of the ischemic period the contralateral kidney was taken out, the clips were removed and the left kidneys were observed for 5 min to ensure reperfusion. Sham animals underwent laparotomy of the same duration without clamping. At pre-determined times of reperfusion, blood samples were collected from the abdominal aorta, the remnant kidneys were harvested, instantly snap-frozen in liquid nitrogen, and stored at −80 °C or fixed in buffered 4% formalin for further processing.

To test the effect of DHEA in the first set of experiments rats were pretreated first 25 hours, then 1 hour before the surgical procedure with (i) isotonic saline as vehicle; (ii) 4 mg/bwkg DHEA (Sigma Aldrich, Budapest, Hungary).

To investigate the effect of FLU in the second set of experiments 30 min prior to the ischemic insult animals were treated as follows: (i) isotonic saline as vehicle; (ii) 20 mg/bwkg fluvoxamine maleate (FLU; Sigma Aldrich, Budapest, Hungary); (iii) 20 mg/bwkg FLU and 1 mg/bwkg N,N-dipropyl-2-[4-methoxy-3-(2-phenylethoxy)-phenyl]-ethylamine monohydrochloride (NE100, selective S1R antagonist) (Tocris Bioscience, Bristol, UK).

In the third set of experiments to test the NO-mediated effect the following

pretreatment was applied 30 min prior to the ischemic insult: 20 mg/bwkg FLU and 10 mg/bwkg N-omega-Nitro-L-arginine methyl ester (L-NAME, non-selective NOS inhibitor) (Sigma Aldrich, Budapest, Hungary) or 20 mg/bwkg *N*5-(1-Iminoethyl)-L-ornithine dihydrochloride (L-NIO, selective eNOS inhibitor; Sigma Aldrich, Budapest, Hungary) or 25 mg/bwkg 7-Nitroindazole (7-NI, selective nNOS inhibitor) (Sigma Aldrich, Budapest, Hungary). DHEA was administered subcutaneously; all other substances were administered intraperitoneally.

Experimental protocol is summarized in *Figure 7.*

In one series postischemic survival was followed for 7 days.

In another series animals were randomly divided into the following groups:

(i) Sham-operated, vehicle treated group as controls; (ii) T30' group that was not subjected to ischemic insult and was sacrificed or underwent intravital two-photon microscopic analysis 30 min after drug pretreatment; (iii) T2 group was subjected to ischemia 30 min after drug pretreatment and was sacrificed after 2 hours of reperfusion; (iv) T24 group was subjected to ischemia 30 min after drug pretreatment and was sacrificed or underwent two-photon microscopic analysis after 24 hours of reperfusion.

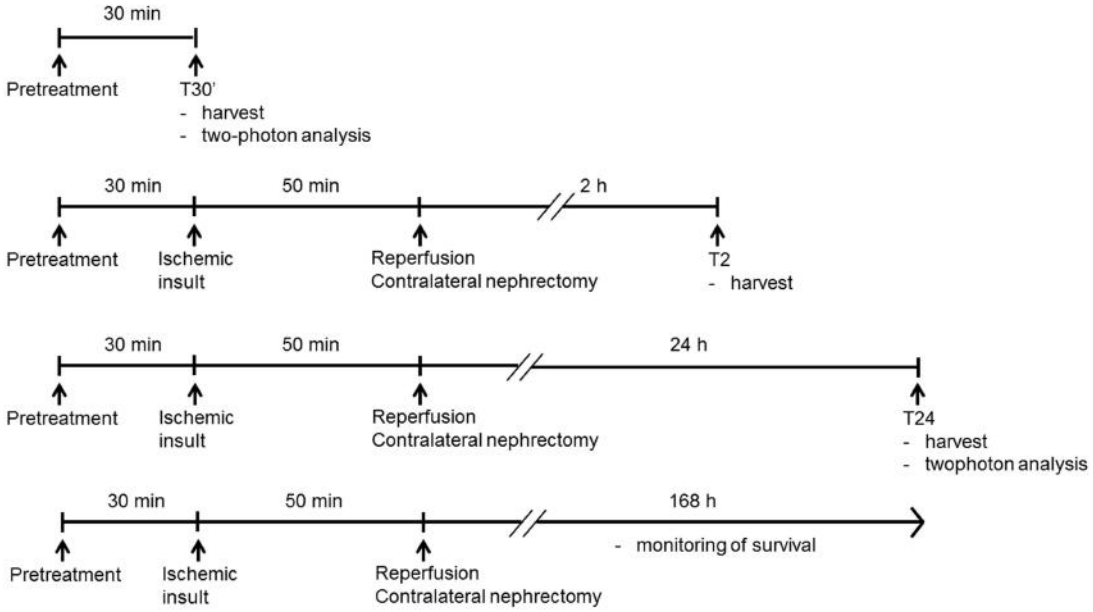

Figure 7. Experimental design of renal IRI

Rat model of kidney isograft autotransplantation

Male Wistar rats (n=8/group) were anesthetized with isoflurane (3% vol/vol) mixed with synthetic air (1 L/min) before surgery and placed on a temperature-controlled table to maintain core body temperature. Left kidneys were perfused with cold Custodiol perfusion solution (Na^+: 15 mmol/L; K^+: 9 mmol/L; Mg^{2+}: 4 mmol/L; Ca^{2+}: 0.015 mmol/L; histidine: 198 mmol/L; tryptophan: 2 mmol/L; ketoglutarate: 1 mmol/L; mannitol: 30 mmol/L) (Franz Kohler Chemie GMBH, Bensheim, Germany), then removed from the animal: kidneys were placed into a container for 2 hours filled with either (i) cold Custodiol perfusion solution (Tx) or (ii) cold Custodiol perfusion solution containing 0.003 mg/mL FLU (Tx FLU). After 2 hours kidneys were placed back into the rats and end-to-end anastomoses of the renal artery, vein and ureter were performed. Contralateral kidneys were removed and the autotransplanted kidneys were observed to ensure reperfusion. Total warm ischemia time was 35 min in all animals. Sham operated animals served as controls (*Figure 8*).

After 24 hours of reperfusion, blood samples were collected from the abdominal aorta, the remnant kidneys were harvested, instantly snap-frozen in liquid nitrogen, and stored at −80 °C or fixed in buffered 4% formalin for further processing.

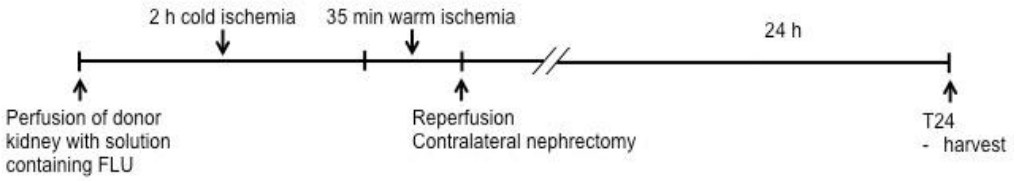

Figure 8. Experimental design of renal autotransplantation

Rat model of type 1 diabetes mellitus (DM1) and experimental groups

DM1 was induced in male Wistar rats (n=6-8/group) by a single intraperitoneal injection of 65 mg/bwkg streptozotocin (STZ, Sigma Aldrich, Budapest, Hungary) in freshly prepared 0.1 M citrate buffer (pH 4.5). Rats were considered diabetic if the peripheral blood glucose concentration in three random samples was higher than 15 mmol/L at 72 hours after the injection of STZ. Age-matched control rats received an equivalent volume of citrate buffer and were used along with diabetic animals.

DM1 rats were randomly divided into four groups and were treated by oral gavage daily at 10:00 AM as follows: (i) DM1 rats treated with isotonic saline as vehicle for 7 weeks (D); (ii) 20 mg/bwkg FLU for 7 weeks (D + 7 wk FLU (20 mg/bwkg)); (iii): 20 mg/bwkg FLU for 2 weeks after 5 weeks of DM1 (D + 2 wk FLU (20 mg/bwkg)); (iv) 2 mg/bwkg FLU for 2 weeks after 5 weeks of DM1 (D + 2 wk FLU (2 mg/bwkg)). Age-matched, non-diabetic control rats (Control) were treated with saline daily for two weeks at the same time as the diabetic animals.

At the end of the experimental protocol all rats were anesthetized with a mixture of 60 mg/bwkg ketamine and 5 mg/bwkg xylazine (rats did not receive drug treatment on this day). Blood samples were collected from the abdominal aorta. Kidney samples were collected and immediately snap-frozen stored at −80 °C or fixed in buffered 4% formalin for further processing.

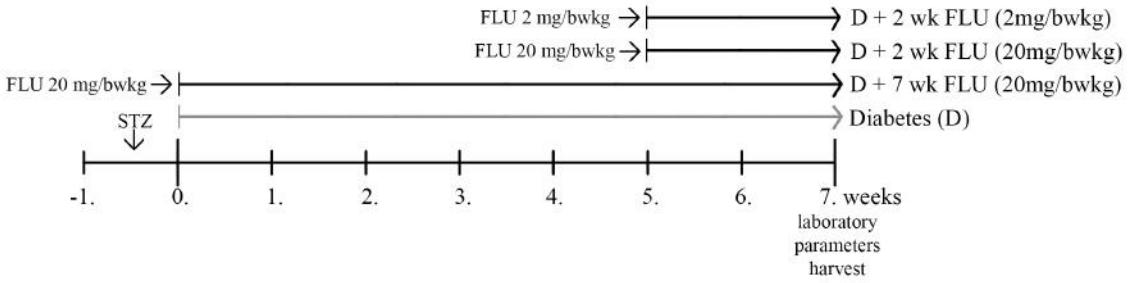

Figure 9. Experimental design of type 1 diabetes mellitus.

Plasma chemistry and metabolic parameters

The development of DM1 was followed by measurement of serum glucose and fructosamine levels. Serum electrolytes (sodium, potassium, chloride), urea, creatinine, albumin, total protein, triglycerides, total cholesterol, aspartate transaminase (AST) and glutamate-pyruvate transaminase (GPT) were evaluated using commercially available kits on a Hitachi 912 photometric chemistry analyzer by our hospital’s research services.

In vitro models

Cell culture and treatment

Human proximal tubular epithelial cell line (HK2; American Type Culture Collection; Rockville, Maryland, USA) were grown in Dulbecco's Modified Eagle Medium (DMEM) (Life Sciences, Budapest, Hungary) supplemented with 10% fetal calf serum (FCS) 1% L-glutamine and 1% antibiotic, antimycotic solution (100x) (Sigma Aldrich, Budapest, Hungary) containing 10000 IU/mL penicillin, 10 mg/mL streptomycin and 25 µg/mL Amphotericin B. The cells were incubated at 37°C in 5% CO_2 and 95% air. In all experiments, there was a "growth arrest" period of 24 hours in serum-free medium before treatment.

Cell viability and proliferation assay

Prior to the experiments the non-toxic dosage of FLU and NE100 was confirmed by methyl-thiazoletetrazolium assay (MTT) (Roche Diagnostics, Mannheim, Germany). Cell viability was determined by MTT assay according to the manufacturer's instructions (*Figure 10/A*).

Cell viability was also assessed by trypan blue exclusion. Cells were detached with trypsin-EDTA and re-suspended in medium diluted 1:1 with trypan blue solution (Sigma Aldrich, Budapest, Hungary). Live cells from triplicate wells were counted in a Burker chamber.

In vitro model of oxidative stress

Oxidative stress was induced by 400 µM hydrogen-peroxide (H_2O_2) treatment for 30 min. Pilot experiments were performed to determine the effective dose and duration of H H_2O_2 treatment (*Figure 10/B*).

Cells were treated as follows: (i) 10 µM FLU (30 min prior to harvest); (ii) FLU + 3 µM NE100 (iii) FLU + 10 µM AktVIII inhibitor (AktVIII; 1 hour prior to harvest; Santa Cruz Biotechnology, Budapest, Hungary); (iv) FLU + 2 µM AktIV inhibitor

(AktIV; 1 hour prior to harvest; Santa Cruz Biotechnology, Budapest, Hungary). After treatment the cells were processed for nitrite measurement.

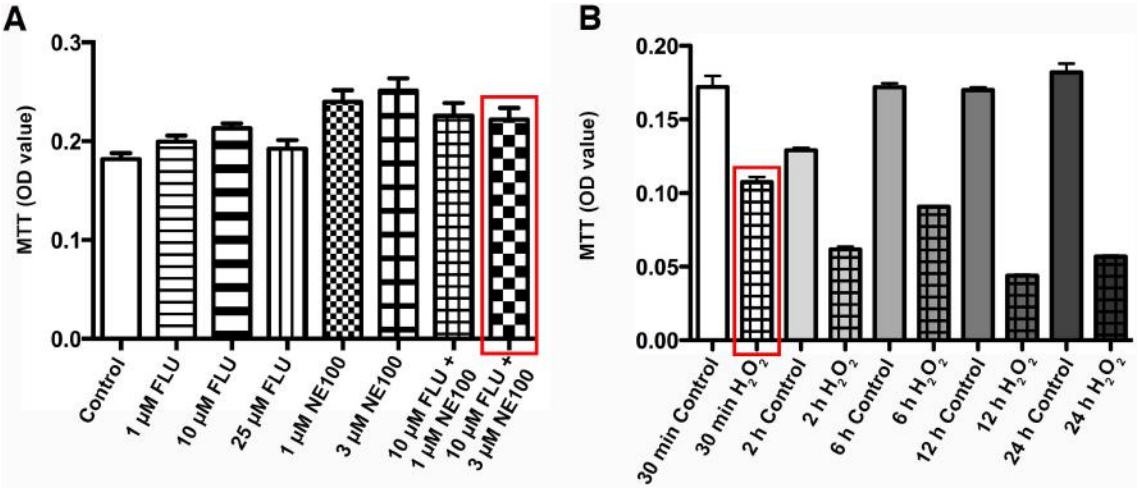

Figure 10. Cell viability assay to confirm the non-toxic dosage of (**A**) Fluvoxamine **(**FLU) and Sigma-1 receptor antagonist NE100. (**B**) Cell viability assay to determine the protocol for hydrogen peroxide (H_2O_2)-induced oxidative stress. The dose and duration for final treatment protocols are marked with red.

RNA interference

All reagents for siRNA were purchased from Invitrogen, Budapest, Hungary. HK2s were transfected with 10 nM S1R specific siRNA or negative control siRNA using Lipofectamine 2000. Successful transfection with 10nM fluorescently labeled siRNA was visualized with an Olympus IX81 (Olympus America, Center Valley, PA) fluorescent microscope. The efficacy of knockdown was determined by Western blot (*Figure 11*).

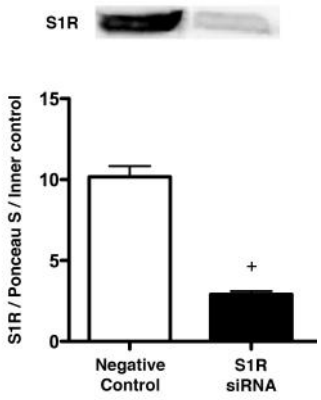

Figure 11. Validation of Sigma-1 receptor (S1R) knockdown. S1R protein level of S1R siRNA-treated HK2 cells compared to scrambled siRNA-treated Negative Control cells. +P<0.05 *versus* Negative Control (n=6/group). Bars indicate means ± SEMs, and data were analyzed by one-way ANOVA with Bonferroni multiple comparison test.

Subcellular protein fractionation

HK2 cells were treated either with 10 μM FLU or 10 μM FLU and 400 μM H_2O_2. After treatment the cells were processed for further analysis by Subcellular Protein Fractionation Kit for Cultured Cells (Thermo Scientific, Budapest, Hungary). The adherent cells were harvested with trypsin - EDTA and separated into cytoplasmic, membrane, soluble nuclear, chromatin-bound nuclear and cytoskeletal extract. After fractionating the different cell extracts S1R protein levels were determined by Western blot.

Imaging techniques

Conventional histology

Paraffin-embedded, 3 μm kidney sections were stained with periodic acid-Schiff (PAS) and haematoxylin eosin or Masson's trichrome or Sirius red to assess injury. Images were taken with a Zeiss AxioImager A1 light microscope (Zeiss, Jena, Germany). Tubular injury was evaluated based on a semi-quantitative scale.[53] Each cortical tubule showing epithelial cell necrosis and brush border loss was assigned a score of 0: normal; 1: loss of brush border; cell necrosis in less than 25% of tubular

cells 2: cell necrosis in 25% - 50% of tubular cells 3: cell necrosis in 50% - 75% of tubular cells; 4: cell necrosis in >75% of tubular cells. Two fields of x200 magnification/animal were examined and averaged in a double - blinded fashion by two different pathologists.

In the case of transplanted kidneys sections were stained with PAS, then tubular lumen areas were measured on 6 fields of x20/animal using Adobe Photoshop (Adobe Systems, San José, California) software.

To evaluate mesangial matrix expansion sections were stained with PAS. 15 fields of x40 magnification containing glomeruli were randomly selected per animal and the ratio of mesangial area per glomerular taft area was measured in each glomerulus using Adobe Photoshop and Image J (US National Institute of Health, Bethesda, USA, http://rsb.info.nih.gov/ij/) softwares.

To evaluate tubulointerstitial fibrosis sections were stained with Masson's trichrome. 10 - 10 fields of x20 magnification were randomly selected from cortical and cortico-medullary regions respectively per animal and the ratio of Masson-stanied fibrotic area per total area was measured in each field using Adobe Photoshop and Image J softwares.

To evaluate collagen accumulation sections were stained with Sirius red. 10-10 fields of x20 magnification were randomly selected from cortical and cortico-medullary regions respectively per animal and the ratio of Sirius red-stanied extracellular matrix area per total area was measured in each field using Adobe Photoshop and Image J softwares.

Two-photon microscopy

Femto 2D high sensitivity galvanoscanner-based two-photon microscope system (Femtonics Inc., Budapest, Hungary) was used for intravital two-photon microscopy. Fluorescence excitation is provided by a Mai Tai mode-locked titanium-sapphire laser (Spectra-Physics Inc., Irvine, CA) and collected in separate photomultiplier tube detectors to a maximal depth of 100 μm. To inject the mixture of dyes the rat was anesthetized as described in the surgical procedure and a cannula was placed in the carotid artery. 70 kDa Rhodamine dextran (Life Technologies, Budapest, Hungary) was

used to label the vasculature, Texas Red (Life Technologies, Budapest, Hungary) to evaluate the reabsorption capacity and the preservation of the brush border and Hoechst 33342 (Life Technologies, Budapest, Hungary) to visualize nuclei.

The changes in capillary diameters were measured continuously in every minute for a 30-min period and the difference in diameter between the first, 10^{th}, 20^{th} and 30^{th} minute was calculated. ~150 capillaries were measured per animal.

Images and data volumes were processed using Matlab (Femtonix Inc., Budapest, Hungary) and Image J softwares.

DAB (3,3'-diaminobenzidine) immunohistochemical staining

Slides were deparaffinized in xylene, rehydrated in graded ethanol series and washed in dH_2O. Heat-induced epitope retrieval was performed by boiling the tissue sections in citrate buffer (HISTOLS®-Citrate Buffer) followed by cooling at room temperature (RT) for 20 min. Nonspecific sites were blocked (HISTOLS® Background Blocking Protein Solution) for 10 min at RT. Without washing, the slides were incubated with the primary antibody (Rabbit anti-S1R, Thermo Scientific, Budapest, Hungary) in 1:50 dilution for 1 hour at RT and repeatedly washed in TBS. Secondary antibody (HISTOLS® MR anti mouse and rabbit Detection Systems Histopathology Ltd., Pecs, Hungary) was applied for 30 min at RT followed by repeated washing in TBS. Sections were incubated with 3-amino-9-ethylcarbazol (HISTOLS® -Resistant AEC Chromogen/Substrate System, Histopathology Ltd., Pecs, Hungary) and washed in dH_2O, counter stained with haematoxylin or PAS followed by washing in tap water.

Fluorescent immunohistochemistry

Frozen kidney sections were embedded in Shandon cryomatrix (Thermo Scientific, Budapest, Hungary) and cut to 5 μm slides. Samples were incubated with the specific rabbit S1R (Invitrogen, Budapest, Hungary); goat Akt (Santa Cruz Biotechnology, Budapest, Hungary) and mouse eNOS (BD Biosciences, Budapest, Hungary) primary antibodies. After repeated washing slides were incubated with the specific secondary anti-rabbit Alexa Fluor 568 (Invitrogen, Budapest, Hungary), anti-

goat Alexa Fluor 647 (Invitrogen, Budapest, Hungary) or anti-mouse Alexa Fluor 488 (Invitrogen, Budapest, Hungary) conjugates and counterstained with Hoechst 33342 (Life Technologies, Budapest, Hungary).

HK2 cells were cultured in tissue culture chambers (Sarstedt Kft., Budapest, Hungary). After repeated washing the cells were fixed in 4% paraformaldehyde, washed again and permeabilized with Triton X-100 (Sigma Aldrich, Budapest, Hungary). Cells were incubated with the specific mouse S1R antibody (Santa Cruz Biotechnology, Budapest, Hungary). After repeated washing the chambers were incubated with anti-mouse Alexa Fluor 488 conjugate and counterstained with Hoechst 33342. Appropriate controls were performed omitting the primary antibody to assure the specificity and to avoid autofluorescence. Sections were analyzed with a Zeiss LSM 510 Meta confocal laser-scanning microscope (Zeiss, Jena, Germany) with objectives of 20x and 63x magnification.

Other molecular biology techniques

Quantitative real-time PCR

Total RNA from kidney, hippocampus and prefrontal area samples was extracted using the RNeasy RNA isolation Kit (Quiagen GmbH, Hilden, Germany). Hif1a, Ngal, Kim1, Sigmar1, glyceraldehyde-3-phosphate dehydrogenase (Gapdh), Mcp1 and 18S ribosomal RNA (Rn18s) mRNA expression were determined in duplicates by real-time (RT-PCR) using SYBR Green I Master enzyme mix (Invitrogen, Budapest, Hungary) and specific primers (*Table 2*). Results were analyzed by LightCycler 480 SYBR Green I Light Cycler system (Roche Diagnostics, Mannheim, Germany). The mRNA expression of Hif1a, Ngal, and Kim1 was normalized against Gapdh as housekeeping gene.

Table 2. Sequence of forward and reverse primers for RT-qPCR

	Forward primer 5'-3'	Reverse primer 5'-3'
Ngal	CAA GTG GCC GAC ACT GAC TA	GGT GGG AAC AGA GAA AAC GA
Hif1a	AAG AAA CCG CTT ATG ACG TG	CCA CCT CTT TTT GCA AGC AT
Kim1	CGC AGA GAA ACC CGA CTA AG	CAA AGC TCA GAG AGC CCA TC
Gapdh	CAC CAC CAT GGA GAA GGC TG	GTC ATG GCA TGG ACT GTG
Mcp1	ATG CAG TTA ATG CCC CAC TC	TTC CTT ATT GGG GTC ACC AC

Measurement of Nitric Oxide Levels

The total stable oxidation products of NO metabolism (NO_2/NO_3) of serum and HK2 cell homogenates were assessed using Griess reagent (Promega, Budapest, Hungary). Following manufacturer's directions 50 μL of the samples were incubated with 50-50 μL Griess reagent (part I: 1% sulphanilamide; part II: 0.1% naphthylethylene diamide dihydrochloride and 2% phosphoric acid) at RT. Ten minutes later the absorbance was measured at 540 nm using a Plate Chameleon V Fluorometer-Luminometer-Photometer reader (Hidex, Turku, Finland). Relative concentration was calculated on the basis of a sodium nitrite reference curve and was expressed as μM.

Detection of microRNA (miRNA) expression

Total RNA was extracted from the kidney using TRIzol Reagent (Invitrogen, Budapest, Hungary) according to the protocol provided by the manufacturer. Micro-RNA expression was evaluated and quantified using TaqMan probes (Applied Biosystems, Budapest, Hungary). First, complementary DNA (cDNA) was reverse-transcribed from 5-ng RNA samples using miRNA-specific primers (for miR-21, miR-17-5p, and U6 snRNA) as described in the manufacturer's protocol. Next, PCR products were amplified from the cDNA samples using the TaqMan Small RNA Assay together with the TaqMan Universal PCR Master Mix 2. All measurements were done in duplicates, and the miRNA expressions were normalized to U6 small nuclear RNA (snRNA).

Western Blot analysis

All reagents for PAGE and Western blot were purchased from Bio-Rad Hungary. Kidney samples were sonicated and re-suspended in lysis buffer. Protein concentration measurement was performed with a detergent-compatible protein assay kit. Samples were electrophoretically resolved on 7.5 %, 10 % or 12% polyacrylamide gels and transferred to nitrocellulose membranes. Membranes were stained with Ponceau S, then washed and blocked with 5 % non-fat dry milk. The membranes were incubated with antibodies specific for rat or human S1R (rat: #423300, Invitrogen, Budapest, Hungary; human: #sc-166392, Santa Cruz Biotechnology, Budapest, Hungary); peNOS (Ser1177) (#9571, Cell Signaling Technology, Budapest, Hungary), pAkt (Ser473) (#9271, Cell Signaling Technology, Budapest, Hungary) and nNOS (#sc-5302, Santa Cruz Biotechnology, Budapest, Hungary) respectively. After repeated washing the blots were incubated with the corresponding horseradish-peroxidase-conjugated secondary antibodies (#7074, goat anti-rabbit, Cell Signaling Technology, Budapest, Hungary; #sc2005, goat anti-mouse, Santa Cruz Biotechnology, Budapest, Hungary).

Bands of interest were detected using enhanced chemiluminescence detection (GE Healthcare Life Sciences, Budapest, Hungary) and quantified by densitometry (VersaDoc, Quantity One Analysis software; Bio-Rad Hungary) as integrated optical density (IOD) after subtraction of background. IOD was factored for Ponceau red staining to correct for any variations in total protein loading and for internal control. Protein abundance is represented as IOD/Ponceau S/Internal control.[54]

Cytometric bead array

All reagents and equipment for CBA were purchased from BD Biosciences (Budapest, Hungary). Saline-perfused kidney homogenates were measured for TNFα, IL-1α, IFN-γ, IL-4, and IL-10 peptide levels using appropriate rat CBA Flex Sets according to the manufacturer's protocol. Measurements have been performed using a FACSVerse flow cytometer and data analyzed using FCAP Array software.

Statistical analysis

Parametrical data are expressed as means ± SEM, while non-parametrical data as median ± range. Statistical analyzes were performed using Prism software (version 5.00; GraphPad Prism Software). Survival studies were assessed by Logrank test. Multiple comparisons and possible interactions were evaluated by one-way ANOVA followed by Bonferroni post-hoc test. For non-parametrical data the Kruskal–Wallis ANOVA on ranks followed by Fischer exacts test was used. *P* values of <0.05 were considered significant.

DOI:10.14753/SE.2017.2251

5. Results

5.1 S1R in the kidney

The peripheral expression, localization and function of S1R are under-discussed in the literature. S1R was first detected in the kidney in 1994 with radioimmunbinding assay (Hellewell 1994), but since then only one group investigated renal S1R (Bhuiyan 2010). However they only measured protein levels from whole kidney lysates, exact localization and subcellular distribution has not been discussed at all. According to the Protein Atlas of human kidney biopsies S1R shows no staining in glomeruli and moderate staining in tubules (online source: http://www.proteinatlas.org/ENSG00000147955-SIGMAR1/tissue/kidney).

Our group is the first to show evidence of S1R expression in different kidney regions. To gain an overview of the renal distribution of the receptor S1R-specific DAB staining was applied on rat kidney sections. S1R expression was most prominent in the renal cortex, but was also present in the medulla and papilla (*Figure 12/A*). Western blot measurement of S1R protein levels from homogenates of renal cortex, medulla and papilla confirmed these results (*Figure 12/B*). Next, co-staining with proximal tubular brush border-specific PAS and anti-S1R DAB revealed that S1R is definitely expressed in proximal tubules but not in glomeruli (*Figure 12/C*).

DOI:10.14753/SE.2017.2251

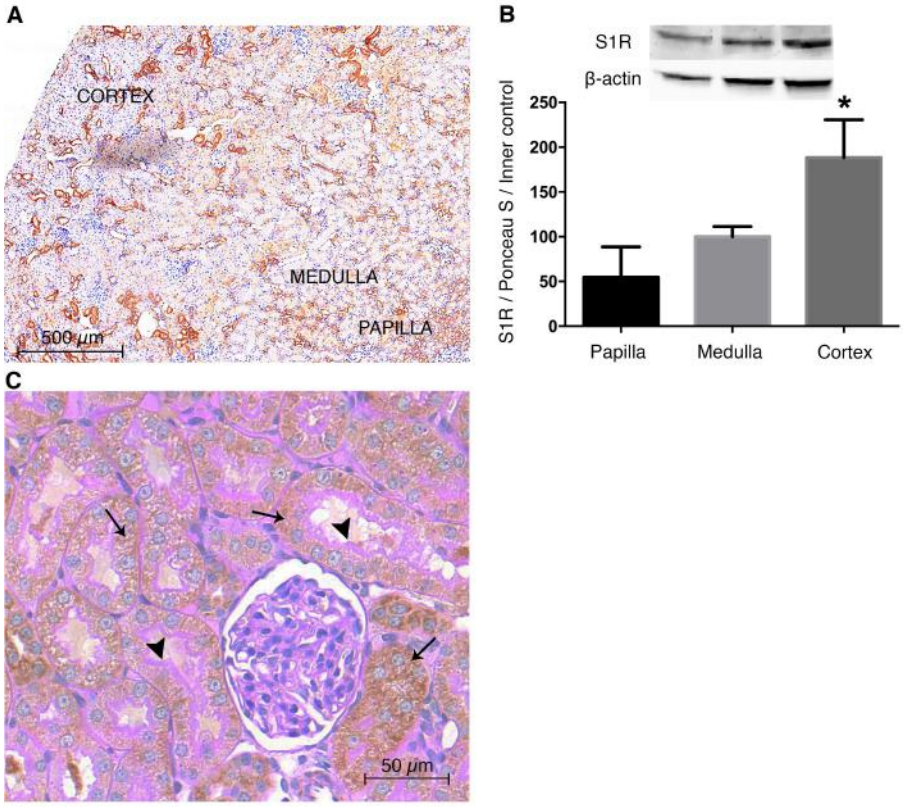

Figure 12. Sigma-1 receptor (S1R) is predominantly expressed in the renal cortex. (**A**) Representative rat kidney section stained with anti-S1R (brown; magnification: 6x DAB). Scale bar=500 μm. (**B**) Immunoblot for renal S1R. S1R is expressed in the papilla, medulla, and most prominently the cortex. Representative blots are shown. Bars indicate means ± SEMs; data were analyzed by one-way ANOVA with Bonferroni multiple comparison test. *P<0.05 *versus* papilla and medulla (n=6/group). (**C**) Representative kidney section developed with peroxidase anti-S1R (brown) and counterstained with PAS (pink). Thin black arrows show S1R in proximal tubules but not in glomerulus. Black arrowheads point to intact, PAS–stained brush borders of proximal tubules. Scale bar=50 μm.

To further clarify the subcellular localization of S1R fluorescent immunohistochemistry double staining with S1R and antibodies specific to different nephron segments was performed as well.

S1R was co-localized with proximal tubule-specific gamma-glutamyltransferase (GGT), but not with Na^+/K^+-ATP-ase in distal tubules, eNOS in glomeruli or neuronal NOS (nNOS) in the macula densa supporting the finding that S1R is mainly present in proximal tubules (*Figure 13*).

DOI:10.14753/SE.2017.2251

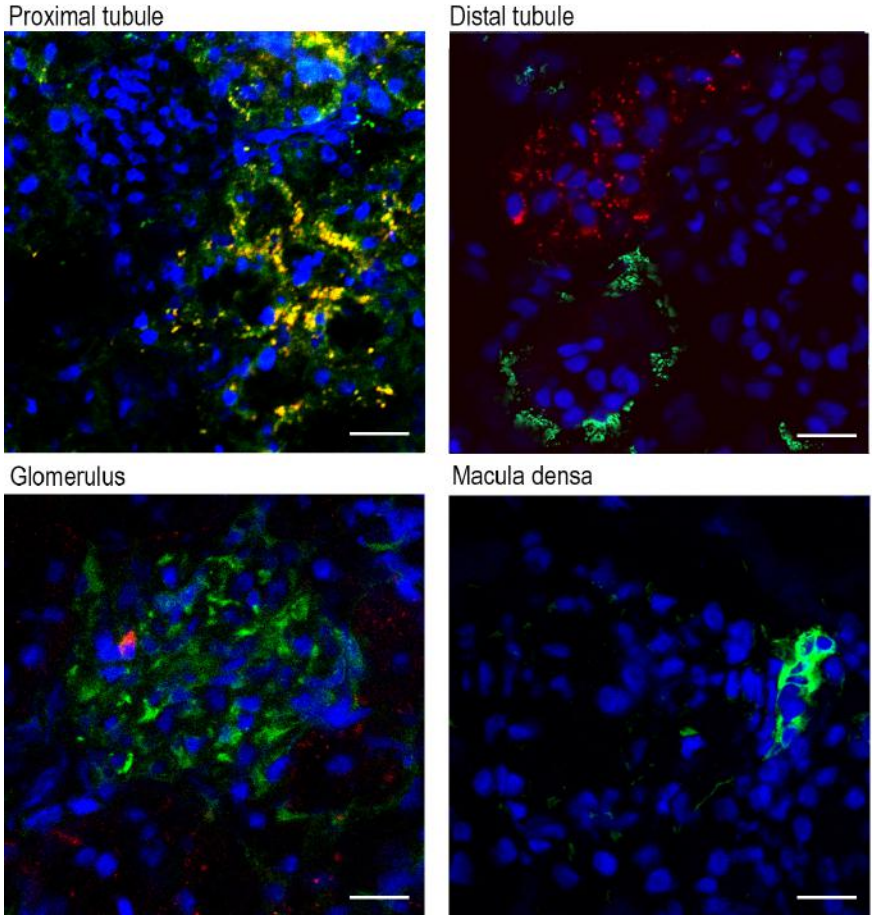

Figure 13. Localization of Sigma-1 receptor in different nephron segments. Representative fluorescent immunohistochemistry images stained for nuclei (blue), S1R (red) in all images. Green represents gamma-glutamyltransferase (GGT) in the proximal tubule, Na^+/K^+-ATPase in the distal tubule, endothelial nitric oxide synthase (eNOS) in the glomerulus or neuronal nitric oxide synthase (nNOS) in the macula densa. Scale bar=25 μm.

5.2 Dehydroepiandrosterone improves post-ischemic kidney function and ameliorates structural injury

After confirming the presence of S1R in the kidney our goal was to investigate the effect of S1R agonist treatment on renal IRI. Dehydroepiandrosterone (DHEA) is a highly abundant steroid hormone, which is also an endogenous agonist of S1R.

To determine the effect of S1R activation rats received only vehicle (ischemia/reperfusion (I/R)) or DHEA (I/R DHEA) pretreatment. In the first series of experiments post-ischemic survival was followed and compared to sham-operated controls (SHAM) for seven days. DHEA-pretreated rats survived longer than vehicle-

treated ones (median survival: 72 versus 36 hours, P<0.001). One third of DHEA-treated rats survived the seven-day period and recovered completely, while all vehicle-treated ones died within 75 hours (*Figure 14/A*).

Another series of animals were sacrificed after 24 hours of reperfusion to investigate the acute effects of IRI (T24 I/R and T24 I/R DHEA groups; resp.). Increased SCr and BUN in all treatment groups confirmed post-ischemic AKI (*Figure 14/B-C*). Intravital two-photon microscopy allowed us to measure changes of peritubular capillary diameters in live rats. Post-ischemic vasoconstriction was apparent (*Figure 14/D*) suggesting that the subsequent decline in renal blood flow could be a causative factor of renal functional and structural damage. DHEA pretreatment (T24 I/R DHEA) improved kidney function and prevented peritubular vasoconstriction *(Figure 14/B-D)*.

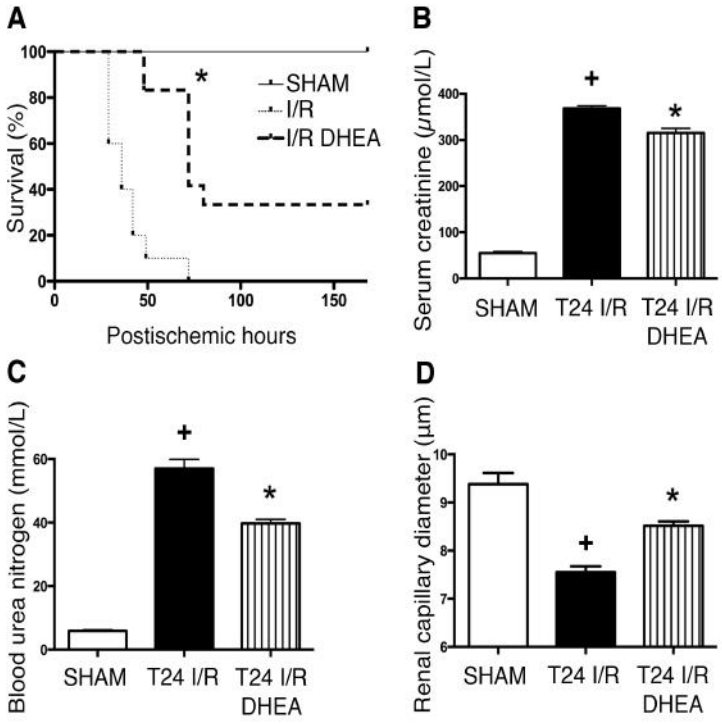

Figure 14. Dehydroepiandrosterone (DHEA) pretreatment is protective against renal ischemia/reperfusion injury. (**A**) Post-ischemic survival was followed for 7 days in rats pretreated with vehicle (I/R) or DHEA (I/R DHEA) 25 and 1 hour before the 50-minute ischemia. Log rank test (n=8/group). *P<0.001 *versus* ischemia/reperfusion (I/R). (**B**) Serum creatinine levels. *P<0.05 *versus* T24 I/R; +P<0.05 *versus* SHAM-operated (SHAM) (n=6/group). (**C**) Blood urea nitrogen levels of vehicle (T24 I/R) and DHEA (T24 I/R DHEA) -pretreated rats after 24 hours of reperfusion.

*P<0.05 *versus* T24 I/R (n=6/group); +P<0.05 *versus* SHAM (n=6/group). (**D**) Renal capillary diameters measured using intravital two–photon microscopy. Approximately 150 capillaries per animal. *P<0.05 versus T24 I/R (n=3/group); +P<0.05 versus SHAM (n=3/group). Bars indicate means ± SEMs, and data were analyzed by one-way ANOVA with Bonferroni multiple comparison test.

Histologic changes were consistent with functional decline: brush borders disappeared, the majority of tubules showed cell necrosis and extensive cast formation (*Figure 15/A-C*). DHEA pretreatment (T24 I/R DHEA) considerably reduced tubular necrosis and partly preserved brush borders *(Figure 15/A-D*).

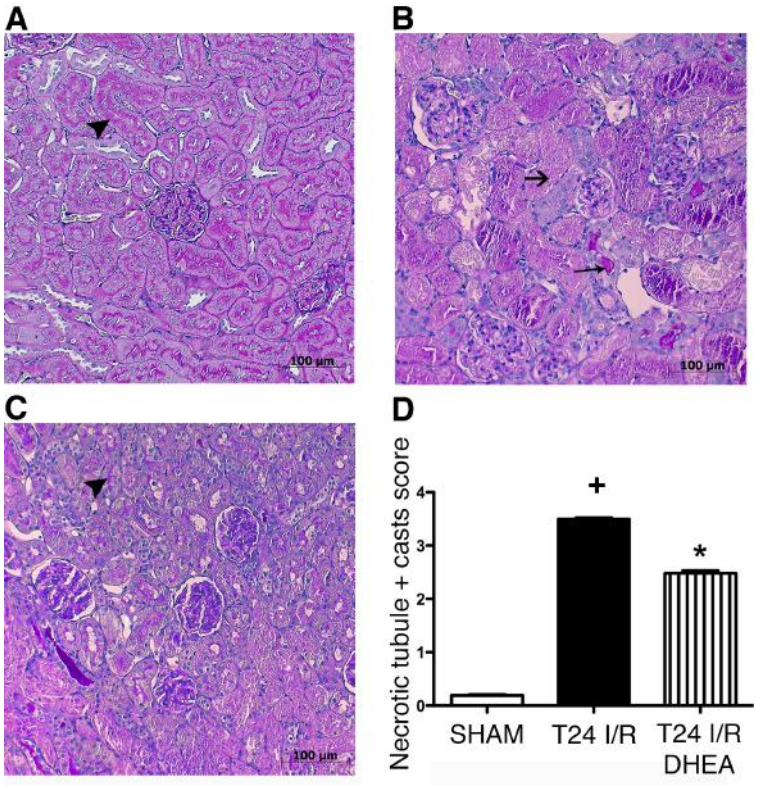

Figure 15. Dehydroepiandrosterone (DHEA) improves renal structure after ischemia/reperfusion injury (IRI). (**A–C**) Representative images of structural damage after IRI on PAS–stained kidney sections of (**A**) SHAM-operated (SHAM), (**B**) T24 ischemia/reperfusion (I/R), or (**C**) T24 I/R DHEA–pretreated rats. Black arrowheads points to intact brush border, long thin black arrow shows hyaline accumulation, and short black arrow shows necrotic tubule. Original magnification: 200x (**D**) Semi-quantitative evaluation of tubular injury on a zero to four scale. *P<0.05 *versus* T24 I/R (n=6/group); +P<0.05 *versus* SHAM (n=6/group). Bars indicate medians ± ranges, and data were analyzed by Kruskal–Wallis test with Dunn correction.

DOI:10.14753/SE.2017.2251

5.3 High affinity S1R agonist fluvoxamine is renoprotective following kidney IRI

On the basis of the first set of experiments our hypothesis was that S1R activation by DHEA is renoprotective in AKI by improving NO-mediated kidney perfusion. To substantiate the crucial role of S1R in IRI, in a second set of experiments rats were pretreated with fluvoxamine (FLU) that has much higher affinity to S1R than DHEA.[55]

Since FLU-treatment has not been studied in the kidney yet we performed pilot experiments (with 2 or 20 mg/bwkg) to determine the minimal effective dose, which is not toxic, but still exerts renoprotection. 20 mg/bwkg is comparable to the regular daily dosage of FLU used chronically in everyday clinical treatment (Morishita S 2003), while 2 mg/bwkg is ten-times less than the dosage used in humans.

To determine optimal timing in one series 20 mg/bwkg was given first 30 minutes prior the ischemic insult and then the dose was repeated right after the clip was removed, just at the beginning of reperfusion. All protocols successfully improved renal function; however 20 mg/bwkg and 40 mg/bwkg dosages were more effective in abating structural damage as well. The highest dosage did not cause additional improvement, therefore 20 mg/bwkg dosage was used further on (*Figure 16*).

A group of rats received selective S1R antagonist N, N-dipropyl-2-[4-methoxy-3-(2-phenylethoxy)-phenyl]-ethylaminemonohydrochloride (NE100) together with FLU to verify the role of S1R in investigated processes. NE100 dosage of 1 mg/bwkg was based on literary data.[56]

DOI:10.14753/SE.2017.2251

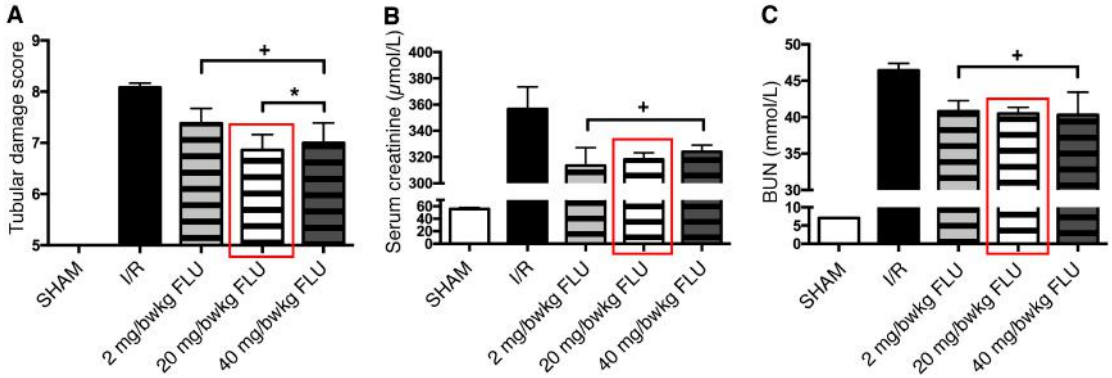

Figure 16. The effect of different dosages of fluvoxamine (FLU) on (**A**) tubular damage, (**B**) serum creatinine and (**C**) Blood urea nitrogen (BUN) levels after ischemia/reperfusion injury. +P<0.05 versus ischemia/reperfusion (I/R), *P<0.05 versus 2 mg/bwkg FLU (n=6/group). SHAM-operated (SHAM). Bars indicate means ± SEMs, and data were analyzed by one-way ANOVA with Bonferroni multiple comparison test. The final dose is marked with red.

5.3.1 FLU pretreatment improves survival after sub-lethal IRI

After determining the 20 mg/bwkg as the minimal effective dose, in the first series of experiments the effect of FLU was tested on post-ischemic survival as the most relevant primary end-point.

FLU-treated rats (I/R F) survived longer than vehicle (I/R) or FLU+NE100 (I/R FN)-treated ones (median survival: 67 *versus* 36 and 49 hours respectively, P<0.001). One third of I/R F rats completely recovered from the ischemic insult, while all I/R and I/R FN rats died within 70 hours (*Figure 17*).

DOI:10.14753/SE.2017.2251

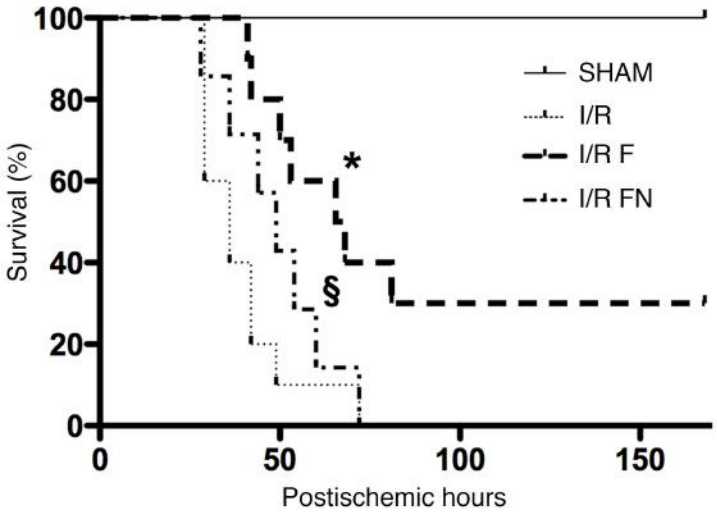

Figure 17. Fluvoxamine (FLU; F) pretreatment improves post-ischemic survival. Rats were pretreated with isotonic saline ischemia/reperfusion (I/R), FLU (I/R F), or FLU and NE100 (I/R FN) 30 minutes before the 50-minute ischemia. *P<0.001 *versus* I/R; §P<0.001 *versus* I/R F. Post-ischemic survival was followed for 7 days. Log rank test (n=8/group).

5.3.2 FLU is protective against renal IRI-induced AKI

Beside SCr and BUN, serum AST is also acknowledged recently as a marker of ischemia induced renal tubular damage. All these three parameters were less elevated in FLU-treated rats after 24 hours of reperfusion (T24 I/R F) and the improvement was neutralized by NE100 (T24 I/R FN) suggesting that S1R agonism successfully diminishes acute renal injury. All functional parameters returned to normal level by 168 hours in FLU-treated survivors (*Figure 18/A-C*).

Since SCr, BUN and AST are widely used, but not specific and higly sensitive markers of AKI, we also measured other biormarkers to further prove the protective effect of FLU. HIF-1α is a known mediator of cell protection and epithelium recovery after IRI (Conde E 2012). Hif-1α mRNA expression increased as soon as 2 hours after ischemia (T2 I/R), especially in FLU-treated rats (T2 I/R F) (Figure 18/D). By T24 the difference was disappeared suggesting the HIF-1 alfa shows a quick response after IRI.

NGAL is an indicator of distal tubular injury that correlates with the severity of renal impairment (Bolignano D 2008). However Ngal mRNA expression was robustly increased after 24 hours of reperfusion (T24 I/R) in all groups, but the increase was milder in FLU-treated rats (Figure 18/E).

KIM-1 is a specific marker of tubular injury.[18] In our study Kim-1 was upregulated in the post-ischemic kidney (T24 I/R). Increased Kim-1 mRNA expression was ameliorated by FLU (T24 I/R F) (Figure 18/F) also suggesting milder proximal tubular damage.

Antagonizing FLU with NE100 diminished functional improvement and suppressed all parameters reflecting milder tubular damage.

MicroRNAs (miRNAs) are short, double-stranded RNAs that can regulate post-transcriptional gene-expression through multiple mechanisms.[57] MicroRNA-21 (miR21) and microRNA-17-5p (miR17-5p) are part of the regulatory network that can determine the outcome of IRI.[58] Others demonstrated that mir21 is involved in the renoprotective effect of ischemic preconditioning.[59] In our experiments both miR21 and miR17-5p expression was elevated after IRI, but no difference was detected between treatment groups (Figure 18/G-H), therefore miRNAs have not been tested further on.

DOI:10.14753/SE.2017.2251

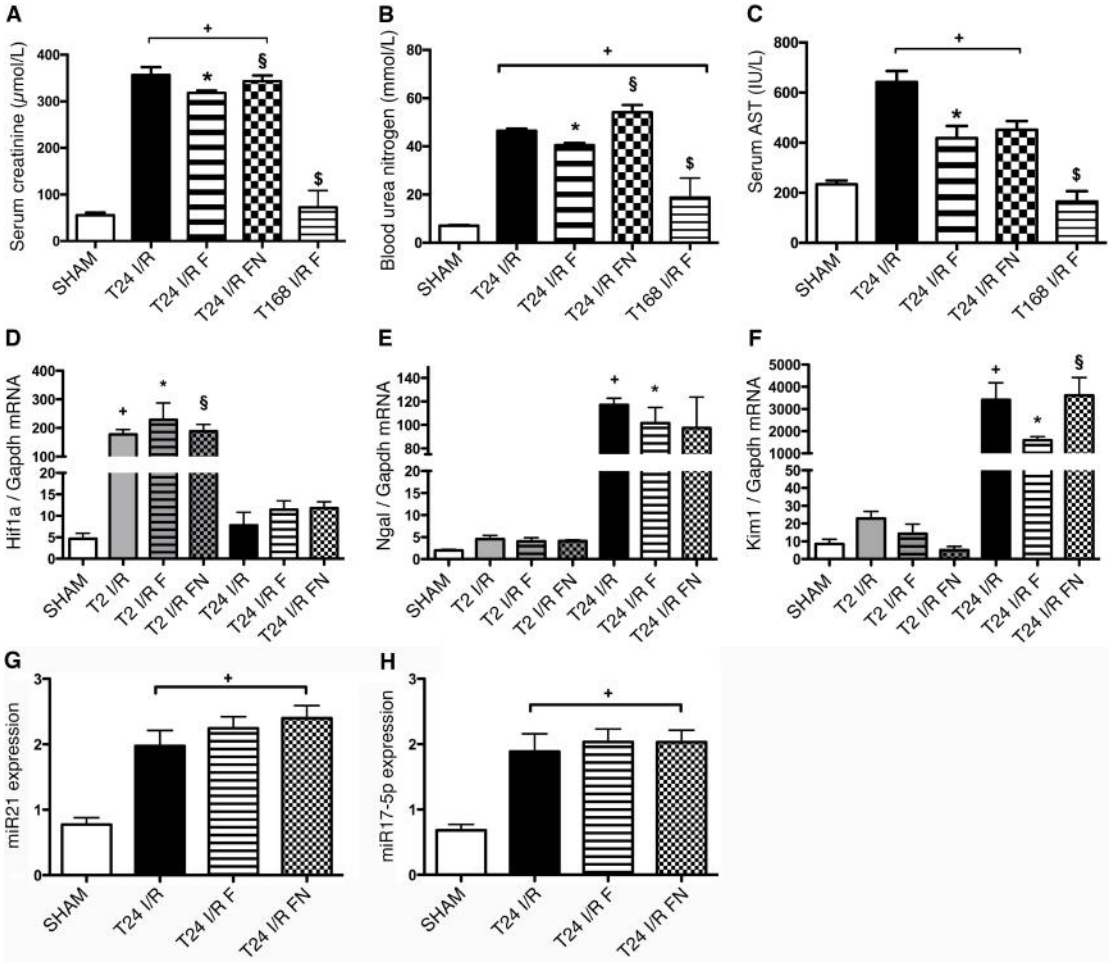

Figure 18. Fluvoxamine (FLU; F) pretreatment is protective against renal ischemia/reperfusion injury. (**A**) Serum creatinine levels after 24 hours of reperfusion in FLU-treated (T24 ischemia/reperfusion (I/R) F) and FLU + NE100 treated (T24 I/R FN) rats and after 168 hours of reperfusion in FLU-treated (T168 I/R F) rats. *P<0.05 *versus* T24 I/R; +P<0.05 *versus* SHAM; §P<0.05 *versus* T24 I/R F; $P<0.05 *versus* T24 I/R (n=8/group). (**B**) Blood urea nitrogen (BUN) levels. *P<0.05 *versus* T24 I/R; +P<0.05 *versus* SHAM-operated (SHAM); §P<0.05 *versus* T24 I/R F; $P<0.05 versus T24 I/R (n=8/group). (**C**) Serum aspartate transaminase (AST) levels. *P<0.05 *versus* T24 I/R; +P<0.05 *versus* SHAM; $P<0.05 versus T24 I/R (n=8/group). (**D**) Renal hypoxia inducible factor alpha (Hif-1a) mRNA expression normalized to glyceraldehyde-3-phosphate dehydrogenase (Gapdh) expression. *P<0.05 versus T24 I/R; +P, 0.05 *versus* SHAM; §P<0.05 *versus* T24 I/R F (n=6/group). (**E**) Renal neutrophil gelatinase-associated lipocalin (Ngal) mRNA expression normalized to Gapdh expression. *P<0.05 *versus* T24 I/R; +P<0.05 *versus* SHAM (n=6/group). (**F**) Renal kidney injury molecule 1 (Kim-1) mRNA expression normalized to Gapdh expression. *P<0.05 *versus* T24 I/R; +P<0.05 *versus* SHAM; §P<0.05 *versus* T24 I/R F (n=6/group). (**G**) Renal micro RNA 21 (miR21) and (**H**) Micro RNA 17-5p (miR17-5p) mRNA expression normalized against U6 small nuclear RNA. +P<0.05 *versus* SHAM; (n=6/group). Bars indicate means ± SEMs, and data were analyzed by one way ANOVA with Bonferroni multiple comparison test.

DOI:10.14753/SE.2017.2251

5.3.3 FLU ameliorates IRI-induced inflammation

Inflammation caused by both the innate and adaptive immune response is an important contributor to ischemic injury. Elevated serum white blood cell count and increased renal inflammatory cytokine levels were indicative of IRI-induced systemic inflammation. White blood cell count was reduced by 30% in FLU-treated rats (T24 I/R F: 4.366 ± 0.523 x 10^9/L versus T24 I/R: 6.236 ± 0.763 x 10^9/L and T24 I/R FN: 6.216 ± 0.583 x 10^9/L; $P<0.05$). Pro-inflammatory IL-1α and IL-6 were reduced by 70% and 80% respectively, IL-4 remained unchanged. Anti-inflammatory cytokine IL-10 was increased by 15% (*Table 3*).

Table 3. Renal cytokine expression. Cytokine levels were measured from renal tissue homogenates by cytometric bead array. Kidney tissues were collected after 24 hours of reperfusion from vehicle (T24 ischemia/reperfusion (I/R)), Fluvoxamine (FLU; F) (T24 I/R F), or FLU + NE100 (T24 I/R FN) –treated rats. *P<0.05 *versus* T24 I/R; +P<0.05 *versus* SHAM-operated (SHAM); §P<0.05 *versus* T24 I/R F (n=6/group). Values indicate means ± SEMs, and data were analyzed by one-way ANOVA with Bonferroni multiple comparison test. Interleukin 1 alpha (IL-1α); interleukin 6 (IL-6); tumor necrosis factor alpha (TNFα); interleukin 10 (IL-10); interleukin 4 (IL-4).

	SHAM	T24 I/R	T24 I/R F	T24 I/R FN
IL-1α (pg/mL)	0.17±0.16	58.7±16.3 $^{+}$	16.1±4.82 *	11.4±6.33
IL-6 (pg/mL)	0.00±0.00	141±14.9 $^{+}$	29.6±3.36 *	32.4±10.4
TNF-α (pg/mL)	106±2.07	138±16.4	149±8.67	135±8.76
IL-10 (pg/mL)	75.6±1.61	98.0±5.87 $^{+}$	113±7.95 *	86.6±2.54 §
IL-4 (pg/mL)	8.74±1.11	9.88±0.80	10.6±0.11	10.1±0.15

5.3.4 FLU ameliorates renal structural damage

IRI-induced histologic injury was assessed on PAS-stained kidney sections and graded on a semi-quantitative zero to four scale by two pathologists in a blinded fashion (please see the Methods section for details). Brush borders in the healthy tubules of SHAM-operated animals were stained dark purple as shown by black arrowheads (*Figure 19/A*). Contrarily, severe structural damage was apparent in ischemic kidneys: leukocyte infiltration, hyaline accumulation (long thin arrows) and necrotic tubules

(short, black arrows) were prevalent as well as loss of brush border indicating loss of reabsorption capacity (*Figure 19/D-E*). On the other hand tubular damage and cell necrosis were only moderate, and brush borders were intact in several regions of FLU-treated kidneys after 24 hours of reperfusion (*Figure 19/B*). Tubular damage was nullified in rats that survived the 168 hours of post-ischemic period: cell necrosis was scarce and brush borders were recovered almost everywhere (*Figure 19/C*).

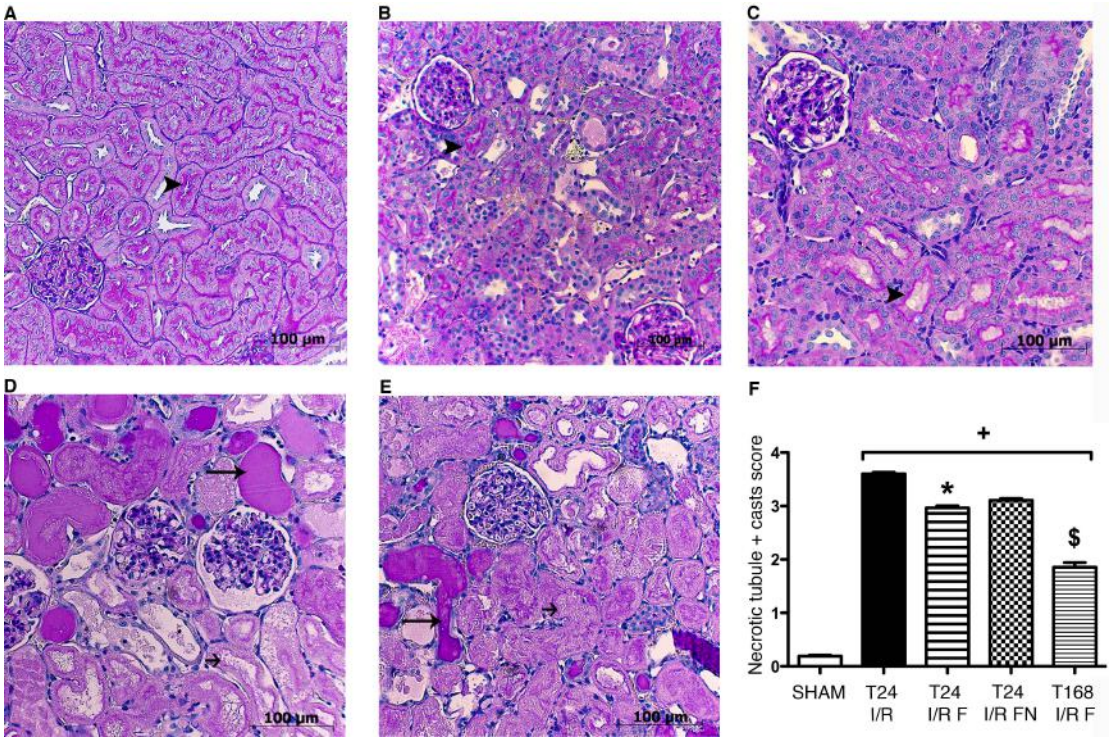

Figure 19. Fluvoxamine (FLU; F) ameliorates renal structural damage. (**A–E**) Representative PAS–stained kidney sections of (**A**) SHAM-operated (SHAM), (**B**) after 24 hours of reperfusion in FLU-treated (T24 ischemia/reperfusion (I/R) F), (**C**) T168 I/R F, (**D**) T24 I/R, and (**E**) T24 I/R FLU+NE100 (FN) rats. Black arrowheads point to intact brush border, long thin black arrows show hyaline accumulation and short black arrows show necrotic tubules. Original magnification: 200x. Scale bar=100 µm. (**F**) Semi-quantitative evaluation of tubular injury on a zero to four scale. *P<0.05 *versus* T24 I/R; +P<0.05 *versus* SHAM; $P<0.05 versus T24 I/R (n=6/group). Bars indicate medians ± ranges and data were analyzed by Kruskal–Wallis test with Dunn correction.

Intravital two– photon microscopic imaging revealed similar tubular structure. Brush borders were intact (white arrows, stained orange by Texas Red dye) in several areas in T24 I/R F rats indicating that FLU preserved renal function, whereas no brush border was visible in the cortex of either T24 I/R or T24 I/R FN animals. In the T24 I/R

F group, nuclei were intact (thin, white arrows, stained blue by Hoechst 33342), and necrotic cast formation was minimal as opposed to severe cell necrosis and cast formation in T24 I/R and T24 I/R FN groups (two-tailed white arrows) (*Figure 20*).

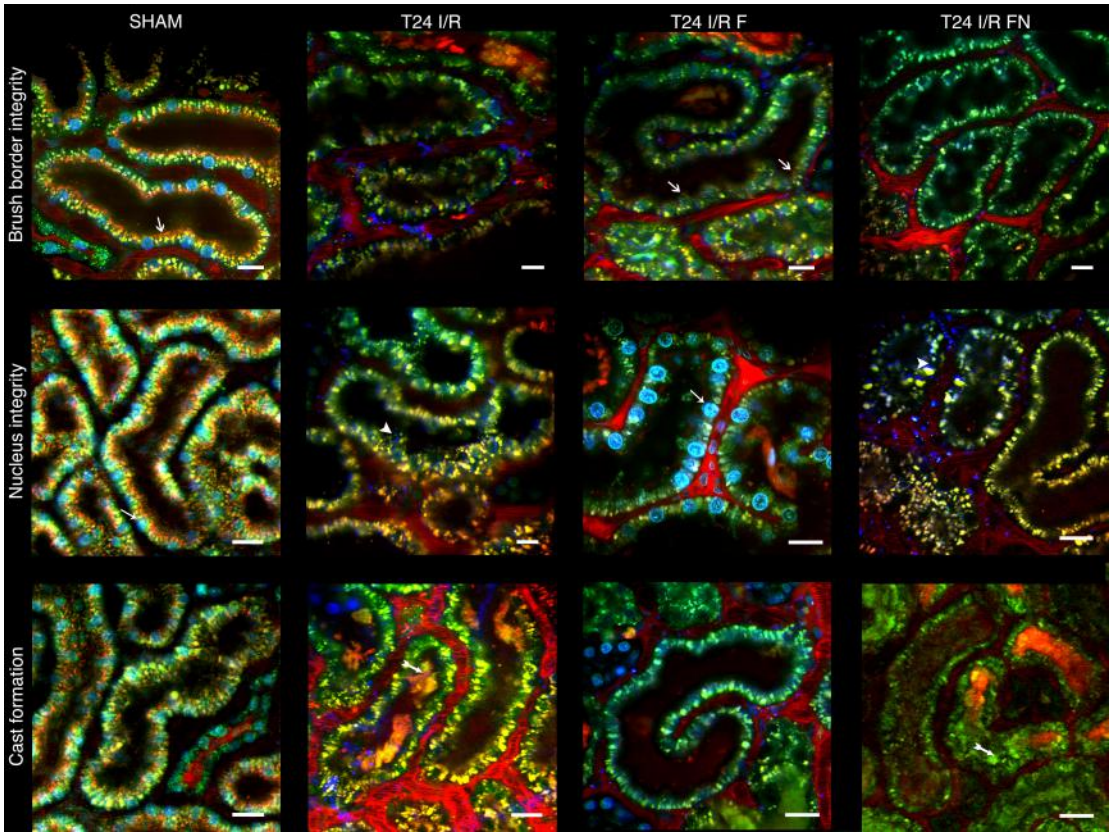

Figure 20. Fluvoxamine (FLU; F) ameliorates post-ischemic renal cortical damage. Representative intravital two–photon images of the rat kidney after 24 hours of reperfusion (T24 ischemia/reperfusion (I/R)) with FLU (T24 I/R F) or FLU and NE100 (T24 I/R FN) pretreatment. Brush border integrity is shown in top panel. White arrows show orange–colored Texas Red staining of intact brush borders. Nucleus integrity is shown in middle panel. Nuclei stained with Hoechst 33342 appear in blue. Thin white arrows point to intact nuclei. White arrowheads show severely damaged, disintegrated nuclei. In bottom row two–tailed white arrows show extensive necrotic cast formation (n=3/group). Scale bar=25 μm.

DOI:10.14753/SE.2017.2251

5.4 S1R in the ischemic kidney

According to the literature in the brain and CNS S1R is localized in the mitochondria-associated ER membrane and upon stimulation it translocates to the cytosol and plasma membrane. However no data is available concerning sub-cellular localization in peripheral tissues.

Anti-S1R DAB and immunofluorescent staining was performed on kidney slides to evaluate localization and abundance of the receptor after IRI. Anti-S1R staining was more intense after IRI, and was most prominent after FLU treatment suggesting higher abundance in this group (*Figure 21/A-D*). Elevated S1R protein levels verified these findings (*Figure 21/I*). Similarly to previous results S1R was not detectable in glomeruli.

High-magnification immunofluorescent images revealed a predominantly perinuclear ring-like expression pattern of S1R in the proximal tubular epithelium of SHAMs. After I/R and FLU treatment S1R was detected in the whole cytoplasm as well as in nuclei (*Figure 21/E-H*).

DOI:10.14753/SE.2017.2251

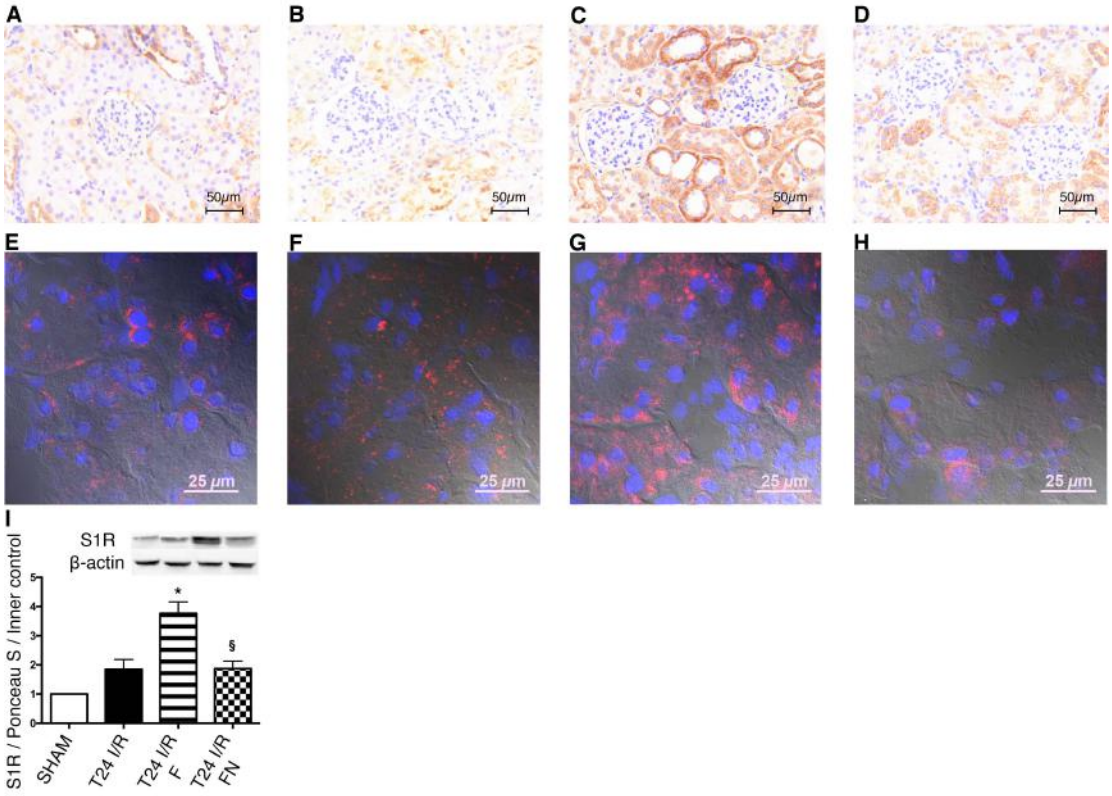

Figure 21. Sigma-1 receptor (S1R) translocation after renal ischemia/reperfusion (I/R) and fluvoxamine (FLU; F) treatment. (**A–D**) Representative anti–S1R DAB–stained kidney sections of (**A**) SHAM-operated (SHAM), (**B**) T24 I/R, (**C**) T24 I/R F, and (**D**) T24 I/R FLU+NE100 (FN) rats. Scale bar=50 μm. (**E–H**) Representative immunohistochemical double–stained kidney sections for nuclei (blue) and S1R (red) of (**E**) SHAM, (**F**) T24 I/R, (**G**) T24 I/R F, and (**H**) T24 I/R FN rats. Scale bar=25 μm. (**I**) Immunoblot for renal S1R protein expression. Representative blots are shown. *P<0.05 *versus* T24 I/R; §P<0.05 *versus* T24 I/R F (n=5–7/group). Bars indicate means ± SEMs, and data were analyzed by one-way ANOVA with Bonferroni multiple comparison test.

5.5 The role of S1R in proximal tubular cells

HK2 human proximal tubular cells were used to examine the role of S1R specifically in these cells and in an *in vitro* model of oxidative stress. Oxidative stress was induced with 400 μM H_2O_2 treatment for 30 min. According to the MTT cell - viability and proliferation assay this protocol caused a rather robust oxidative insult, but the number of viable cells was still enough to perform the experiments (*Figure 10/B in the Methods section*). The non-toxic dosages of FLU and NE100 were also determined using MTT assay (*Figure 10/A in the Methods section*).

To our best knowledge our group is the first to show that S1R is expressed in human proximal tubular cells. S1R abundance remained unchanged after FLU or H_2O_2 treatment; however localization was different under normal conditions and oxidative stress. The receptor showed perinuclear localization in control cells (*Figure 22/A*), but was detected everywhere in the cytosol and also in nuclei after H_2O_2 or FLU (F) treatment (*Figure 22/A-D*). Subcellular fractionation followed by Western blot confirmed that although the abundance of S1R remains unaltered, the receptor translocates from the ER to the cytosol and/or nucleus upon stimulation and might activate signaling pathways (*Figure 22/E-G*).

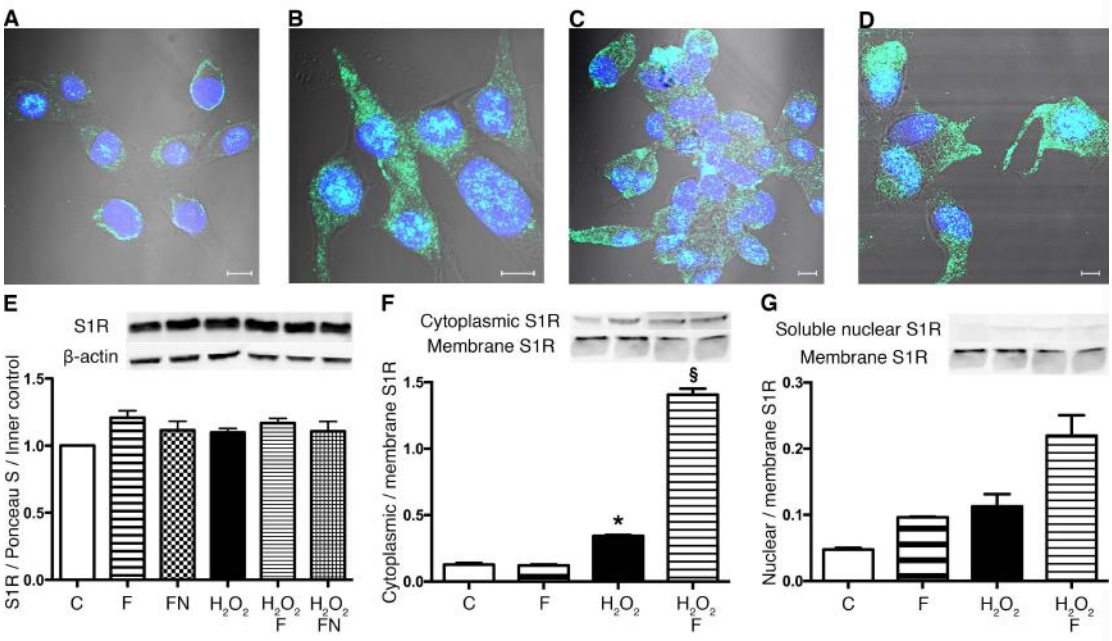

Figure 22. Sigma-1 receptor (S1R) translocation to the cytoplasm and nucleus after ligand stimulation and oxidative stress. (**A–D**) Representative images of fluorescent immunohistochemistry double staining of (**A**) control (C), (**B**) hydrogen-peroxide (H_2O_2) (**C**) Fluvoxamine (FLU; F), and (**D**) H_2O_2 and FLU–treated human kidney-2 cell line (HK2). Nuclei (blue) and anti-S1R (green). Scale bar=5 μm. (**E**) Immunoblot for S1R protein in HK2 cells after FLU (F), FLU + NE100 (FN), H2O2, H2O2 + FLU (H2O2 F), and H2O2 + FLU + NE100 (H2O2 FN) treatment compared with untreated control (C) cells (n=6/group). (**F**) Cytoplasmic-to-membrane ratio of S1R in HK2 cells after various treatments. Representative blots are shown. *P<0.05 *versus* C; §P<0.05 *versus* H_2O_2 (n=5/group). (**G**) Nuclear-to-membrane ratio of S1R in HK2 cells after various treatments. Representative blots are shown (n=5/group). Bars indicate means ± SEMs and data were analyzed by one-way ANOVA with Bonferroni multiple comparison test.

DOI:10.14753/SE.2017.2251

5.5.1 FLU induces S1R-mediated NO production in HK2 cells

A possible signaling pathway by which vasodilatative NO could be produced is the Akt-eNOS pathway. First, we wanted to assess whether this pathway is induced by S1R activation in HK2 cells.

FLU increased phospho-eNOS (peNOS, Ser1177; the active form of the eNOS enzyme) protein levels in HK2 cells both under normal conditions (group: F) and oxidative stress (H_2O_2 F). The S1R antagonist NE100 blocked this increase (FN; H_2O_2 FN) (*Figure 23/A*). nNOS was not detectable in proximal tubular cells in any of the treatment groups (data not shown).

The direct role of S1R in eNOS production was further proven by siRNA knockdown of the receptor. siRNAs are man-made short RNA molecules which interfere with the expression of specific genes resulting in no translation. Parallel with successful S1R knockdown (*Figure 10 in the Methods section*) peNOS protein was also lower compared to scrambled siRNA-treated negative control cells. Decreased peNOS production in FLU-treated S1R knockdown cells (S1R siRNA F) verified the regulatory role of S1R in peNOS expression (*Figure 23/B*).

To confirm the role of Akt in FLU-induced NOS activation and NO production, various Akt inhibitors were used to suppress both the upstream (Akt IV) and downstream (Akt VIII, which inhibits the phosphorylation of all Akt isoenzymes) activation and/or phosphorylation of Akt. Inhibition of Akt suppressed peNOS and subsequently NO production in FLU-treated cells (*Figure 23/C-D*).

DOI:10.14753/SE.2017.2251

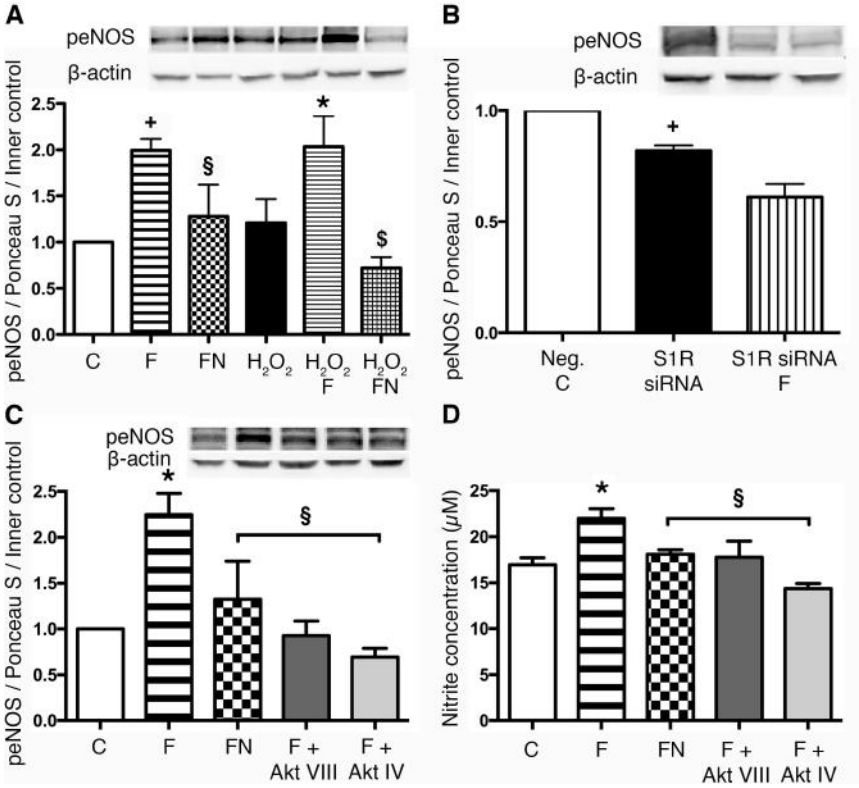

Figure 23. Sigma-1 receptor (S1R) induces protein kinase B (Akt)-mediated phspho-endothelial nitric oxide synthase (peNOS) and nitrite production in human kidney-2 cell line (HK2). (**A**) Immunoblot for peNOS (Ser1177) protein level of HK2 cells after various treatments compared with control (C) cells. *P<0.05 *versus* hydrogen-peroxide (H_2O_2); +P<0.05 *versus* C; §P<0.05 *versus* fluvoxamine (FLU; F); $P<0.05 *versus* H_2O_2 F (n=6/group). Immunoblot (**B**) peNOS expression of S1R knockdown HK2 cells compared with scrambled siRNA–treated negative control (Neg. C) cells. Representative blots are shown. +P<0.05 *versus* Neg.C (n=6/group). (**C**) Immunoblot for peNOS protein level of HK2 cells after FLU (F), FLU + NE100 (FN), FLU + AktVIII inhibitor (F + Akt VIII) and FLU + AktIV inhibitor (F + Akt IV) treatment. *P<0.05 *versus* C; §P<0.05 *versus* F (n=6/group). (**D**) Nitrite production of HK2 cells after FLU and various inhibitor treatments. *P<0.05 *versus* C (n=6/group); §P<0.05 *versus* F (n=6/group). Bars indicate means ± SEMs and data were analyzed by one-way ANOVA with Bonferroni multiple comparison test.

DOI:10.14753/SE.2017.2251

5.6 FLU induces S1R-mediated vasodilatative NO production in the rat kidney

5.6.1 S1R-mediated renal vasoregulation in SHAM-operated rats

Once the role of S1R in NO production was characterized under *in vitro* circumstances the next step was to investigate the vasoregulatory effect of FLU in the rat kidney. Intravital two-photon microscopy was used to measure peritubular capillary diameters in SHAM-operated rats after 30 minutes of FLU treatment. Parallel with increased peNOS (*Figure 24/E*) and NO production (*Figure 24/C*) FLU pretreatment (T30’ F) caused peritubular capillary dilatation. The addition of NE100 (T30’ FN), nonselective NOS blocker N-ω-Nitro-L-arginine methyl ester (T30’ F + NAME), selective nNOS blocker 7-Nitroindazole (T30’ F + 7-NI), and most prominently selective eNOS blocker N -5-(1-Iminoethyl)-L-ornithine dihydrochloride (T30’ F+NIO) inhibited FLU-mediated vasodilation (*Figure 24/A*).

5.6.2 S1R-mediated vasodilatation in the post-ischemic kidney

Peritubular capillaries showed significant vasoconstriction after 24 hours of reperfusion: diameters were ~2 μm less in average compared to SHAM-operated rats. Parallel with increased nitrite production (*Figure 24/C*) capillary dilatation was significant in FLU-treated rats after 24 hours of reperfusion (T24 I/R F) as well, which was diminished by NE100 (T24 I/R FN) or various NOS inhibitors supporting that the vasodilative effect of FLU is S1R-mediated and NOS-dependent (*Figure 24/B*).

DOI:10.14753/SE.2017.2251

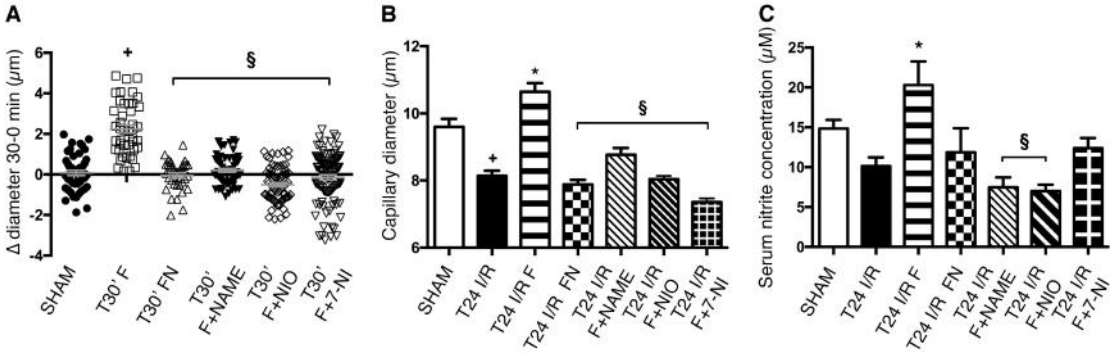

Figure 24. Fluvoxamine (FLU; F) induces sigma-1 receptor (S1R)–mediated nitric oxide synthase (NOS) production and vasodilation in the rat kidney. (**A**) Changes in capillary diameters 30 minutes after FLU (T30' F), FLU + NE100 (T30' FN), FLU + nonselective NOS blocker N-v-Nitro-L-arginine methyl ester (T30' F + NAME), FLU + selective endothelial nitric oxide synthase (eNOS) blocker N-5-(1-Iminoethyl)-L-ornithine dihydrochloride (F + NIO), and FLU + selective neuronal nitric oxide synthase (nNOS) blocker 7-Nitroindazole (F + 7-NI) treatment in SHAM-operated (SHAM) rats. Approximately 150 capillaries per animal. +P<0.05 *versus* SHAM-operated; §P<0.05 *versus* T30' F (n=3/group). (**B**) Capillary diameters after 24 hours of reperfusion. Approximately 150 capillaries per animal. *P<0.05 *versus* T24 ischemia/reperfusion (I/R); +P<0.05 *versus* SHAM; §P<0.05 *versus* T24 I/R F (n=3/group). (**C**) Serum nitrite concentration of rats after 24 hours of reperfusion. *P<0.05 *versus* T24 I/R; §P<0.05 *versus* T24 I/R F (n=6/group). Bars indicate means ± SEMs, and data were analyzed by one-way ANOVA with Bonferroni multiple comparison test.

5.6.3 The S1R - Akt - NOS signaling pathway in the kidney

S1R, pAkt (Ser473), peNOS (Ser1177) and nNOS protein levels were measured 30 minutes after treatment in SHAM-operated rats and also after 24 hours of reperfusion to evaluate the effect of FLU on the S1R signaling pathway. FLU increased pAkt and peNOS protein abundance as soon as 30 minutes after treatment, whereas S1R and nNOS remained unchanged (*Figure 25/A-D*). On the other hand after 24 hours of reperfusion all measured proteins were increased especially in FLU-treated rats (T24 I/R F) (*Figure 25/A-D*). These results indicate that S1R signaling is instantly activated by FLU and is rapidly followed by peNOS production, but nNOS generation only increases later during reperfusion (*Figure 25/C-D*). As a result of increased NOS abundance NO production was also considerably increased contributing to vasodilatation in the post-ischemic kidney (*Figure 24/C*).

DOI:10.14753/SE.2017.2251

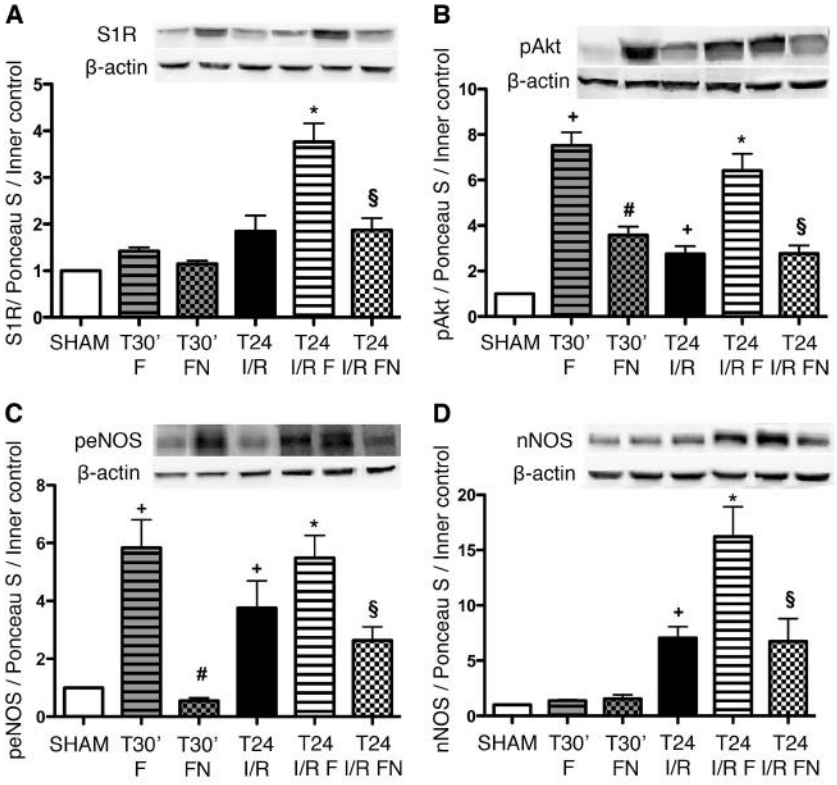

Figure 25. Sigma-1 receptor (S1R) signaling pathway in the kideny. Immunoblot for renal (**A**) S1R, (**B**) phospho - protein kinase B (pAkt) (Ser473), (**C**) phospho-endothelial nitric oxide synthase (peNOS) (Ser1177), and (**D**) phospho-neuronal nitric oxide synthase (nNOS) expression in fluvoxamine (FLU, F) (T30' F) and FLU + NE100 (T30' FN) –treated SHAM–operated (SHAM) rats and after 24 hours of ischemia/reperfusion (I/R) injury . Representative blots are shown. *P<0.05 *versus* T24 I/R; +P<0.05 *versus* SHAM; #P<0.05 *versus* T30' I/R F; §P<0.05 *versus* T24 I/R F (n=5–7/group). Bars indicate means ± SEMs, and data were analyzed by one-way ANOVA with Bonferroni multiple comparison test.

5.7 The effect of FLU-treatment on the transplanted kidney

To evaluate the effect of FLU in a rat model comparable to the clinical setting kidneys were autotransplanted with 2 hours of cold ischemia. FLU was added to the perfusion solution in which kidneys were kept during cold ischemia and rats were sacrificed 24 hours after the KTx procedure.

DOI:10.14753/SE.2017.2251

5.7.1 FLU improves kidney function after transplantation

Kidney function was substantially improved in FLU-treated rats as shown by decreased SCr and AST levels (*Figure 26/A-C*), however BUN was not decreased at this early time point yet. Early markers of kidney injury NGAL, KIM-1 and MCP-1 were also significantly less elevated in FLU-treated kidneys (*Figure 26/D-F*).

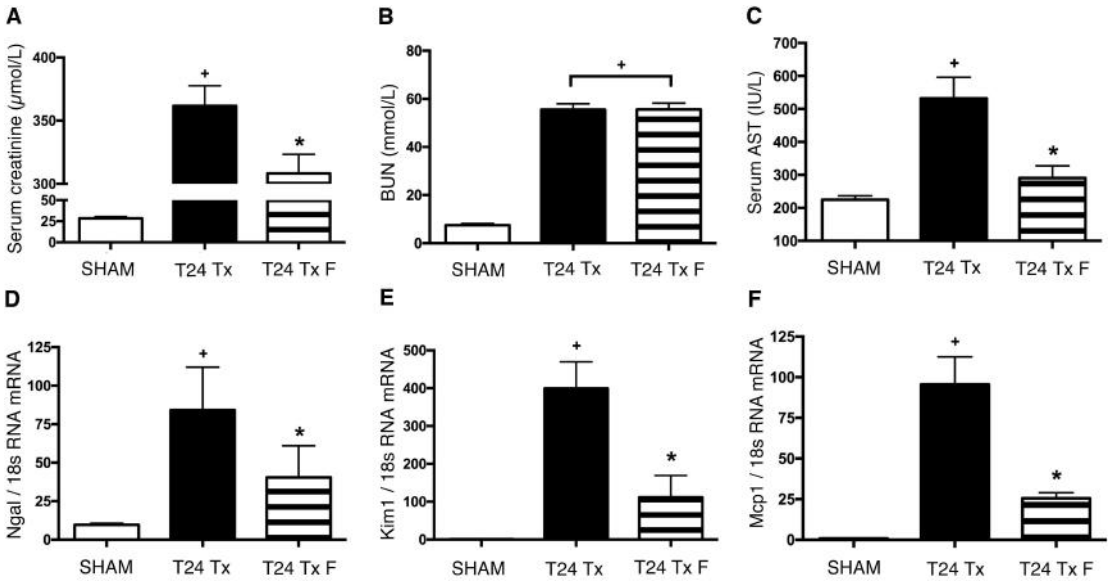

Figure 26. Fluvoxamine (FLU; F) ameliorates post-transplantational kidney damage. (**A**) Serum creatinine levels 24 hours after kidney transplantation in vehicle (T24 Tx) and FLU-treated (T24 Tx F) rats. *P<0.05 *versus* T24 Tx; +P<0.05 *versus* SHAM-operated (SHAM); (n=8/group). (**B**) Blood urea nitrogen (BUN) levels. *P<0.05 *versus* T24 Tx; +P<0.05 *versus* SHAM; (n=8/group). (**C**) Serum aspartate transaminase (AST) levels. *P<0.05 *versus* T24 Tx; +P<0.05 *versus* SHAM; (n=8/group). (**D**) Renal neutrophil gelatinase-associated lipocalin (Ngal) mRNA expression normalized to 18s RNA expression. *P<0.05 versus T24 Tx; +P.0.05 *versus* SHAM; (n=8/group). (**E**) Renal kidney injury molecule 1 (Kim-1) mRNA expression normalized to 18s RNA expression. *P<0.05 *versus* T24 Tx; +P<0.05 *versus* SHAM (n=8/group). (**F**) Renal monocyte chemoattractant protein 1 (Mcp-1) mRNA expression normalized to 18s RNA expression. *P<0.05 *versus* T24 Tx; +P<0.05 *versus* SHAM; (n=8/group). Bars indicate means ± SEMs, and data were analyzed by one-way ANOVA with Bonferroni multiple comparison test.

DOI:10.14753/SE.2017.2251

5.7.2 FLU improves kidney structure after transplantation

Histologic evaluation after KTx was performed on PAS-stained kidney sections. Severe tubular and glomerular injury was observed in vehicle-treated rats (CP + T24 Tx). Glomeruli were collapsed, their structure was damaged and degraded. Excessive signs of necrosis and picnotic nuclei were observed in tubular epithelial cells (*Figure 27/B*). FLU-treated kidneys (CP + T24 Tx F) showed milder histological damage. Glomeruli were intact, tubular nuclei and plasma showed normal staining. Tubular brush borders were preserved (*Figure 27/C*). Similarly, structure was better preserved in kidneys that were perfused with FLU (CP F), but harvested after 2 hours of cold ischemia (CP) (*Figure 27/D-E*). The degree of tubular damage was quantified by measuring tubular lumen areas. Dilatation of the tubular lumen is caused by degradation of tubular epithelial cells and is a good indicator of tubular damage. Tubular lumens were less dilated in FLU-treated kidneys with (CP + T24 Tx F) or without (CP F) reperfusion (*Figure 27/F*).

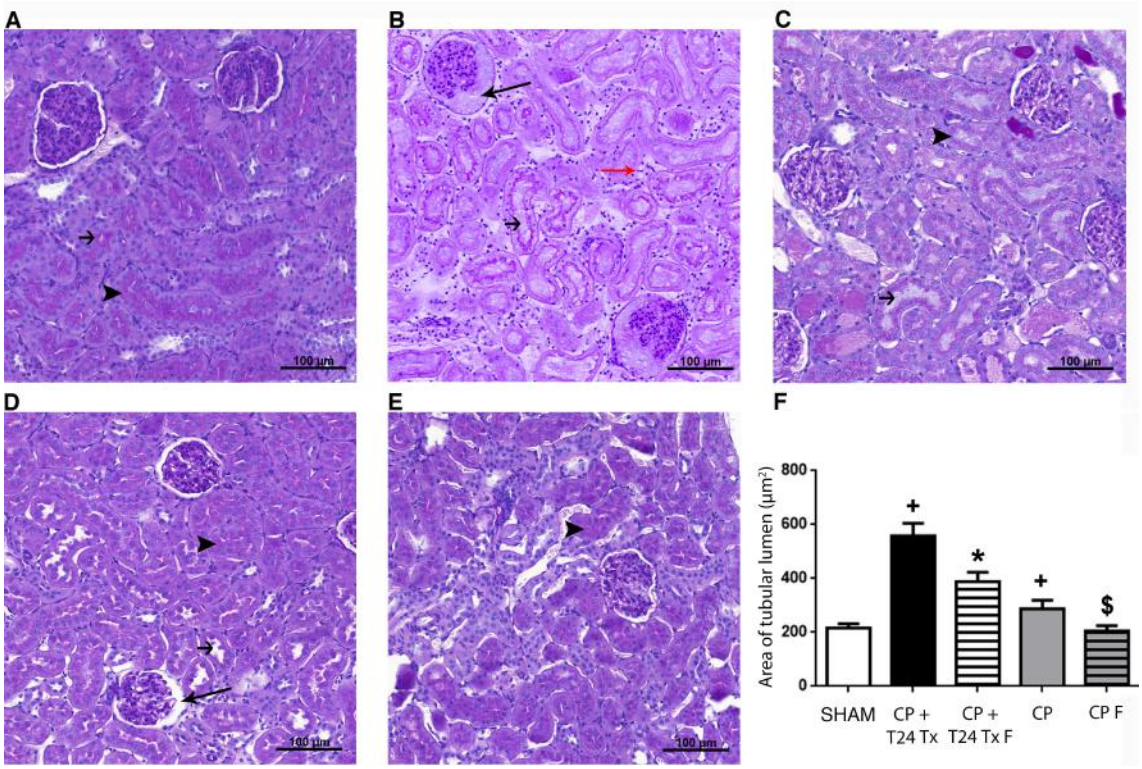

Figure 27. Fluvoxamine (FLU; F) ameliorates structural kidney damage after transplantation. (**A–E**) Representative PAS–stained kidney sections of (**A**) SHAM-operated (SHAM), (**B**) after 24 hours of reperfusion in vehicle-treated (Cold perfusion (CP) + T24 transplantation (Tx)), (**C**) after 24 hours of

reperfusion in FLU-treated (CP + T24 Tx F), (**D**) after 2 hours of cold ischemia in vehicle-treated (CP) and (**E**) after 2 hours of cold ischemia in FLU-treated (CP F) rats. Black arrowheads point to intact brush border, long thin black arrows show collapsed glomerulus, short black arrows show tubular lumens and long red arrow shows picntic nucleus. Original magnification: 200x. Scale bar=100 μm. (**F**) Semi-quantitative measurement of tubular lumen areas. *P<0.05 *versus* CP + T24 Tx; +P<0.05 *versus* SHAM; $P<0.05 versus CP (n=8/group). Bars indicate means ± SEMs, and data were analyzed by one-way ANOVA with Bonferroni multiple comparison test.

5.8 Chronic FLU-treatment is protective in DNP

DNP develops in roughly one-third of DM cases representing a major risk factor for ESRD. Hyperglicaemia and activated RAAS system lead to chronic vasoconstriction, which is an important contributor to kidney damage. Considering our promising results about the renoprotective effect of S1R agonism in the AKI model and in KTx; it was rational to investigate the effect of chronic FLU treatment on the long-run in a rat model of DNP.

5.8.1 FLU improves renal function in DNP

In a rat model of DM1 indued chronic kidney disease three treatment protocols were tested: long-term treatment with 20 mg/bwkg/day FLU for 7 weeks or short-term treatment with 2 or 20 mg/bwkg/day FLU for 2 weeks started 5 weeks after the onset of DM. Metabolic and renal parameters are summarized in *Table 4* and *Table 5*, respectively. After 7 weeks of DM rats had significant weight loss, higher blood glucose and increased serum fructosamine levels and lipid levels reflecting to metabolic changes associated with the development of DM (*Table 4*).

Table 4. Metabolic parameters of fluvoxamine (FLU)-treated type 1 diabetes mellitus DM1 rats. Metabolic parameters were measured in control and diabetic animals (D) treated with fluvoxamine (FLU) for 7 weeks (D + 7wk FLU (20mg/bwkg)) and for 2 weeks in a dose of 20 mg/bwkg (D + 2wk FLU (20mg/bwkg)) and 2 mg/bwkg (D + 2wk FLU (2mg/bwkg)). Se: serum; Se-GOT: serum glutamate-oxaloacetate transaminase; Se-GPT: serum glutamate-pyruvate transaminase. *P<0.05 *versus* Control*;* §P<0.05 *versus* D (n=8-10/group). Data are represented as means ± SEMs, and were analyzed by one-way ANOVA with Bonferroni multiple comparison test.

	Control	**Diabetes (D)**	**D + 7wk FLU (20 mg/bwkg)**	**D + 2wk FLU (20 mg/bwkg)**	**D + 2wk FLU (2 mg/bwkg)**
Total weight gain (g)	136±9.05	60.7±8.34*	91.3±10.4	91.2±12.6	85.0±12.5
Se-blood glucose (mmol/L)	12.3±0.59	44.5±3.22*	45.4±2.86	34.5±2.27	30.2±4.61
Se-fructosamine (µmol/L)	149±2.17	254±3.48*	276±4.25	252±7.58	242±4.86
Se-triglycerides (mmol/L)	1.38±0.23	2.84±0.51*	1.12±0.18§	1.26±0.09§	1.26±0.25§
Se-total cholesterol (mmol/L)	1.97±0.05	2.69±0.16*	2.56±0.12	1.96±0.06§	1.72±0.12§
Se-GOT (U/L)	127±7.15	346±69.5*	160±8.98§	209±26.4§	203±20.5§
Se-GPT (U/L)	42.7±3.07	165±33.5*	76.1±8.48§	74.5±3.18§	74.0±6.70§

DM induced severe renal impairment with increased SCr and BUN values. Fractional sodium excretion (FeNa) (reflecting tubular function) was increased and significant albuminuria (representing mainly glomerular function) were present indicating the development of DNP. Both long- and short-term treatment with FLU remarkably improved renal function parameterers (*Table 5*).

Table 5. Laboratory parameters of fluvoxamine (FLU)-treated type 1 diabetes mellitus rats. Rats were treated *per os* with: isotonic saline as vehicle (D); FLU *(*20 mg/bwkg/day) for 7 weeks (D7FLU); FLU (20 mg/bwkg/day) for 2 weeks from the 5th week of DM1 (D+FLU); FLU (2 mg/bwkg/day) for 2 weeks from the 5th week of DM1 (D+FLU2). Blood urea nitrogen (BUN); fractional sodium excretion (FeNa). *P<0.05 *versus* Control*;* §P<0.05 *versus* D (n=8-10/group). Data are represented as means ± SEMs, and were analyzed by one-way ANOVA with Bonferroni multiple comparison test.

	Control	**Diabetes (D)**	**D + 7wk FLU (20 mg/bwkg)**	**D + 2wk FLU (20 mg/bwkg)**	**D + 2wk FLU (2 mg/bwkg)**
BUN (mmol/L)	7.06±0.19	26.6±2.42*	17.3±1.49§	17.3±2.30§	18.8±1.68§
Serum creatinine (µmol/L)	22.0±0.93	42.0±2.39*	27.0±2.24§	34.5±2.74§	31.8±2.94§
FeNa (%)	0.22±0.02	3.12±0.75*	0.40±0.03§	0.90±0.23§	0.62±0.12§
Urinary albumin excretion (mg/mL)	3.25±2.39	42.5±6.38*	20.8±9.51§	21.5±4.99§	24.3±5.77

DOI:10.14753/SE.2017.2251

5.8.2 FLU improves histological parameters in DNP

Kidney sections were stained with PAS and mesangial fractional volume values (Vv) were defined by the ratio of mesangial area/glomerular taft area. Mesangial area was determined by assessment of PAS-positive and nucleus-free areas in the mesangium. FLU decreased DM-induced mesangial matrix expansion in long-term, as well as short-term treatment in both dosages (*Figure 28/A-F*). As the 20 mg/bwkg/day dosage was more effective, only this was used subsequently.

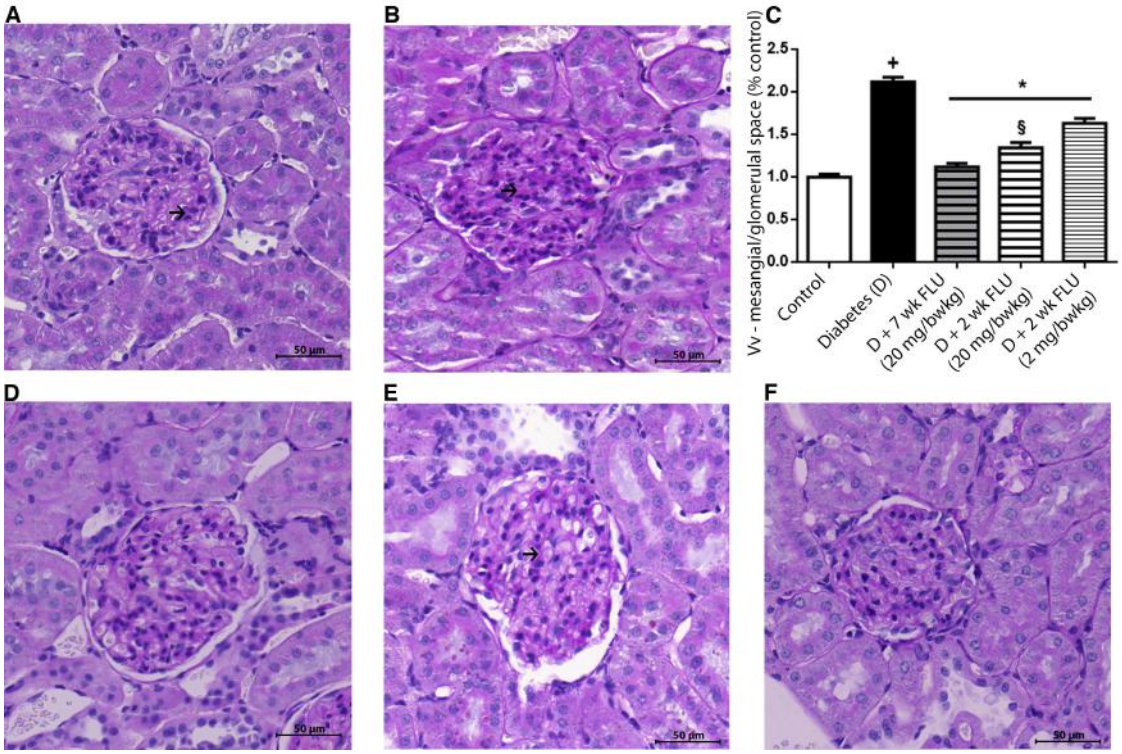

Figure 28. Fluvoxamine (FLU) decreases diabetes (DM) -induced mesangial matrix expansion. (**A-B**) Representative PAS–stained kidney sections of (**A**) Control, (**B**) Diabetic rats. (**C**) Semi-quantitative measurement of glomerular mesangial area. *P<0.05 *versus* Diabetes (D); +P<0.05 *versus* Control; §P<0.05 versus D + 2 wk FLU (2 mg/bwkg) (n=6-8/group). Bars indicate means ± SEMs, and data were analyzed by one-way ANOVA with Bonferroni multiple comparison test. (**D-F**) Representative PAS–stained kidney sections (**D**) D + 7 wk FLU (20 mg/bwkg), (**E**) D + 2 wk FLU (20 mg/bwkg) and (**F**) D + 2 wk FLU (2 mg/bwkg) rats. Short black arrows show dark purple-stained mesangial tissue in glomeruli. Original magnification: 200x. Scale bar=50 µm.

The extent of DM-induced tubulointerstitial fibrosis was evaluated on Masson's trichrome-stained sections. Fibrotic areas were extensive in DM kidneys. Both long- and short-term treatment with 20 mg/bwkg/day FLU successfully reduced tubulointerstitial fibrosis (*Figure 29/A-E*).

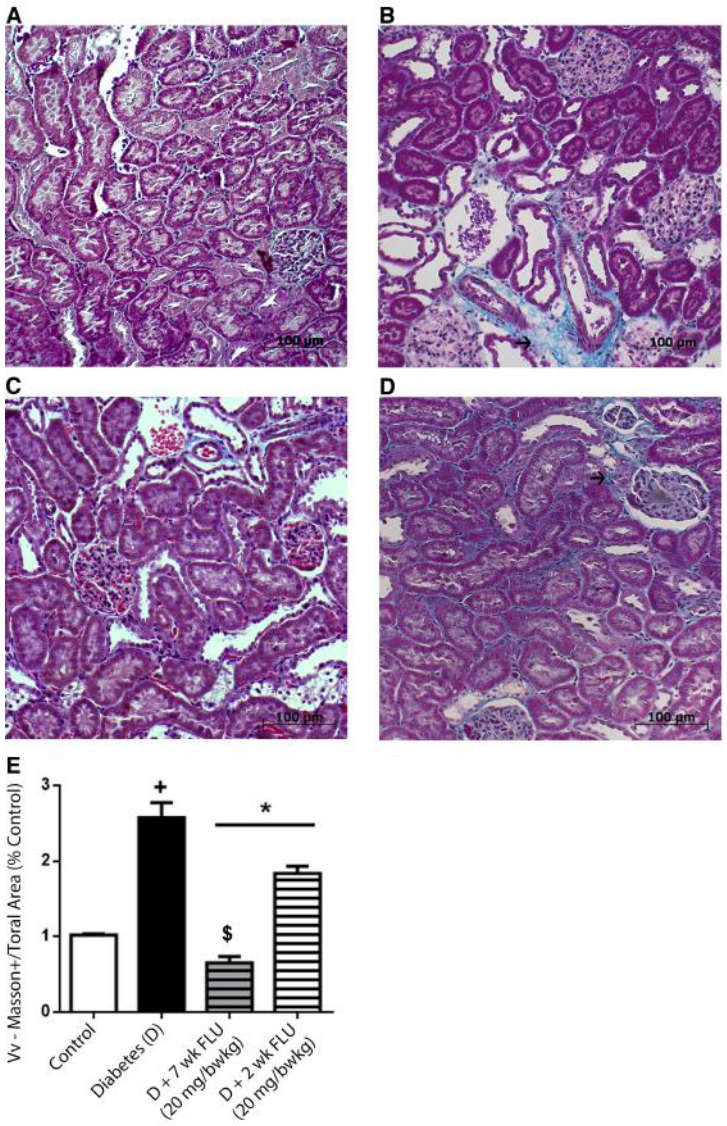

Figure 29. Fluvoxamine (FLU) decreases diabetes-induced mesangial matrix expansion. (**A-D**) Representative Masson's trichrome–stained kidney sections of (**A**) Control, (**B**) Diabetic (D), (**C**) D + 7 wk FLU (20 mg/bwkg) and (**D**) D + 2 wk FLU (20 mg/bwkg) rats. Short black arrows show blue tubulointerstitial fibrotic tissue. Original magnification: 200x. Scale bar=100 µm. rats. (**E**) Semi-quantitative measurement of Masson-positive fibrotic area. *P<0.05 *versus* Diabetes; +P<0.05 *versus* Control; $P<0.05 versus D + 2 wk FLU (20 mg/bwkg); (n=6-8/group). Bars indicate means ± SEMs, and data were analyzed by one-way ANOVA with Bonferroni multiple comparison test.

DOI:10.14753/SE.2017.2251

Extracellular matrix production is also a prominent pathological feature of DNP. Slides were stained with Sirius red to determine the ratio of Sirius-red positive collagen fibrils. The amount of extracellular matrix was doubled in DM kidneys compared to controls, but was significantly reduced after long-term FLU treatment (*Figure 30/A-E*). Short-term FLU treatment did not reduce collagen production.

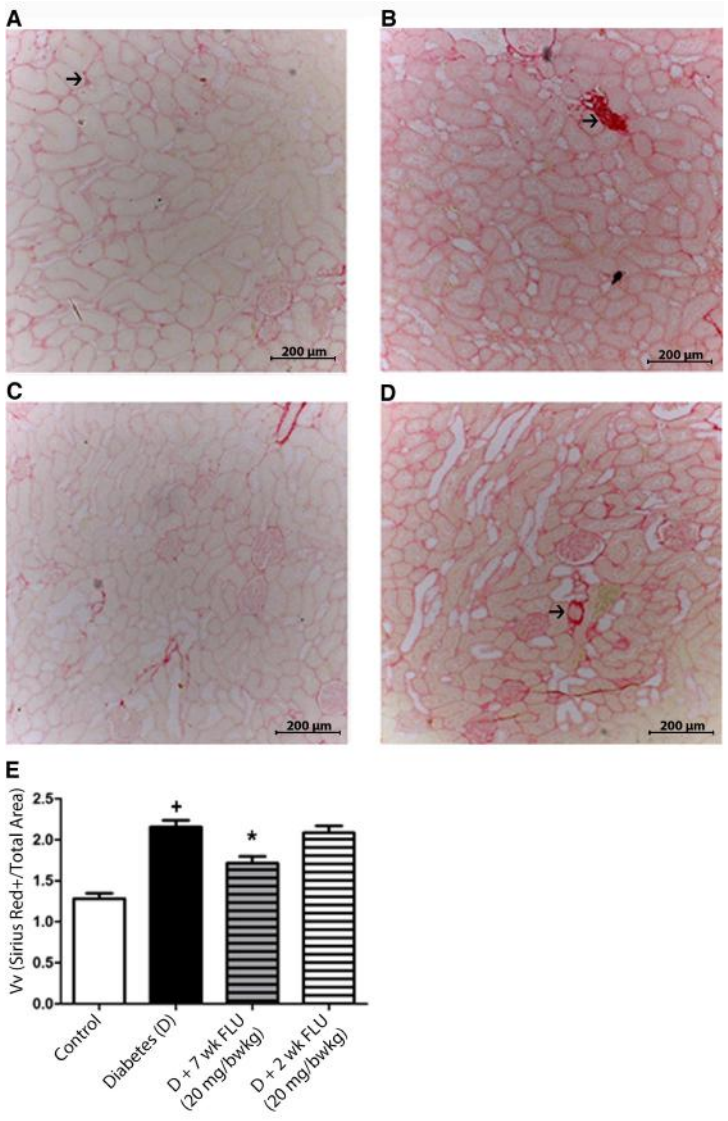

Figure 30. Fluvoxamine (FLU) decreases diabetes-induced collagen accumulation. (**A-D**) Representative Sirius red–stained kidney sections of (**A**) Control, (**B**) Diabetic (D), (**C**) D + 7 wk FLU (20 mg/bwkg) (**D**) D + 2 wk FLU (20 mg/bwkg) rats. Short black arrows show Sirius red-positive collagen tissue. Original magnification: 200x. Scale bar=200 µm. (**E**) Semi-quantitative measurement collagen accumulation. *P<0.05 *versus* Diabetes (D); +P<0.05 *versus* Control; (n=6-8/group). Bars indicate means ± SEMs, and data were analyzed by one-way ANOVA with Bonferroni multiple comparison test.

DOI:10.14753/SE.2017.2251

5.8.3 FLU rescues depressed peNOS production in DNP

Changes in the S1R-Akt-eNOS signaling pathway were evaluated after long- and short-term FLU treatment. There was an increasing tendency in S1R and pAkt protein levels, however did not reach the level of significance (p=0.06, *Figure 31/A-B*). On the other hand depressed peNOS production in DM was rescued by both long- and short-term FLU treatment (*Figure 31/C*).

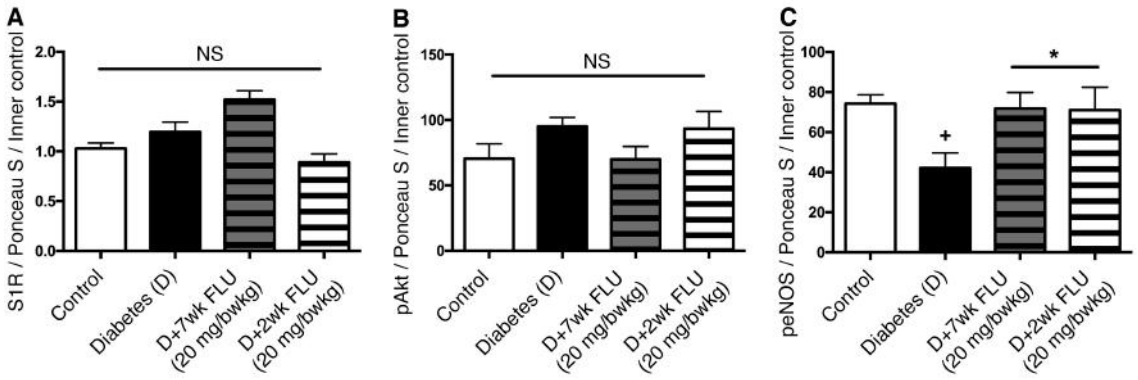

Figure 31. The Sigma-1 receptor (S1R) signaling pathway in the diabetic kidney. Immunoblot for renal (**A**) S1R, (**B**) phospho - protein kinase B (pAkt) (Ser473) and (**C**) phospho-endothelial nitric oxide synthase (peNOS) (Ser1177) in Control, Diabetic (D), D + 7 wk FLU (20 mg/bwkg) and D + 2 wk FLU (20 mg/bwkg) rats. *P<0.05 *versus* Diabetes (D); +P<0.05 *versus* Control; (n=6–8/group). Bars indicate means ± SEMs, and data were analyzed by one-way ANOVA with Bonferroni multiple comparison test.

DOI:10.14753/SE.2017.2251

6. Discussion

CKD is a global health problem affecting at least one in every ten person on the planet. The incidence of CKD is rapidly growing due to growing incidence of causative diseases, primarily DM and hypertension. ESRD is the final stage of CKD where kidneys become dysfunctional and RRT is needed. KTx is the primary treatment option for ESRD, but a number of factors can determine outcomes. The most important allogen-independent factor of long-term graft survival is renal IRI, which is unavoidable during KTx, especially in the case of cadaver donors. Our experiments aimed to explore the main pathomechanisms of acute and chronic kidney injury, and to identify possible new targets for therapeutic intervention.

Our group previously proved that female rats are more resistant to IRI than males[24, 26], mainly due to sex hormones, females have lower endothelin expression[22] and higher NOS enzyme levels. We also showed the renoprotective effect of steroid hormone DHEA in male rats, which seems to be rather estrogen-independent[60] suggesting that DHEA activates signal transduction pathways through other receptors. However DHEA does not have its own DHEA-specific receptor, it triggers Akt - eNOS signaling via various plasma membrane receptors.[61] One of these is the S1R.

Until the most recent past, most of the research on S1R focused on the brain. We are the first to describe S1R distribution in different kidney regions as well as subcellular localization of the receptor in proximal tubular cells.

Although it has been known for a decade now that S1R is neuroprotective[44], nobody came up with the idea to investigate its role in the kidney. Our study is the first to demonstrate that S1R agonism either by DHEA or FLU is protective in renal IRI essentially by improving postischemic survival, renal function and ameliorating renal

structural damage. In fact one week after the ischemic insult renal function returned to almost normal and kidney histology was similar to that of healthy rats. We were also the first to detect S1R in proximal tubular cells and proved its direct effect on NO production. We showed *in vivo* that the activation of S1R leads to NO – mediated vasodilatation and has a beneficial effect on renal perfusion.

Based on our first series of experiments we speculated that S1R activation by DHEA is renoprotective in AKI by improving NO - mediated kidney perfusion. In a second series we proceeded with the exogenous agonist FLU, which has a much higher affinity to S1R than DHEA (K_iFLU 36 nM *vs.* K_iDHEA <10 μM)[55] and is a commonly used drug in the treatment of chronic depression.

The protective effect of FLU was substantiated by a robust improvement in postischemic survival. In fact the FLU treated group was the only one where 30% of the animals survived the one-week period and completely recovered from the ischemic insult. Improvement of SCr and BUN values after 24 hours of reperfusion was significant, but not as convincing as survival data. One must consider that kidney damage is the most severe in the first days of reperfusion therefore moderate difference could be considered as non-significant at this time point. However several clinical studies underline that during/post AKI even a minimal increase in SCr has of outmost importance since it is associated with increased mortality.[62, 63] These observations are in line with our study where a 13% acute improvement in renal function was coupled with substantial improvement in survival.

Recent papers widely discuss that SCr and BUN are suboptimal markers of AKI, especially in rodents[64], as they are non-specific, insensitive and are inadequate for early detection. Therefore we measured several other probably more sensitive early

biomarkers, which were all upregulated after IRI. Ngal expression is strongly and very rapidly upregulated in the post-ischemic kidney making it a sensitive marker of distal tubular damage. NGAL also induces proliferation and has a strong anti-apoptotic effect in tubular epithelial cells.[65] Kim-1 mRNA is expressed at very low levels in the normal human and rodent kidney, but in hypoxia or ischemia it is upregulated in proximal tubules more than any other known transcript. It is mainly expressed in the S3 segment of proximal tubules, a region which is highly susceptible to injury. KIM-1 is involved in the regeneration process by clearing apoptotic cell debris from the tubular lumen (Mussap M 2014). Here we found that parallel to Kim-1 and Ngal, reperfusion injury marker serum AST (Bolignano D 2008, HAN WK 2002) was considerably less elevated after FLU treatment, which also confirmed milder renal injury.[18, 66]

HIF-1α is not only a hypoxic kidney injury marker, but also the master regulator of cell response to hypoxia. It induces the expression of a large number of target genes, by which it mediates cell protection and tubular recovery during renal IRI.[67] Numerous reports indicate that Akt is involved in the regulation of HIF-1α expression[68, 69], and since we found that S1R activation induces Akt phosphorylation we suspect that Akt could be one link between S1R and HIF-1α. This pathway however has to be further investigated.

Both conventional histology and intravital two-photon imaging revealed that FLU blunted the development of tubular damage. One week after FLU-treatment kidney structure was almost completely amended and only remote leukocyte infiltration pointed to ceased inflammation.

Cytokine profile of the kidney verified a dulled inflammatory response. IL-1α has been recently identified as an early pro-inflammatory mediator in cerebral ischemia

and a key driver of cerebrovascular inflammation[70, 71], however its role in renal IRI has not been investigated yet. Here we found that IL-1α levels were less elevated in rats receiving FLU pretreatment, while the powerful regulatory cytokine IL-10 was increased by FLU. IL-10 can block pro-inflammatory processes and inhibit leukocyte activation and in various rodent models IL-10 administration has been shown to prevent ischemic injury.[72, 73] We hypothesize that inflammatory response could be highly regulated by IL-10 in FLU treated rats, opposed to vehicle treated ones where the increase in pro-inflammatory cytokine levels (TNF- α, IL-1α and IL-6) was more robust. Weakened regulation was associated with worse outcome in these rats. AKI is known to cause multi-organ dysfunction (heart, brain and lungs) via increasing inflammatory cytokines and causing systemic inflammation.[74] In models of brain and heart ischemia the protective effect of S1R agonists has partly been attributed to their anti-inflammatory actions.[46, 75] Therefore it is very plausible that alongside renoprotection, the systemic anti-inflammatory actions of FLU also contribute to better outcomes in our study.

The proximal tubular epithelium, especially in the S3 segment is particularly sensitive to IRI due to its high energy demand and relatively low blood flow. This makes the proximal tubular epithelium an optimal target for therapeutic intervention. In contrast to studies on S1R in neuronal systems, surprisingly there is no data available regarding peripheral tissues. We are the first to detect S1R expression in proximal tubular cells. Subcellularly S1R is localized in the mitochondria-associated ER membrane and the nuclear envelope, but can translocate to the cytoplasm or even the plasma membrane using lipid rafts.[47] The exact mechanism of how the receptor translocation is initiated is still not fully known, but S1R localization at organelle-to-

organelle interfaces suggests that the receptor serves as a modulator of inter-organelle communications that are mediated by direct membrane associations. Upon ligand stimulation or ER stress S1Rs dissociate from binding immunoglobulin protein and act as interorganelle signaling modulators.[37] Congruently we observed a perinuclear, "ring-like" pattern of S1R in proximal tubular epithelial cells under normal conditions, but the receptor was expressed everywhere in the cytosol and nucleus after FLU treatment or under H_2O_2-induced oxidative stress.

Akt and NO signaling is one of the most complex signaling pathways involved in vasoregulation and ischemia. There are certain "players" that have already been mapped in detail (e.g. Akt-eNOS activation), while a lot of components are not yet characterized at all. The renal production of NO is mediated mainly by eNOS and to a much lesser extent by nNOS. We suggested the S1R – Akt - NOS signaling as a possible route of NO production in the kidney. Decreased peNOS levels in S1R knockdown cells or after the inhibition of Akt proved the role of S1R and Akt in peNOS production. There are also literary data that support the S1R involvement in eNOS production. The group of Fukunaga published a series of experiments describing the association between S1R and eNOS in the heart:[45, 46, 76-78] Very recently it has been also reported that S1R mediated NO production plays a role in neuropathic pain.38 In hippocampal neurons DHEA has been shown to act on NO production via 1R.39 NO mediation (however rather via nNOS than eNOS) was also described in S1R-induced spinal neuronal hypersensitivity.[79]

The generation of ER- and mitochondria - derived ROS is a well - known phenomenon in IRI. It triggers the unfolded protein response, which involves the activation of three main pathways: the PKR-like endoplasmic reticulum kinase (PERK); the inositol

requiring enzyme 1 (IRE1) protein kinase and the activating transcription factor 6 (ATF6) pathway. IRE1 is one of the ER stress sensor proteins that are localized in the mitochondria-associated ER membrane. Upon ER stress caused by ROS generation IRE1 is stabilized by S1R, which further prolongs the stabilization of IRE1-X-box binding protein 1 (XBP1) signaling. This signal is an essential step of transduction pathways involved in cell survival, such as the phosphoinositide 3-kinase (PI3K) - Akt pathway.[80] Moreover S1R has been demonstrated to regulate the pro-brain-derived neurotrophic factor (BDNF) *in vitro*[81], which is known to activate the PI3K-Akt pathway via tropomyosin receptor kinase B. Our results (data not shown) showing that FLU increases the expression of pro and mature BDNF in the brain suggests a similar mechanism in the kidney. Despite these significant efforts the downstream signal transduction regulated by S1R is still not fully elucidated and the mechanism by which S1R activates Akt needs further investigation.

To determine the effect of FLU-mediated NOS production on renal perfusion we measured peritubular capillary diameters in the living kidney. Evidence for active control of capillary diameter by pericytes in response to vasoactive molecules such as NO has already been demonstrated.[82, 83] Pericytes can be found on almost all capillaries as well as on small arterioles and venules. Indeed, in line with increased NO production vasodilatation was apparent within minutes after FLU treatment. Similarly, IRI-induced vasoconstriction was reversed by FLU. Vasodilatation did not occur if either S1R antagonist or NOS inhibitors were administered together with FLU validating the hypothesis that S1R activation enhances NO production in the kidney resulting in better blood supply, which leads to milder ischemic injury.

There is a general agreement that the macula densa is the principle site of nNOS production in the kidney, but a less amount is also present in proximal and distal tubules.[84] Here we detected prompt eNOS production after S1R stimulation, while nNOS was elevated only later during reperfusion. This is congruent with an earlier study where eNOS activity peaked 2 hours after reperfusion and returned to baseline after 3 days[85] and confirms our previous results in a different renal disease model showing that eNOS and nNOS have different expression patterns in time.[86]

FLU as an SSRI can also influence the serotonergic and noradrenergic systems in the brain, therefore their role cannot be fully ruled out. However it has already been proven in the heart and brain that paroxetine, an SSRI with very low affinity to S1R was unable to produce the same protective effects as FLU.[46, 87] Furthermore various studies demonstrated that FLU is the only SSRI that has no appreciable effect on the norepinephrine system either.[88]

From the first part of our experiments one can conclude, in this rat model of IRI S1R agonists successfully minimize renal IRI injury, improve postischemic survival and renal function *via* activation of Akt–mediated NO signaling in the kidney.

KTx is the best choice among RRTs; it is a life-saving treatment for ESRD patients. However in the past decades there has been a constant struggle to minimize renal IRI during KTx, it is still a major obstacle that contributes to delayed graft function and graft failure. Organs from expanded criteria donors are even more susceptible to IRI. Around 80% of transplants are from cadaver donors where cold ischemia time is an even more significant risk factor for delayed graft function.[89] As cold ischemia is unavoidable in the majority of cases it is a logical and needed time-point for intervention. Therefore in our experiments we used the rat kidney

autotransplantation model that allows us to eliminate the confounding effects of an immune response and the toxicities related to immunosuppression to prevent allograft rejection, thus allowing us to focus entirely on IRI effects.

Cold ischemia time in our experimental setting was set for 2 hours according to literary data and was validated by markedly impaired renal functional parameters.[90] Several other groups treated the donor rats in order to achieve better transplantation outcomes[90, 91], but we deliberately designed our study in a way that the preservation liquid contained FLU, as donor-pretreatment is not possible in the case of cadaver donors. Moreover treating the donor rat would be a systemic intervention, opposed to adding a S1R agonist to the perfusion solution where only the transplanted kidney is affected. We calculated the FLU concentration of the preservation fluid based on the results of our renal IRI model, where 20 mg/bwkg dose exerted significant vasodilatative effects.

Here we showed that perfusion and cold storage of the graft in FLU containing perfusion solution exerted remarkable renoprotection marked by improved functional and histological parameters in autotransplanted kidneys. Since literary data suggest that histological changes in the autotransplanted grafts are the most prominent after 6 hours[90] of cold storage we are planning additional studies with longer cold ischemia times to further charachterize the protective effects of FLU.

As we showed in our renal IRI model S1R agonism had a strong anti-inflammatory effect in the kidney. Concurrently MCP-1 was less elevated in FLU-treated autotransplanted kidneys as well. MCP-1 is known to be up - regulated in IRI and is also referred to as a biomaker for mononuclear inflammatory processes.[92] Increase in MCP-1 expression correlates with the increase in monocyte infiltration in

the kidney. Thus inflammatory cytokine profile of transplanted kidneys perfused with FLU could be of significance as well.

High NGAL and KIM-1level shortly after KTx have been shown to be good predictors of delayed graft function in clinical and there is an ongoing attempt to use these factors as early biomarkers to foresee rejection episodes.[93, 94] Here we detected that higher Ngal and Kim-1 mRNA levels are massively reduced in grafts stored in FLU-containing fluid indicating promising long-term results, but further experiments have to be performed for confirmation.

Parallel to functional improvements healthy structure of the kidneys was also more preserved in FLU-treated groups. Not only autotransplanted kidneys were in better condition; kidneys that were not subjected to autotransplantation, but were perfused and stored in FLU-containing cold perfusion solution for 2 hours showed significantly better histology than vehicle treated grafts. Thus it is rather feasible that FLU-pretreated kidneys are already in a better overall condition when they are implanted into the recipient and therefore are more resistant to IRI injury later during KTx.

To determine the vasoregulation and renal perfusion of autotransplanted kidneys intravital two-photon microscopic analysis was attempted, but it was unsuccessful due to technical difficulties. Currently we still insist on answering this question therefore other methods such a single photon emission computed tomography and Doppler ultrasound of renal vessels are planned for the future. These measurements will provide valuable data that could accentuate our results regarding the role of S1R agonism in renal vasodilatation during KTx. Furthermore molecular biology analysis of the S1R – Akt - eNOS pathway is in progess.

As it has been emphasized several times in the dissertation DNP is of particular interest. Not only does it account for nearly the half of ESRD cases, but DNP is also the primary cause of KTx in westernized countries. Furthermore DM has significant impact on renal function after KTx, since post-transplant DM can occur in approx. 7-15% of renal transplanted patients (depending on age, body weight, immunosuppressive regimen etc). As for post-transplant DM it is estimated that the number of cases will increase significantly in the next few decades.[95] Post-transplant DM reduces renal function in the graft and increases patient cardiovascular morbidity and mortality following KTx.[96]

Based on all these observations it was evident that we wanted to assess the relevance and possible renoprotective effects of our "newly discovered" S1R pathway in a DNP model. To our surprise the relevance of S1R in DM was only investigated in one, oldish study measuring decreased S1R expression in the brain.[97] Even after carefully reviewing the literature we did not find any data about the possible effects of S1R agonists. Neither has S1R been discussed in the diabetic kidney at all.

However based on the first results of *Aragno et al.* one could have already suspected the role of S1R in DNP for 15 years.

Aragno et al. investigated the effect of DHEA in an STZ model of DM. Altough none of the animal models can ideally mimic the human disesase, considering the validation criteria of the Animal Models of Diabetic Complications Consortium, STZ-induced DNP is still one of the most widely used non-genetic rat model of DM1 (AMDCC website http://www.amdcc.org). Following STZ induction hyperglicaemia and RAAS activation lead to renal vasoconstriction, increased glomerular basement membrane thickening, fibrosis and accelerated inflammation.[98] The development of

nephropathy is accelerated if no insulin is given to the animals. Without insulin supplementation microalbuminuria and increased renal functional parameters parallel to the first fibrotic changes can be measured earliest 3 weeks after STZ induction. By the 6th-7th week ESRD develops represented by markedly higher SCr, BUN, massive proteinuria, and lower GFR.[99]

Aragno et al. used the STZ model that is the same as ours.[100, 101] They showed that 3-weeks of chronic DHEA-treatment has a strong anti-oxidant effect and rescues Na^+-K^+-ATP-ase function. They suggested that DHEA might be protective by reducing lipid oxidation and disturbances in the arachidonic acid metabolism, but they could not explain the exact mechanism.[101]

The first report on the renal effects of DHEA was in an obese Zucker rat DM2 model. From the clinical view DM2 is also highly relevant as it accounts for the majority of DM cases. The molecular mechanisms of DM1 and DM2 are very similar: nephropathy develops as the consequence of persistent high blood glucose due to insulin deficiency or insulin resistance, intrarenal RAAS is activated, various inflammatory and fibrotic pathways are induced. In this study *Richards et al.* showed that DHEA lowered SCr and reduced albuminuria, improved GFR and FeNa. DHEA also decreased serum concentration of inflammatory cytokine TNF-α and additionally it slowed the progression of DNP-induced fibrosis demonstrated by reduced α-smooth muscle actin levels.[102] Even though they showed these very convincing data, this group did not investigate the molecular mechanisms of DHEA-mediated renoprotection. Taken together all these results and the fact that DHEA has been known as a S1R agonist since 1996[103] point to a rather straightforward connection, but neither of the mentioned groups associated the renoprotective effects of DHEA with S1R.

To our best knowledge we are the first in the literature to investigate the effects of S1R agonism in DNP, therefore based on our acute studies we used FLU as one of the most potent S1R agonists. In our experimental setup we wanted to answer two questions in parallel. In the first series we gave FLU from the beginning to assess whether S1R agonist treatment can prevent the development of DNP. Secondly, FLU was administered only in the last two weeks of the protocol to confirm whether it is effective enough to stop or slower disease progression. Both long- and short-term FLU-treatment improved metabolic and functional parameters, but there was no significant difference between the two protocols in this regard. On the other hand long-term treatment was more effective in hindering structural deterioration, indicating a beneficial anti-fibrotic effect of S1R agonists. Additional experiments are in process to explore the molecular mechanisms of renal fibrosis.

Previous studies suggest that progressive fibrosis during DNP is a consequence of long-term NO deficiency and loss of the antifibrotic action of NO, but the underlying mechanism is not fully understood. Administration of NO-donor L-arginine-supplemented drinking water for two weeks ameliorated proteinuria and diminished glomerulosclerosis in STZ diabetic rats.[104] Recent observations in clinical studies of *eNOS* 4b/a and G894T polymorphism[105] and experimental models in *eNOS*-/- mice have suggested that genetic deficiency of eNOS predisposes the development of renal injury in DM. Similarly to observations in the acute IRI model, we found that chronic treatment with S1R agonist FLU increases peNOS production. All these data underlines the importance of FLU-mediated eNOS effects in DNP, however there is a long way to go to clarify the exact molecular pathways.

It is worth to consider that beside its S1R agonist property FLU is mainly used as an SSRI. SSRIs are the routinely recommended treatment for depressed patients

even with DM due to their high efficacy and tolerability[106], however one should be cautious because of the possible disadvantages of chronic treatment. Although liver injury is one of the most frequently reported adverse effects of SSRIs; in our experiments serum liver enzymes were in the normal range supporting the clinical observation that FLU is the least hepatotoxic among SSRIs.[107] Antidepressants are also assumed to significantly alter glucose homeostasis. However, there are only two studies saying that FLU induces hyperglycemia; a transient increase in blood glucose level was documented after acute FLU treatment in non-diabetic mice.[108] The other study is a case report of a DM2 woman with depression, where FLU elevated the random blood glucose level.[109] The effect of FLU in DM1 has not been studied at all. In our study, chronic FLU administration did not influence blood-glucose or fructosamine values suggesting that FLU does not alter glucose homeostasis significantly on the long run. Abnormalities of lipoprotein metabolism contribute to the development of atherosclerosis and are independent risk factors of cardiovascular mortality in DNP patients.[110] The effect of FLU on serum lipid panel is poorly investigated. There are only a few studies showing that FLU reduces cholesterol levels and has beneficial effects on the lipid panel.[111, 112] Here we showed that FLU decreases DM-induced hyperlipidemia, which has the additional benefit of reducing cardiovascular risk.

In conclusion our findings have outlined a molecular pathway of S1R–mediated renal vasodilatation, which suggests that S1R could be an ideal target to prevent both acute and chronic renal injury. During KTx the supplementation of graft preservation fluid with S1R agonist FLU might be a novel tool to minimize cold ischemia-induced injury and to optimize overall graft condition. Our observations will be submitted for patent application in the near future.

DOI:10.14753/SE.2017.2251

7. Conclusions

1. We were the first to clarify that S1R is expressed in different nephron segments, predominantly in the cortex, but also in the medulla and papilla.

2. Our *in vivo* and *in vitro* experiments revealed that upon stimulation S1R translocates from the mitochondria-associated ER to the cytoplasm and nucleus.

3. We showed that treatment with endogenous S1R agonist DHEA is renoprotective in a rat model of IRI.

4. We demonstrated that exogenous, high-affinity S1R agonist FLU treatment is protective in renal IRI. It substantially improves post-ischemic survival, ameliorates functional and structural kidney damage, as well as inflammation.

5. We described the role of S1R in improving perfusion in the post-ischemic kidney by inducing Akt-NOS signaling and NO production.

6. We demonstrated the renoprotective effect of FLU treatment in KTx.

7. We showed that chronic FLU treatment ameliorates functional and structural kidney damage in diabetic nephropathy, presumably via hindering fibrosis and rescuing eNOS production.

DOI:10.14753/SE.2017.2251

8. Summary

Today chronic kidney disease (CKD) is a global health crisis creating a huge financial burden. More than 10% of the worldwide population is affected by CKD and the number of cases is constantly increasing. Growing incidence of end-stage renal disease (ESRD) can be attributed to the rapidly escalating incidence of causative disorders, mainly diabetes mellitus and hypertension. According to the latest WHO statistics the number of diabetic patients will double by 2030 making the situation even worse.

ESRD is the last and most severe stage of CKD where renal replacement therapy (dialysis or kidney transplantation (KTx)) is required. Transplantation is the preferred treatment option due to its superiority in prolonging the longevity of patients and also in providing a much valuable quality of life compared to dialysis. Outcome of KTx is determined by a number of different issues among which renal ischemia/reperfusion injury (IRI) is the most important allogen-independent factor of long-term graft survival.

Endothelial dysfunction, peritubular capillary loss, and increased reactivity to vasoconstrictive agents are all leading to tubular damage during the progression of IRI. All of these processes contribute to decreased production and impaired responsiveness to nitric oxide (NO). Despite improvements in therapy IRI is still associated with unacceptably high mortality; therefore new treatment approaches are urgently needed.

This dissertation discusses the main pathomechanisms of acute and chronic kidney injury. Special emphasis is put on the pathological processes of renal IRI, since it has a central role in long term graft survival. Our results demonstrate as first in the literature that the Sigma-1 receptor (S1R) - NO signaling pathway plays a central role in the pathomechanism of kidney injury. We showed that treatment with various S1R agonists substantially improves renal function and minimizes renal structural damage in rat models of both renal IRI, KTx and diabetic nephropathy.

Our findings have chalked out a new molecular pathway of S1R–mediated renal vasodilation involving S1R translocation, activation of protein kinase B (Akt) and NO production. All our data suggest that S1R agonism might provide a novel therapeutic option for renoprotective therapy.

DOI:10.14753/SE.2017.2251

Összefoglalás

A krónikus veseelégtelenség (CKD) napjaink egyik legjelentősebb népegészségügyi problémája, mely világszerte komoly egészség-gazdasági terhet jelent a társadalom számára. A népesség több mint 10%-a szenved CKD-ban és a betegek száma egyre nő. A felnőttkori végstádiumú veseelégtelenség (ESRD) emelkedő tendenciájának hátterében főként a civilizációs betegségek, a diabétesz mellitusz (DM) és magas vérnyomás rohamosan növekvő incidenciája áll. A WHO becslései alapján a cukorbetegségben szenvedők száma 2030-ra várhatóan megduplázódik, mely tovább fokozza a vesebetegség kockázatát.

A CKD utolsó stádiumában végállapotú veseelégtelenség alakul ki, melyben a vesepótló kezelés megkezdése (dialízis vagy vesetranszplantáció (KTx)) már elkerülhetetlen. A vesepótló kezelések közül a KTx egyértelműen előnyösebb, növeli a várható élettartamot és jelentősen javítja a betegek életminőséget. A renális iszkémia/reperfúziós károsodás (IRI) az egyik legjelentősebb allogén-független tényező a hosszú távú graft túlélés szempontjából

Az IRI során kialakuló endotéliális diszfunkció, a fokozott vazokonstrikció és a nitrogén-monoxid (NO) csökkent termelődése mind hozzájárul a tubuláris károsodás kialakulásához. Bár az elmúlt évtizedekben jelentős előrelépés történt az IRI mérséklésében, a hosszútávú graft-túlélés számottevően továbbra sem javult, így hatékonyabb kezelési stratégiák kidolgozása szükséges.

A disszertáció bemutatja az akut és krónikus vesekárosodás patomechanizmusát kiemelve a renális IRI - mint a hosszú távú graft túlélés szempontjából legjelentősebb faktor - szerepét. Kísérleteink során egy Sigma-1-receptor (S1R) – mediált, új jelátviteli útvonalat azonosítottunk, mely a S1R transzlokációján és az Akt aktivációján keresztül serkenti a vazodilatatív hatású NO termelődését. Eredményeinkkel elsőként igazoltuk a S1R agonizmus renoportektív hatását: az előkezelés javítja a vesefunkciót és csökkenti a vese strukturális károsodását IRI, KTx és diabéteszes nefropátiás patkány modellekben.

Eredményeink alapján azt reméljük, hogy a S1R agonisták új terápiás célpontot jelenthetnek a vesekárosodás kivédésében és alapvetően változtathatják meg a renoprotektív kezelések kelléktárát.

9. Bibliography

1. Lozano, R, Naghavi, M, Foreman, K, Lim, S, Shibuya, K, Aboyans, V, Abraham, J, Adair, T, Aggarwal, R, Ahn, SY, Alvarado, M, Anderson, HR, Anderson, LM, Andrews, KG, Atkinson, C, Baddour, LM, Barker-Collo, S, Bartels, DH, Bell, ML, Benjamin, EJ, Bennett, D, Bhalla, K, Bikbov, B, Bin Abdulhak, A, Birbeck, G, Blyth, F, Bolliger, I, Boufous, S, Bucello, C, Burch, M, Burney, P, Carapetis, J, Chen, H, Chou, D, Chugh, SS, Coffeng, LE, Colan, SD, Colquhoun, S, Colson, KE, Condon, J, Connor, MD, Cooper, LT, Corriere, M, Cortinovis, M, de Vaccaro, KC, Couser, W, Cowie, BC, Criqui, MH, Cross, M, Dabhadkar, KC, Dahodwala, N, De Leo, D, Degenhardt, L, Delossantos, A, Denenberg, J, Des Jarlais, DC, Dharmaratne, SD, Dorsey, ER, Driscoll, T, Duber, H, Ebel, B, Erwin, PJ, Espindola, P, Ezzati, M, Feigin, V, Flaxman, AD, Forouzanfar, MH, Fowkes, FG, Franklin, R, Fransen, M, Freeman, MK, Gabriel, SE, Gakidou, E, Gaspari, F, Gillum, RF, Gonzalez-Medina, D, Halasa, YA, Haring, D, Harrison, JE, Havmoeller, R, Hay, RJ, Hoen, B, Hotez, PJ, Hoy, D, Jacobsen, KH, James, SL, Jasrasaria, R, Jayaraman, S, Johns, N, Karthikeyan, G, Kassebaum, N, Keren, A, Khoo, JP, Knowlton, LM, Kobusingye, O, Koranteng, A, Krishnamurthi, R, Lipnick, M, Lipshultz, SE, Ohno, SL, Mabweijano, J, MacIntyre, MF, Mallinger, L, March, L, Marks, GB, Marks, R, Matsumori, A, Matzopoulos, R, Mayosi, BM, McAnulty, JH, McDermott, MM, McGrath, J, Mensah, GA, Merriman, TR, Michaud, C, Miller, M, Miller, TR, Mock, C, Mocumbi, AO, Mokdad, AA, Moran, A, Mulholland, K, Nair, MN, Naldi, L, Narayan, KM, Nasseri, K, Norman, P, O'Donnell, M, Omer, SB, Ortblad, K, Osborne, R, Ozgediz, D, Pahari, B, Pandian, JD, Rivero, AP, Padilla, RP, Perez-Ruiz, F, Perico, N, Phillips, D, Pierce, K, Pope, CA, 3rd, Porrini, E, Pourmalek, F, Raju, M, Ranganathan, D, Rehm, JT, Rein, DB, Remuzzi, G, Rivara, FP, Roberts, T, De Leon, FR, Rosenfeld, LC, Rushton, L, Sacco, RL, Salomon, JA, Sampson, U, Sanman, E, Schwebel, DC, Segui-Gomez, M, Shepard, DS, Singh, D, Singleton, J, Sliwa, K, Smith, E, Steer, A, Taylor, JA, Thomas, B, Tleyjeh, IM, Towbin, JA, Truelsen, T, Undurraga, EA, Venketasubramanian, N, Vijayakumar, L, Vos, T, Wagner, GR, Wang, M, Wang, W, Watt, K, Weinstock, MA, Weintraub, R, Wilkinson, JD, Woolf, AD, Wulf, S, Yeh, PH, Yip, P, Zabetian, A, Zheng, ZJ, Lopez, AD, Murray, CJ, AlMazroa, MA, Memish, ZA. (2012) Global and regional mortality from 235 causes

of death for 20 age groups in 1990 and 2010: a systematic analysis for the Global Burden of Disease Study 2010. *Lancet,* 380**:** 2095-2128,

2. Molitch, ME, DeFronzo, RA, Franz, MJ, Keane, WF, Mogensen, CE, Parving, HH, Steffes, MW. (2004) Nephropathy in diabetes. *Diabetes Care,* 27 Suppl 1**:** S79-83,

3. Ninomiya, T, Perkovic, V, de Galan, BE, Zoungas, S, Pillai, A, Jardine, M, Patel, A, Cass, A, Neal, B, Poulter, N, Mogensen, CE, Cooper, M, Marre, M, Williams, B, Hamet, P, Mancia, G, Woodward, M, Macmahon, S, Chalmers, J. (2009) Albuminuria and kidney function independently predict cardiovascular and renal outcomes in diabetes. *J Am Soc Nephrol,* 20**:** 1813-1821,

4. Coca, SG, Singanamala, S, Parikh, CR. (2012) Chronic kidney disease after acute kidney injury: a systematic review and meta-analysis. *Kidney Int,* 81**:** 442-448,

5. Hsu, CY, Ordonez, JD, Chertow, GM, Fan, D, McCulloch, CE, Go, AS. (2008) The risk of acute renal failure in patients with chronic kidney disease. *Kidney Int,* 74**:** 101-107,

6. Levey, AS, Eckardt, KU, Tsukamoto, Y, Levin, A, Coresh, J, Rossert, J, De Zeeuw, D, Hostetter, TH, Lameire, N, Eknoyan, G. (2005) Definition and classification of chronic kidney disease: a position statement from Kidney Disease: Improving Global Outcomes (KDIGO). *Kidney Int,* 67**:** 2089-2100,

7. Liyanage, T, Ninomiya, T, Jha, V, Neal, B, Patrice, HM, Okpechi, I, Zhao, MH, Lv, J, Garg, AX, Knight, J, Rodgers, A, Gallagher, M, Kotwal, S, Cass, A, Perkovic, V. (2015) Worldwide access to treatment for end-stage kidney disease: a systematic review. *Lancet,* 385**:** 1975-1982,

8. Kulcsár, I, Szegedi, J, Ladányi, E, Török, M, Túri, S, Kiss, I. (2010) Dialíziskezelés Magyarországon: 2003-2009. *Hypertonia és Nephrologia,* 14**:** 247-253,

9. Tonelli, M, Wiebe, N, Knoll, G, Bello, A, Browne, S, Jadhav, D, Klarenbach, S, Gill, J. (2011) Systematic review: kidney transplantation compared with dialysis in clinically relevant outcomes. *Am J Transplant,* 11**:** 2093-2109,

10. Ponticelli, C. (2004) Renal transplantation 2004: where do we stand today? *Nephrol Dial Transplant,* 19**:** 2937-2947,

11. Szederkenyi, E, Szenohradszky, P, Csajbok, E, Perner, F, Asztalos, L, Kalmar Nagy, K, Langer, R. (2013) [50-year history of kidney transplantation in Hungary]. *Orv Hetil,* 154**:** 846-849,

12. Lamb, KE, Lodhi, S, Meier-Kriesche, HU. (2011) Long-term renal allograft survival in the United States: a critical reappraisal. *Am J Transplant,* 11**:** 450-462,

13. Legendre, C, Canaud, G, Martinez, F. (2014) Factors influencing long-term outcome after kidney transplantation. *Transpl Int,* 27**:** 19-27,

14. Kasiske, BL, Snyder, JJ, Gilbertson, D, Matas, AJ. (2003) Diabetes mellitus after kidney transplantation in the United States. *Am J Transplant,* 3**:** 178-185,

15. (2012) Section 2: AKI Definition. *Kidney Int Suppl (2011),* 2**:** 19-36,

16. Mehta, RL, Kellum, JA, Shah, SV, Molitoris, BA, Ronco, C, Warnock, DG, Levin, A. (2007) Acute Kidney Injury Network: report of an initiative to improve outcomes in acute kidney injury. *Crit Care,* 11**:** R31,

17. Bellomo, R, Ronco, C, Kellum, JA, Mehta, RL, Palevsky, P. (2004) Acute renal failure - definition, outcome measures, animal models, fluid therapy and information technology needs: the Second International Consensus Conference of the Acute Dialysis Quality Initiative (ADQI) Group. *Crit Care,* 8**:** R204-212,

18. Han, WK, Bailly, V, Abichandani, R, Thadhani, R, Bonventre, JV. (2002) Kidney Injury Molecule-1 (KIM-1): a novel biomarker for human renal proximal tubule injury. *Kidney Int,* 62**:** 237-244,

19. Mishra, J, Mori, K, Ma, Q, Kelly, C, Yang, J, Mitsnefes, M, Barasch, J, Devarajan, P. (2004) Amelioration of ischemic acute renal injury by neutrophil gelatinase-associated lipocalin. *J Am Soc Nephrol,* 15**:** 3073-3082,

20. Racusen, LC. (1998) Epithelial cell shedding in acute renal injury. *Clin Exp Pharmacol Physiol,* 25**:** 273-275,

21. Layton, AT, Vallon, V, Edwards, A. (2015) Modeling oxygen consumption in the proximal tubule: effects of NHE and SGLT2 inhibition. *Am J Physiol Renal Physiol,* 308**:** F1343-1357,

22. Muller, V, Losonczy, G, Heemann, U, Vannay, A, Fekete, A, Reusz, G, Tulassay, T, Szabo, AJ. (2002) Sexual dimorphism in renal ischemia-reperfusion injury in rats: possible role of endothelin. *Kidney Int,* 62**:** 1364-1371,

23. Schrier, RW, Wang, W, Poole, B, Mitra, A. (2004) Acute renal failure: definitions, diagnosis, pathogenesis, and therapy. *J Clin Invest,* 114**:** 5-14,

24. Fekete, A, Vannay, A, Ver, A, Vasarhelyi, B, Muller, V, Ouyang, N, Reusz, G, Tulassay, T, Szabo, AJ. (2004) Sex differences in the alterations of Na(+), K(+)-ATPase following ischaemia-reperfusion injury in the rat kidney. *J Physiol,* 555**:** 471-480,

25. Basile, DP. (2007) The endothelial cell in ischemic acute kidney injury: implications for acute and chronic function. *Kidney Int,* 72**:** 151-156,

26. Fekete, A, Vannay, A, Ver, A, Rusai, K, Muller, V, Reusz, G, Tulassay, T, Szabo, AJ. (2006) Sex differences in heat shock protein 72 expression and localization in rats following renal ischemia-reperfusion injury. *Am J Physiol Renal Physiol,* 291**:** F806-811,

27. Devarajan, P. (2005) Cellular and molecular derangements in acute tubular necrosis. *Curr Opin Pediatr,* 17**:** 193-199,

28. Lastra-Lastra, G, Sowers, JR, Restrepo-Erazo, K, Manrique-Acevedo, C, Lastra-Gonzalez, G. (2009) Role of aldosterone and angiotensin II in insulin resistance: an update. *Clin Endocrinol (Oxf),* 71**:** 1-6,

29. Ribeiro-Oliveira, A, Jr., Nogueira, AI, Pereira, RM, Boas, WW, Dos Santos, RA, Simoes e Silva, AC. (2008) The renin-angiotensin system and diabetes: an update. *Vasc Health Risk Manag,* 4**:** 787-803,

30. Kinsey, GR, Okusa, MD. (2012) Role of leukocytes in the pathogenesis of acute kidney injury. *Crit Care,* 16**:** 214,

31. Elsherbiny, NM, Al-Gayyar, MM, Abd El Galil, KH. (2015) Nephroprotective role of dipyridamole in diabetic nephropathy: Effect on inflammation and apoptosis. *Life Sci,* 143**:** 8-17,

32. Brune, S, Pricl, S, Wunsch, B. (2013) Structure of the sigma1 receptor and its ligand binding site. *J Med Chem,* 56**:** 9809-9819,

33. Ortega-Roldan, JL, Ossa, F, Amin, NT, Schnell, JR. (2015) Solution NMR studies reveal the location of the second transmembrane domain of the human sigma-1 receptor. *FEBS Lett,* 589**:** 659-665,

34. Mavlyutov, TA, Epstein, ML, Andersen, KA, Ziskind-Conhaim, L, Ruoho, AE. (2010) The sigma-1 receptor is enriched in postsynaptic sites of C-terminals in mouse motoneurons. An anatomical and behavioral study. *Neuroscience,* 167**:** 247-255,

35. Hellewell, SB, Bruce, A, Feinstein, G, Orringer, J, Williams, W, Bowen, WD. (1994) Rat liver and kidney contain high densities of sigma 1 and sigma 2 receptors:

characterization by ligand binding and photoaffinity labeling. *Eur J Pharmacol,* 268**:** 9-18,

36. Ela, C, Barg, J, Vogel, Z, Hasin, Y, Eilam, Y. (1994) Sigma receptor ligands modulate contractility, Ca++ influx and beating rate in cultured cardiac myocytes. *J Pharmacol Exp Ther,* 269**:** 1300-1309,

37. Hayashi, T, Su, TP. (2003) Intracellular dynamics of sigma-1 receptors (sigma(1) binding sites) in NG108-15 cells. *J Pharmacol Exp Ther,* 306**:** 726-733,

38. Martin-Fardon, R, Maurice, T, Aujla, H, Bowen, WD, Weiss, F. (2007) Differential effects of sigma1 receptor blockade on self-administration and conditioned reinstatement motivated by cocaine vs natural reward. *Neuropsychopharmacology,* 32**:** 1967-1973,

39. Stefanski, R, Justinova, Z, Hayashi, T, Takebayashi, M, Goldberg, SR, Su, TP. (2004) Sigma1 receptor upregulation after chronic methamphetamine self-administration in rats: a study with yoked controls. *Psychopharmacology (Berl),* 175**:** 68-75,

40. Maurice, T, Urani, A, Phan, VL, Romieu, P. (2001) The interaction between neuroactive steroids and the sigma1 receptor function: behavioral consequences and therapeutic opportunities. *Brain Res Brain Res Rev,* 37**:** 116-132,

41. Narita, N, Hashimoto, K, Tomitaka, S, Minabe, Y. (1996) Interactions of selective serotonin reuptake inhibitors with subtypes of sigma receptors in rat brain. *Eur J Pharmacol,* 307**:** 117-119,

42. Rogoz, Z, Skuza, G, Maj, J, Danysz, W. (2002) Synergistic effect of uncompetitive NMDA receptor antagonists and antidepressant drugs in the forced swimming test in rats. *Neuropharmacology,* 42**:** 1024-1030,

43. Lucas, G, Rymar, VV, Sadikot, AF, Debonnel, G. (2008) Further evidence for an antidepressant potential of the selective sigma1 agonist SA 4503: electrophysiological, morphological and behavioural studies. *Int J Neuropsychopharmacol,* 11**:** 485-495,

44. Ajmo, CT, Jr., Vernon, DO, Collier, L, Pennypacker, KR, Cuevas, J. (2006) Sigma receptor activation reduces infarct size at 24 hours after permanent middle cerebral artery occlusion in rats. *Curr Neurovasc Res,* 3**:** 89-98,

45. Bhuiyan, MS, Tagashira, H, Shioda, N, Fukunaga, K. (2010) Targeting sigma-1 receptor with fluvoxamine ameliorates pressure-overload-induced hypertrophy and dysfunctions. *Expert Opin Ther Targets,* 14**:** 1009-1022,

46. Tagashira, H, Bhuiyan, S, Shioda, N, Hasegawa, H, Kanai, H, Fukunaga, K. (2010) Sigma1-receptor stimulation with fluvoxamine ameliorates transverse aortic constriction-induced myocardial hypertrophy and dysfunction in mice. *Am J Physiol Heart Circ Physiol,* 299**:** H1535-1545,

47. Hayashi, T, Su, TP. (2007) Sigma-1 receptor chaperones at the ER-mitochondrion interface regulate Ca(2+) signaling and cell survival. *Cell,* 131**:** 596-610,

48. Tagashira, H, Bhuiyan, MS, Shioda, N, Fukunaga, K. (2014) Fluvoxamine rescues mitochondrial Ca2+ transport and ATP production through sigma(1)-receptor in hypertrophic cardiomyocytes. *Life Sci,* 95**:** 89-100,

49. Soriani, O, Le Foll, F, Galas, L, Roman, F, Vaudry, H, Cazin, L. (1999) The sigma-ligand (+)-pentazocine depresses M current and enhances calcium conductances in frog melanotrophs. *Am J Physiol,* 277**:** E73-80,

50. Cheng, ZX, Lan, DM, Wu, PY, Zhu, YH, Dong, Y, Ma, L, Zheng, P. (2008) Neurosteroid dehydroepiandrosterone sulphate inhibits persistent sodium currents in rat medial prefrontal cortex via activation of sigma-1 receptors. *Exp Neurol,* 210**:** 128-136,

51. Yang, S, Bhardwaj, A, Cheng, J, Alkayed, NJ, Hurn, PD, Kirsch, JR. (2007) Sigma receptor agonists provide neuroprotection in vitro by preserving bcl-2. *Anesth Analg,* 104**:** 1179-1184, tables of contents,

52. Tchedre, KT, Yorio, T. (2008) sigma-1 receptors protect RGC-5 cells from apoptosis by regulating intracellular calcium, Bax levels, and caspase-3 activation. *Invest Ophthalmol Vis Sci,* 49**:** 2577-2588,

53. Rong, S, Park, JK, Kirsch, T, Yagita, H, Akiba, H, Boenisch, O, Haller, H, Najafian, N, Habicht, A. (2011) The TIM-1:TIM-4 pathway enhances renal ischemia-reperfusion injury. *J Am Soc Nephrol,* 22**:** 484-495,

54. Romero-Calvo, I, Ocon, B, Martinez-Moya, P, Suarez, MD, Zarzuelo, A, Martinez-Augustin, O, de Medina, FS. (2010) Reversible Ponceau staining as a loading control alternative to actin in Western blots. *Anal Biochem,* 401**:** 318-320,

55. Cobos, EJ, Entrena, JM, Nieto, FR, Cendan, CM, Del Pozo, E. (2008) Pharmacology and therapeutic potential of sigma(1) receptor ligands. *Curr Neuropharmacol,* 6**:** 344-366,

56. Li, Z, Zhou, R, Cui, S, Xie, G, Cai, W, Sokabe, M, Chen, L. (2006) Dehydroepiandrosterone sulfate prevents ischemia-induced impairment of long-term potentiation in rat hippocampal CA1 by up-regulating tyrosine phosphorylation of NMDA receptor. *Neuropharmacology,* 51**:** 958-966,

57. Eulalio, A, Huntzinger, E, Izaurralde, E. (2008) Getting to the root of miRNA-mediated gene silencing. *Cell,* 132**:** 9-14,

58. Kaucsar, T, Revesz, C, Godo, M, Krenacs, T, Albert, M, Szalay, CI, Rosivall, L, Benyo, Z, Batkai, S, Thum, T, Szenasi, G, Hamar, P. (2013) Activation of the miR-17 family and miR-21 during murine kidney ischemia-reperfusion injury. *Nucleic Acid Ther,* 23**:** 344-354,

59. Jia, P, Teng, J, Zou, J, Fang, Y, Zhang, X, Bosnjak, ZJ, Liang, M, Ding, X. (2013) miR-21 contributes to xenon-conferred amelioration of renal ischemia-reperfusion injury in mice. *Anesthesiology,* 119**:** 621-630,

60. Vannay, A, Fekete, A, Langer, R, Toth, T, Sziksz, E, Vasarhelyi, B, Szabo, AJ, Losonczy, G, Adori, C, Gal, A, Tulassay, T, Szabo, A. (2009) Dehydroepiandrosterone pretreatment alters the ischaemia/reperfusion-induced VEGF, IL-1 and IL-6 gene expression in acute renal failure. *Kidney Blood Press Res,* 32**:** 175-184,

61. Liu, D, Dillon, JS. (2004) Dehydroepiandrosterone stimulates nitric oxide release in vascular endothelial cells: evidence for a cell surface receptor. *Steroids,* 69**:** 279-289,

62. Chertow, GM, Burdick, E, Honour, M, Bonventre, JV, Bates, DW. (2005) Acute kidney injury, mortality, length of stay, and costs in hospitalized patients. *J Am Soc Nephrol,* 16**:** 3365-3370,

63. Smith, GL, Vaccarino, V, Kosiborod, M, Lichtman, JH, Cheng, S, Watnick, SG, Krumholz, HM. (2003) Worsening renal function: what is a clinically meaningful change in creatinine during hospitalization with heart failure? *J Card Fail,* 9**:** 13-25,

64. Keppler, A, Gretz, N, Schmidt, R, Kloetzer, HM, Groene, HJ, Lelongt, B, Meyer, M, Sadick, M, Pill, J. (2007) Plasma creatinine determination in mice and rats: an enzymatic method compares favorably with a high-performance liquid chromatography assay. *Kidney Int,* 71**:** 74-78,

65. Zang, X, Zheng, F, Hong, HJ, Jiang, Y, Song, Y, Xia, Y. (2014) Neutrophil gelatinase-associated lipocalin protects renal tubular epithelial cells in hypoxia-reperfusion by reducing apoptosis. *Int Urol Nephrol,* 46**:** 1673-1679,

66. Bolignano, D, Donato, V, Coppolino, G, Campo, S, Buemi, A, Lacquaniti, A, Buemi, M. (2008) Neutrophil gelatinase-associated lipocalin (NGAL) as a marker of kidney damage. *Am J Kidney Dis,* 52**:** 595-605,

67. Conde, E, Alegre, L, Blanco-Sanchez, I, Saenz-Morales, D, Aguado-Fraile, E, Ponte, B, Ramos, E, Saiz, A, Jimenez, C, Ordonez, A, Lopez-Cabrera, M, del Peso, L, de Landazuri, MO, Liano, F, Selgas, R, Sanchez-Tomero, JA, Garcia-Bermejo, ML. (2012) Hypoxia inducible factor 1-alpha (HIF-1 alpha) is induced during reperfusion after renal ischemia and is critical for proximal tubule cell survival. *PLoS One,* 7**:** e33258,

68. Movafagh, S, Crook, S, Vo, K. (2015) Regulation of hypoxia-inducible factor-1a by reactive oxygen species : new developments in an old debate. *J Cell Biochem,* 116**:** 696-703,

69. Sun, G, Zhou, Y, Li, H, Guo, Y, Shan, J, Xia, M, Li, Y, Li, S, Long, D, Feng, L. (2013) Over-expression of microRNA-494 up-regulates hypoxia-inducible factor-1 alpha expression via PI3K/Akt pathway and protects against hypoxia-induced apoptosis. *J Biomed Sci,* 20**:** 100,

70. Hacham, M, Argov, S, White, RM, Segal, S, Apte, RN. (2002) Different patterns of interleukin-1alpha and interleukin-1beta expression in organs of normal young and old mice. *Eur Cytokine Netw,* 13**:** 55-65,

71. Luheshi, NM, Kovacs, KJ, Lopez-Castejon, G, Brough, D, Denes, A. (2011) Interleukin-1alpha expression precedes IL-1beta after ischemic brain injury and is localised to areas of focal neuronal loss and penumbral tissues. *J Neuroinflammation,* 8**:** 186,

72. Deng, J, Kohda, Y, Chiao, H, Wang, Y, Hu, X, Hewitt, SM, Miyaji, T, McLeroy, P, Nibhanupudy, B, Li, S, Star, RA. (2001) Interleukin-10 inhibits ischemic and cisplatin-induced acute renal injury. *Kidney Int,* 60**:** 2118-2128,

73. Jung, M, Sola, A, Hughes, J, Kluth, DC, Vinuesa, E, Vinas, JL, Perez-Ladaga, A, Hotter, G. (2012) Infusion of IL-10-expressing cells protects against renal ischemia through induction of lipocalin-2. *Kidney Int,* 81**:** 969-982,

74. Yap, SC, Lee, HT. (2012) Acute kidney injury and extrarenal organ dysfunction: new concepts and experimental evidence. *Anesthesiology*, 116**:** 1139-1148,

75. Allahtavakoli, M, Jarrott, B. (2011) Sigma-1 receptor ligand PRE-084 reduced infarct volume, neurological deficits, pro-inflammatory cytokines and enhanced anti-inflammatory cytokines after embolic stroke in rats. *Brain Res Bull*, 85**:** 219-224,

76. Bhuiyan, MS, Tagashira, H, Fukunaga, K. (2011) Sigma-1 receptor stimulation with fluvoxamine activates Akt-eNOS signaling in the thoracic aorta of ovariectomized rats with abdominal aortic banding. *Eur J Pharmacol*, 650**:** 621-628,

77. Tagashira, H, Bhuiyan, S, Shioda, N, Fukunaga, K. (2011) Distinct cardioprotective effects of 17beta-estradiol and dehydroepiandrosterone on pressure overload-induced hypertrophy in ovariectomized female rats. *Menopause*, 18**:** 1317-1326,

78. Bhuiyan, MS, Tagashira, H, Fukunaga, K. (2013) Crucial interactions between selective serotonin uptake inhibitors and sigma-1 receptor in heart failure. *J Pharmacol Sci*, 121**:** 177-184,

79. Roh, DH, Choi, SR, Yoon, SY, Kang, SY, Moon, JY, Kwon, SG, Han, HJ, Beitz, AJ, Lee, JH. (2011) Spinal neuronal NOS activation mediates sigma-1 receptor-induced mechanical and thermal hypersensitivity in mice: involvement of PKC-dependent GluN1 phosphorylation. *Br J Pharmacol*, 163**:** 1707-1720,

80. Mori, T, Hayashi, T, Hayashi, E, Su, TP. (2013) Sigma-1 receptor chaperone at the ER-mitochondrion interface mediates the mitochondrion-ER-nucleus signaling for cellular survival. *PLoS One*, 8**:** e76941,

81. Fujimoto, M, Hayashi, T, Urfer, R, Mita, S, Su, TP. (2012) Sigma-1 receptor chaperones regulate the secretion of brain-derived neurotrophic factor. *Synapse*, 66**:** 630-639,

82. Chaigneau, E, Oheim, M, Audinat, E, Charpak, S. (2003) Two-photon imaging of capillary blood flow in olfactory bulb glomeruli. *Proc Natl Acad Sci U S A*, 100**:** 13081-13086,

83. Crawford, C, Kennedy-Lydon, T, Sprott, C, Desai, T, Sawbridge, L, Munday, J, Unwin, RJ, Wildman, SS, Peppiatt-Wildman, CM. (2012) An intact kidney slice model to investigate vasa recta properties and function in situ. *Nephron Physiol*, 120**:** p17-31,

84. Smith, C, Merchant, M, Fekete, A, Nyugen, HL, Oh, P, Tain, YL, Klein, JB, Baylis, C. (2009) Splice variants of neuronal nitric oxide synthase are present in the rat kidney. *Nephrol Dial Transplant,* 24**:** 1422-1428,

85. Shoskes, DA, Xie, Y, Gonzalez-Cadavid, NF. (1997) Nitric oxide synthase activity in renal ischemia-reperfusion injury in the rat: implications for renal transplantation. *Transplantation,* 63**:** 495-500,

86. Szabo, AJ, Wagner, L, Erdely, A, Lau, K, Baylis, C. (2003) Renal neuronal nitric oxide synthase protein expression as a marker of renal injury. *Kidney Int,* 64**:** 1765-1771,

87. Nishimura, T, Ishima, T, Iyo, M, Hashimoto, K. (2008) Potentiation of nerve growth factor-induced neurite outgrowth by fluvoxamine: role of sigma-1 receptors, IP3 receptors and cellular signaling pathways. *PLoS One,* 3**:** e2558,

88. Miller, HL, Ekstrom, RD, Mason, GA, Lydiard, RB, Golden, RN. (2001) Noradrenergic function and clinical outcome in antidepressant pharmacotherapy. *Neuropsychopharmacology,* 24**:** 617-623,

89. Quiroga, I, McShane, P, Koo, DD, Gray, D, Friend, PJ, Fuggle, S, Darby, C. (2006) Major effects of delayed graft function and cold ischaemia time on renal allograft survival. *Nephrol Dial Transplant,* 21**:** 1689-1696,

90. Shihab, FS, Bennett, WM, Andoh, TF. (2009) Donor preconditioning with a calcineurin inhibitor improves outcome in rat syngeneic kidney transplantation. *Transplantation,* 87**:** 326-329,

91. Cicora, F, Roberti, J, Lausada, N, Gonzalez, P, Guerrieri, D, Stringa, P, Cicora, P, Vasquez, D, Gonzalez, I, Palti, G, Intile, D, Raimondi, C. (2012) Donor preconditioning with rabbit anti-rat thymocyte immunoglobulin ameliorates ischemia reperfusion injury in rat kidney transplantation. *Transpl Immunol,* 27**:** 1-7,

92. Rice, JC, Spence, JS, Yetman, DL, Safirstein, RL. (2002) Monocyte chemoattractant protein-1 expression correlates with monocyte infiltration in the post-ischemic kidney. *Ren Fail,* 24**:** 703-723,

93. Ramirez-Sandoval, JC, Herrington, W, Morales-Buenrostro, LE. (2015) Neutrophil gelatinase-associated lipocalin in kidney transplantation: A review. *Transplant Rev (Orlando),* 29**:** 139-144,

94. Yadav, B, Prasad, N, Agrawal, V, Jaiswal, A, Agrawal, V, Rai, M, Sharma, R, Gupta, A, Bhadauria, D, Kaul, A. (2015) Urinary Kidney injury molecule-1 can predict delayed graft function in living donor renal allograft recipients. *Nephrology (Carlton),* 20**:** 801-806,

95. Gomes, MB, Cobas, RA. (2009) Post-transplant diabetes mellitus. *Diabetol Metab Syndr,* 1**:** 14,

96. Cosio, FG, Pesavento, TE, Osei, K, Henry, ML, Ferguson, RM. (2001) Post-transplant diabetes mellitus: increasing incidence in renal allograft recipients transplanted in recent years. *Kidney Int,* 59**:** 732-737,

97. Mardon, K, Kassiou, M, Donald, A. (1999) Effects of streptozotocin-induced diabetes on neuronal sigma receptors in the rat brain. *Life Sci,* 65**:** Pl 281-286,

98. Ortiz, A, Sanchez-Nino, MD, Izquierdo, MC, Martin-Cleary, C, Garcia-Bermejo, L, Moreno, JA, Ruiz-Ortega, M, Draibe, J, Cruzado, JM, Garcia-Gonzalez, MA, Lopez-Novoa, JM, Soler, MJ, Sanz, AB. (2015) Translational value of animal models of kidney failure. *Eur J Pharmacol,* 759**:** 205-220,

99. Tesch, GH, Allen, TJ. (2007) Rodent models of streptozotocin-induced diabetic nephropathy. *Nephrology (Carlton),* 12**:** 261-266,

100. Aragno, M, Tamagno, E, Gatto, V, Brignardello, E, Parola, S, Danni, O, Boccuzzi, G. (1999) Dehydroepiandrosterone protects tissues of streptozotocin-treated rats against oxidative stress. *Free Radic Biol Med,* 26**:** 1467-1474,

101. Aragno, M, Parola, S, Brignardello, E, Manti, R, Betteto, S, Tamagno, E, Danni, O, Boccuzzi, G. (2001) Oxidative stress and eicosanoids in the kidneys of hyperglycemic rats treated with dehydroepiandrosterone. *Free Radic Biol Med,* 31**:** 935-942,

102. Richards, RJ, Porter, JR, Inserra, F, Ferder, LF, Stella, I, Reisin, E, Svec, F. (2001) Effects of dehydroepiandrosterone and quinapril on nephropathy in obese Zucker rats. *Kidney Int,* 59**:** 37-43,

103. Bergeron, R, de Montigny, C, Debonnel, G. (1996) Potentiation of neuronal NMDA response induced by dehydroepiandrosterone and its suppression by progesterone: effects mediated via sigma receptors. *J Neurosci,* 16**:** 1193-1202,

104. Trachtman, H, Futterweit, S, Pine, E, Mann, J, Valderrama, E. (2002) Chronic diabetic nephropathy: role of inducible nitric oxide synthase. *Pediatr Nephrol,* 17**:** 20-29,

105. He, Y, Fan, Z, Zhang, J, Zhang, Q, Zheng, M, Li, Y, Zhang, D, Gu, S, Yang, H. (2011) Polymorphisms of eNOS gene are associated with diabetic nephropathy: a meta-analysis. *Mutagenesis,* 26**:** 339-349,

106. Markowitz, SM, Gonzalez, JS, Wilkinson, JL, Safren, SA. (2011) A review of treating depression in diabetes: emerging findings. *Psychosomatics,* 52**:** 1-18,

107. Voican, CS, Corruble, E, Naveau, S, Perlemuter, G. (2014) Antidepressant-induced liver injury: a review for clinicians. *Am J Psychiatry,* 171**:** 404-415,

108. Yamada, J, Sugimoto, Y, Inoue, K. (1999) Selective serotonin reuptake inhibitors fluoxetine and fluvoxamine induce hyperglycemia by different mechanisms. *Eur J Pharmacol,* 382**:** 211-215,

109. Oswald, P, Souery, D, Mendlewicz, J. (2003) Fluvoxamine-induced hyperglycaemia in a diabetic patient with comorbid depression. *Int J Neuropsychopharmacol,* 6**:** 85-87,

110. Reddy, MA, Natarajan, R. (2015) Recent developments in epigenetics of acute and chronic kidney diseases. *Kidney Int,* 88**:** 250-261,

111. de Zwaan, M, Nutzinger, DO. (1996) Effect of fluvoxamine on total serum cholesterol levels during weight reduction. *J Clin Psychiatry,* 57**:** 346-348,

112. Tse, L, Procyshyn, RM, Fredrikson, DH, Boyda, HN, Honer, WG, Barr, AM. (2014) Pharmacological treatment of antipsychotic-induced dyslipidemia and hypertension. *Int Clin Psychopharmacol,* 29**:** 125-137,

10. Bibliography of the candidate's publications

Publications related to the theme of the Ph.D. thesis

1. Hosszu, A, Antal, Z, Lenart, L, Hodrea, J, Koszegi, S, Balogh, DB, Banki, NF, Wagner, L, Denes, A, Hamar, P, Degrell, P, Vannay, A, Szabo, AJ, Fekete, A. (2016) Sigma1-Receptor Agonism Protects against Renal Ischemia-Reperfusion Injury. *J Am Soc Nephrol* In press. **IF=8.491**

2. Lenart, L, Hodrea, J, Hosszu, A, Koszegi, S, Zelena, D, Balogh, D, Szkibinszkij, E, Veres-Szekely, A, Wagner, L, Vannay, A, Szabo, AJ, Fekete, A. (2016) The role of sigma-1 receptor and brain-derived neurotrophic factor in the development of diabetes and comorbid depression in streptozotocin-induced diabetic rats. *Psychopharmacol*, 233: 1269-1278. **IF=3.540**

Other publications

1. Gellai, R, Hodrea, J, Lenart, L, Hosszu, A, Koszegi, S, Balogh, D, Ver, A, Banki, NF, Fulop, N, Molnar, A, Wagner, LJ, Vannay, A, Szabo, AJ, Fekete, A. (2016) The role of O-linked N-Acetylglucosamine modification in diabetic nephropathy. *Am J Physiol Ren Physiol*: ajprenal.00545.02015. **IF=3.390**

2. Denes, J, Katona, M, Hosszu, A, Czuczy, N, Takats, Z. (2009) Analysis of biological fluids by direct combination of solid phase extraction and desorption electrospray ionization mass spectrometry. *Anal Chem*, 81: 1669-1675. **IF=5.214**

DOI:10.14753/SE.2017.2251

11. Acknowledgment

First and foremost I am profoundly thankful to my supervisor Andrea Fekete for being a role model and showing me the value of hard work. Her tireless dedication and guidance is indispensable to everyone in our lab.

I wish to sincerely thank Professors Attila Szabo and Tivadar Tulassay for the proud privilege to work as a PhD student in their Research Laboratory of the 1st Department of Pediatrics, Semmelweis University.

I wish to express my gratitude to my PhD supervisors at Georgetown University, Prof. Christopher Wilcox and Dr. William Welch for their constant support and guidance. My stay at the Hypertension, Kidney and Vascular Research Center was an outmost challenging and encouraging experience. I also thank the Rostoczy Foundation for the financial support that made my stay possible.

I am also very grateful to the „seniors" of our lab, Adam Vannay, Laszlo Wagner and Judit Hodrea for their valuable experience and suggestions that helped me throughout the experiments. I learned a lot from their critical advice when I was writing my manuscripts.

I would like to thank all my colleagues at the lab for creating a motivating and friendly atmosphere. Special thanks to Sandor Koszegi for preparing the histological evalution, to Zsuzsanna Antal for her invaluable help in animal surgeries, to Lilla Lenart for her ongoing efforts to manage all my projects when I was abroad, to Agnes Prokai for teaching me two-photon microscopy. I could not be more thankful to Maria Bernath for her help with cell cultures and laboratory work, not to mention the delicious birthday cakes. I am priviliged of having the Lendulet colleagues as well: Fanni Banki, Dora Balogh, Edgar Szkibinszkij, Renata Gellai, thanks to you all for helping me survive these years.

Above all special thanks to Lilla Lenart and to my whole family; without their constant support and love this work could not have been completed.